Title	COUPLED ROTATIONAL BEHAVI0R OF METHYL GROUPS IN SOME MOLECULAR SOLIDS AS STUDIED BY THE PROTON N,M,R, METHOD
Author(s)	Takeda, Sadamu
Citation	大阪大学, 1982, 博士論文
Version Type	VoR
URL	https://hdl.handle.net/11094/27706
rights	
Note	

COUPLED ROTATIONAL BEHAVIOR OF METHYL GROUPS IN SOME MOLECULAR SOLIDS AS STUDIED BY THE PROTON N.M.R. METHOD

by

Sadamu Takeda

M.S., Osaka University, 1979

Thesis

Submitted to the Graduate School of Faculty of Science,
Osaka University,
in partial fulfilment of the requirements
for the degree of Doctor of Science

Osaka University
1982

Doctoral Committee:
- Professor Hideaki Chihara, Chairman
- Professor Keiji Kuwata
- Professor Yoshimasa Kyogoku

Acknowledgments

I would like to express my sincere thanks to Professor Hideaki Chihara for his kind guidance, many valuable suggestions, and encouragement, as well as for critical reading of this thesis. I would like to thank late Dr. Gen Soda for introducing me to nuclear magnetic resonance method and for his fruitful suggestions and discussions at the biginning of this study. I wish to thank Dr. Nobuo Nakamura and Dr. Tooru Atake for their valuable suggestions , criticism, and encouragement. I also wish to thank all the members of the Chihara's laboratry for their useful discussions and kindness, especially Dr. Taisei Yamamoto and Mr. Kiyoshi Ichimura.

Thanks are also due to Professor Tsunenobu Yamamoto and his co-workers for their useful discussions.

I am grateful to Misses Mariko Nakayama and Ryoko Yagi for typing a part of this manuscript.

Abstract

Coupled rotational behavior of methyl groups in some molecular solids was studied by nuclear magnetic resonance methods.

The proton spin-lattice relaxation due to the rotation of methyl groups was investigated for trichloromethylsilane (CH_3SiCl_3), tetramethylpyrazine (T.M.P.), 1,2,4,5,-tetramethylbenzene (durene), and tetramethylsilane ($Si(CH_3)_4$). The magnetization recoveries of these materials were non-exponential and depended on the pulse sequence employed. These behaviors are understood in the framework of symmetry restricted spin diffusion theory by Emid, et al.. The tunneling assisted minima of the spin-lattice relaxation time were clearly observed in the T_{1f} curve vs. temperature in the β and γ phases of $Si(CH_3)_4$, where T_{1f} is the fast-relaxing component of spin-lattice relaxation time.

The tunneling frequencies of the methyl groups of CH_3SiCl_3, durene, T.M.P., $Si(CH_3)_4$, and hexamethylbenzene (H.M.B.) were directly observed by the "N.M.R. field cycling technique". CH_3SiCl_3 showed two kinds of tunneling splittings. These are 34.6 MHz and 40.4MHz. These frequencies come from the different methyl groups which are hindered by slightly different potential barrier in the crystal. For durene and T.M.P., three kinds of tunneling splittings are identified (29.3, 25.3, and 17.8 MHz in durene; 26.8, 20.2, and 14.3 (or 6.4) in T.M.P.). There are only two crystalographically inequivalent methyl groups in both crystals of durene and T.M.P.. These facts indicate that the two methyl groups which are close to one another in these molecules are not independent but coupled to one another. Indirect evidence of the decrease of tunneling

frequencies of T.M.P. as temperature rised was obtained. In the γ phase of $Si(CH_3)_4$, two kinds of tunneling frequencies of the methyl groups were identified (20.4 and 15.8 MHz in the low temperature limit These two tunneling frequencies decrease with increasing temperature in a similar way. The β phase showed more complicated tunneling spectra. Hexamethylbenzene showed two kinds of tunneling frequencies. These are 9.6 MHz (A) and 7.9 MHz (B) in the low temperature limit. The frequency A was almost independent of the temperature whereas the frequency B decreased as temperature increased and became so small as it was unobservable below 30.9 K. These behavior also indicate that the effect of mechanical coupling between the methyl groups plays an important role in the rotational tunneling of these methyl groups. The new feature of "coupled rotational tunnel state" in the solid state was demonstrated experimentally in the first time.

The effect of collective rotation or "geared rotation" of two methyl groups, which are close to one another, on their proton spin-lattice relaxation rate was also discussed in the classical limit.

For CH_3SiCl_3, T.M.P., and $Si(CH_3)_4$, the small reduction of N.M.R. line width was observed. Comparing the experimental results of these materials with each other, this reduction is that of inter-methyl dipolar broadning. The mechanism of the reduction is probably the increase of the rate of non-magnetic transitions between the rotational levels or the increase of the population of higher rotational levels.

Table of contents

I. Introduction

The dynamical properties of molecules or molecular groups in solid have been studied by many workers using a wide range of different experimental techniques.

It has been revealed by N.M.R. studies that molecules and molecular groups rotate even in the solid state.$^{1)}$ The value of second moment of N.M.R. absorption line enable us to know what mode of molecular motion takes place. The spin-lattice relaxation time (T_1) vs. temperature reveals the time scale of the motion. Especially the dynamical behavior of a methyl group in solid has been studied by N.M.R. method, because it is one of the simple molecular groups. The activation energy and the time scale (correlation time τ_c) of the classical rotation in solid were obtained for many materials. The classical rotation means such a rotation that a methyl group is hindered by rather higher barrier than the thermal energy at corresponding temperature and the rotation is described as the random hopping reorientation over the barrier top by the thermal excitation. The correlation time τ_c corresponds to the residence time of a methyl group in one of the potential wells.

The spin-lattice relaxation time (T_1) against temperature show a minimum due to the reorientation of a methyl group at the condition that $\omega_0 \tau_c = 0.6$, where ω_0 is the Larmor frequency. The activation energy for methyl reorientation vs. temperature of the T_1 minimum holds a nearly linear relation for many materials.$^{2)}$ This result can be understood, when we consider that the reorientaion of a methyl group can be described by

Arrhenius type activation process,

$$\tau_c = \tau_c^{0} \exp (E_a / RT) \qquad (1)$$

and that the pre-exponental factor τ_c^{0} is similar to each other for the methyl groups in many materials.

Quasi-elastic neutron scattering experiment also revealed the dynamical behavior of a methyl group. From the analysis of the quasi-elastic peak, we can obtain the time scale and activation energy of the methyl reorientation3).

E_a and τ_c may be obtained from the analysis of the band shape and/or band width of the Raman band and infrared absorption line. With respect to the molecular rotation as a whole in the solid state (plastically crystalline phase) such studies were performed4) but for the the case of internal rotation of a methyl group there was no such a precise study.

In many cases it was assumed that the potential barrier to rotation of a methyl group is a simple three fold potential. It is

$$V = (V_3)/2 (1-\cos \theta), \qquad (2)$$

where θ is the rotation angle of a methyl group about its C_3 symmetry axis.

In addition to such a classical rotation at considerably high temperature, the tunneling effect plays an important role for the low barrier case and at sufficiently low temperature at which the thermally activated rotation over the barrier top is frozen. This tunneling-assisted rotation of some simple molecules and molecular groups (CH_3-, CH_4, NH_4^+) is one of the interesting subjects, which has been investigated by many workers. The tunneling rotation is usually characterized by the magnitude of energy splitting of the librational (torsional) levels which is called the tunneling frequency. The detailed investigations of the tunneling frequency have been performed mainly by N.M.R. method5) and inelastic neutron scattering technique6). Other methods, e.g. electron paramagnetic resonance7), were also used. The main problems of the studies are to observe the tunneling frequency directly and to measure its dependence on the temperature. One of the ultimate purposes of these studies is to understand the dynamical feature of these molecular groups and its temperature variation as temperature rises from low to high.

Because the precise energy separations between the rotational states (torsional or tunneling states) of a methyl group has been observed, it becomes clear that the hindering potential is not so simple for many case as it can be safely described only by the three fold potential term (V_3, see Eq.(1))8). The shape of the hindering potential plays an important role for the dynamical properties of a methyl group. A special interest exists in the case that some methyl groups come near each other.

It has been considered from the early days that the motion of such adjacent methyl groups is described as a "geared rotation". This idea is a classical one but it is important concept for the rotational dynamics of such system. In other words, the potential barrier hindering the rotation of a methyl group is affected rather strongly by the change of rotation angle of a neighbouring methyl group. This situation is called the "mechanical coupling" between the methyl groups, which causes the "collective rotation". In many cases collective rotation or collective libration is characterized by the symmetry, corresponding to the "normal mode".

An experimental evidence of mechanical coupling between the methyl groups is the energy difference between the torsional modes. The investigations have been performed for several materials with various methods. The splitting of 35 cm^{-1} was reported from newtron inelastic scattering for the torsional sublevels (A_2 and B_2 symmetry levels) of the first excited state in durene and o-xyline[9]. Infrared spectra led to the values, 60 cm^{-1} and 14 cm^{-1} (the separation between A_2 and F_2 symmetry levels), for $C(CH_3)_4$ and $Si(CH_3)_4$, respectively[10], the latter value being also supported by inelastic neutron scattering[11]. The case of four rotors in a molecule of T_d symmetry shows no torsional mode in the infrared spectra in the first approximation, because these molecules with T_d symmetry possess no permanent dipole moment. But the torsional modes inactive in the oscillator approximation become active due to Coriolis coupling, according to the perturbation treatment of the multiple top molecules[10]. On fusion, the separation in $C(CH_3)_4$ changes little (to 55 cm^{-1})[12] indicating that the torsional normal modes are primarily determined by intramolecular interaction in this case.

In microwave studies of the ground vibrational state of double top molecules in the gas phase, finite top-top (methyl-methyl) interactions can be treated as perturbations[13]. The torsional energy levels in the ground vibrational state of a two top molecule are nine-fold degenerate in the limit when both barriers are very high, but as the barriers become lower, this degeneracy is partially lifted to give four levels which are labeled, AA, EE, AE, and EA (tunneling sublevels). The predicted "quartet" absorption pattern is observed for many rotational transitions of acetone[13)] for example where V_3=3.26 kJ mol^{-1}, whereas for molecules with somewhat higher barriers, e.g. dimethyl ether,[13)] where V_3=11.38 kJ mol^{-1} the ground state rotational spectrum consists of many "triplet" absorption lines.

The rotational tunnel state is more sensitive to the situation of the hindering barrier than the torsional state, especially near the bottom of the potential well. The mechanical coupling between the methyl groups is expected to be very effective on the rotational tunnel state and its effect plays an important role for the rotational tunneling of the methyl groups. But the coupling effect on the rotational tunneling state of methyl groups in the solid state has not been demonstrated experimentally.

The main purpose of this thesis is to demonstrate this mechanical coupling effect on the rotational tunnel state of the methyl groups in solid.

When the methyl groups are situated so closely to each other that the coupling effect is observable, the hindering barrier to rotation of a methyl group is probably not so small, i.e. the tunneling splitting is not so large. Therefore N.M.R. relaxation method was employed in this thesis. This method is useful for the tunneling splittings of the order of Larmor frequency ($10^0 \sim 10^2$ MHz, see in Section IV). Four materials, i.e. 1,2,4,5-tetramethylbenzene, tetramethylpyrazine, tetramethylsilane, and hexamethylbenzene, which contain different numbers of adjacent methyl groups with rather high symmetry, were chosen to be studied for this purpose.

The tunneling energy scheme (spectrum) can be obtained through the spin-lattice relaxation phenomena of the protons within a methyl group. In recent years, the novel theory for descibing the spin-lattice relaxation due to methyl rotation (tunneling rotation and/or jump-reorientation) has been proposed by Emid and Wind and their co-workers14,15). It is symmetry restricted spin diffusion theory (SRSD theory). This theory seems to be most universal for the problem of nuclear spin relaxation in solids and it includes the previous theories. But it has scarcely been used by other workers until now. We should examine whether the spin-lattice relaxation behaviour of the materials cited in this thesis are understood in the framework of the theory by Emid, or not. This problem is also one of the purpose of this thesis. After this examination is performed (Section VI.1), the tunneling energy scheme of the methyl groups is to be discussed (Section VI.2 VI.6).

The problem of the tunneling energy scheme relates to the static feature of the methyl group and it is the basis of the dynamical problems of the mehtyl groups in solids. To investigate the dynamical features of the methyl groups, the correct energy scheme is to be taken into account in order to eliminate the mis-understanding. The dynamical problems of the methyl groups in solid are, for example, as follows.

i) The principal mechanism of the methyl rotation, i.e. the jump rotation over the potential or the tunneling rotation through the barrier, and its dependence on the temperature.

ii) The temperature dependence of the observable tunneling frequencies. This problem is deeply connected to the problem i).

These problems i) and ii) will be discussed.

For a tunneling methyl group, of which the tunneling splitting is much larger than the dipolar energy (local field H_d, $H_d \lesssim 10^2$ kHz), the reduced second moment of the N.M.R. absorption line was observed for several materials[16) even at liquid helium temperature region. Some of these materials showed the small narrowing of the maximum slope width or small reduction of second moment at about 10 ~ 50 K. The origin of this phenomenon has not been known. It is one of the purposes of this thesis to make contribution to the elucidation of the problem (Section VI.7).

The theoretical description and the concepts of a single methyl group in solid, which have been proposed until now by many workers, is summarized in Section II. The important points of the theoretical treatment of the spin-lattice relaxation of a single methyl group in solid is also summarized in Section II. This Section does not include the original work of the author.

References

1) C.P. Slichter, "Principles of Magnetic Resonance", second revised expanded edition (1978).
"Specialist Periodical Reports", Nuclear Magnetic Resonance vol.1 (1972) and other vols, The Chemical Society, Burlington House, London.
2) T. Eguch, Thesis (1977), Osaka University.
3) for example
W. Muller-Warmuth, R. Schuler, M. Prager, and K. Kollmar, J. Mag. Reson., 34 (1979) 83.
S. Clough and A. Heidemann, J. Phys., C12 (1979) 761.
4) R.T. Bailey, "The plasticaly crystalline state, orientationaly disordered crystal",Chapter 7, Infrared and Raman studies of moleculer motion in plastic crystals, (1979), Ed. by J.N. Sherwood, A wiley-Interscience publication.
5) see the references 20 - 30 in Section IV.
6) see the references 1 -14 in Section IV.
7) see the references 15 - 19 in Section IV.
8) for example
B. Alefeld, A. Kollmar, and B.A. Dasannachaya, J. Chem. Phys., 63 (1975) 4415.
W. Muller-Warmuth, R. Shuler, M. Prager, and A. Kollmar, J. Chem. Phys., 69 (1978) 2382.
9) R. C. LIvingston, D.M. Grant, R.T. Puquie, K.A. Strong, and R.M. Brugger, J. Chem. Phys., 58 (1973) 1438.
10) J.R. Durig, S.M. Craven, and J. Bragin, J. Chem. Phys., 52 (1970) 2046.
11) C.I. Ratcliffe and T.C. Waddington, J. Chem. Soc. Far. II, 72

(1976) 1840.

12) D.M. Grant, K.A. Strong, and R.M. Brugger, Phys. Rev. Lett., 20 (1968) 983.

13) D.G. Lister, J.N. Macdnald, and N.C. Owen, "Internal Rotation and Inversion", (1978), Academic Press, and the references cited therein.

14) S. Emid, R.J. Baarda, J. Smidt, and R.A. Wind, Physica, 93B (1978) 327, and the references cited therein.

15) S. Emid and R.A. Wind, Chem. Phys. Lett., 33 (1975) 269.

16) for example

P.S. Allen and A. Cowking, J. Chem. Phys., 49 (1968) 789.

T. Hasebe, G. Soda, and H. Chihara, Proc. Japan Acad., 51 (1975) 168.

II Review of theoretical treatment of methyl rotation.

Tunneling behavior of molecular groups (especially a methyl group) in solid and its effect on the nuclear relaxation have been well treated previously. Therefore, in this Section we limit ourselves to an outline of definitions and previous results needed for the understanding of the results of the present study.

II. 1 Quantum-mechanical calculation of the spin-lattice ralaxation rate of a methyl group.

The spin-lattice relaxation rate of a methyl group should be calculated quantum-mechanically for understanding the behavior of the spin-lattice relaxation of a methyl group. The calculation is based on the semiclassical description1-4) in which the energy reservoir is considered classically and a methyl group (spin and totor states) quantum-mechanically.

II. 1.1 Hamiltonian of a methyl group in solid.

The Hamiltonian of a methyl group under consideration is given by1-4)

$$H = H_P + H_R + H_{RP} + H_Z + H_D. \tag{1}$$

H_P describes the phonon system and H_R describes the methyl-rotor system. H_{RP} means the coupling between the phonon and the hindered methyl-rotor systems. H_z is the Zeeman Hamiltonian and H_D represents the dipolar interactions among the protons. H_D includs the intra- and intermethyl dipolar interactions.

Now we will outline the meaning and the role of each term separately.

1) H_P

H_P denotes the Hamiltonian corresponding to the phonon system which is the energy reservoir of the spin system. We consider that the phonon system is in thermal equilibrium characterized by a temperature T which equals the temperature of the sample. This phonon system interacts with methyl-rotor system through the rotation-phonon coupling H_{RP}.

2) H_R

H_R represents the sum of kinetic and potential energy of a methyl group in terms of the rotation angle about its symmetry axis and is given by

$$H_R = - \frac{\hbar^2}{2I} \frac{d^2}{d\theta^2} + V(\theta), \qquad (2)$$

where I is the moment of inertia of a methyl group about its symmetry axis and $V(\theta)$ is the potential barrier hindering the rotation of a methyl group. Due to the three-fold symmetry of the CH_3-group, the most general shape of the potential can be written as

$$V(\theta) = \frac{1}{2} \sum_n V_{3n} \left\{ 1 - \cos(3n\theta) \right\} . \qquad (3)$$

But we will now consider the case in which V_3 is dominant and $V(\theta)$ can be approximated by $V_3(1 - \cos 3\theta)/2$. The eigen functions $\Phi_n{}^S$ and eigen energies $E_n{}^S$ follow from the well known equation,

$$H_R \Phi_n^S = E_n^S \Phi_n^S . \tag{4}$$

n is a quantum number belonging to the n-th rotor level. The superscript S describes the irreducible representations A, E^a, or E^b of the point group C_3. The E^a and E^b states have the same eigen value with respect to any amplitude of V_3. Equation (3) includes the general cases. In the limiting case of $V_3 = 0$, the methyl group is a free rotor and the energy states are identified by the free rotation quantum number. If V_3 is infinite, the energy scheme can be approximated by the harmonic oscillator levels and the eigen value E_n^A becomes equal to $E_n^{E^a}$ ($E_n^{E^b}$). This degenerate n-th level is well known as the torsional (librational) level. The variation of energy scheme of a rotor due to growth of a hindering barrier from zero to a finite magnitude is shown in Fig. 1. The level scheme of a methyl group with a finite potential V_3 is illustrated in Fig. 2. The energy separation between E_n^A and $E_n^{E^a}$ ($E_n^{E^b}$) is well known as the tunneling splitting Δ_n.

The eigen values E_n^S can be calculated numericlly with the wave function of a free rotor$^{7,8)}$ (free rotor approximation) or by other method$^{9)}$. The eigen functions Φ_n can approximated by a series of free rotor wave functions$^{4)}$,

$$\Phi_n = \sum_{m=-\infty}^{\infty} a_m e^{im\theta} \tag{5}$$

Here a_m are expansion coefficients. Because the eigen states have to reflect the symmetry of the potential $V(\theta)$ which is now considered as three-fold, we can express the eigen functions Φ_n in terms of the irreducible representations A, E^a, and E^b of the point group C_3

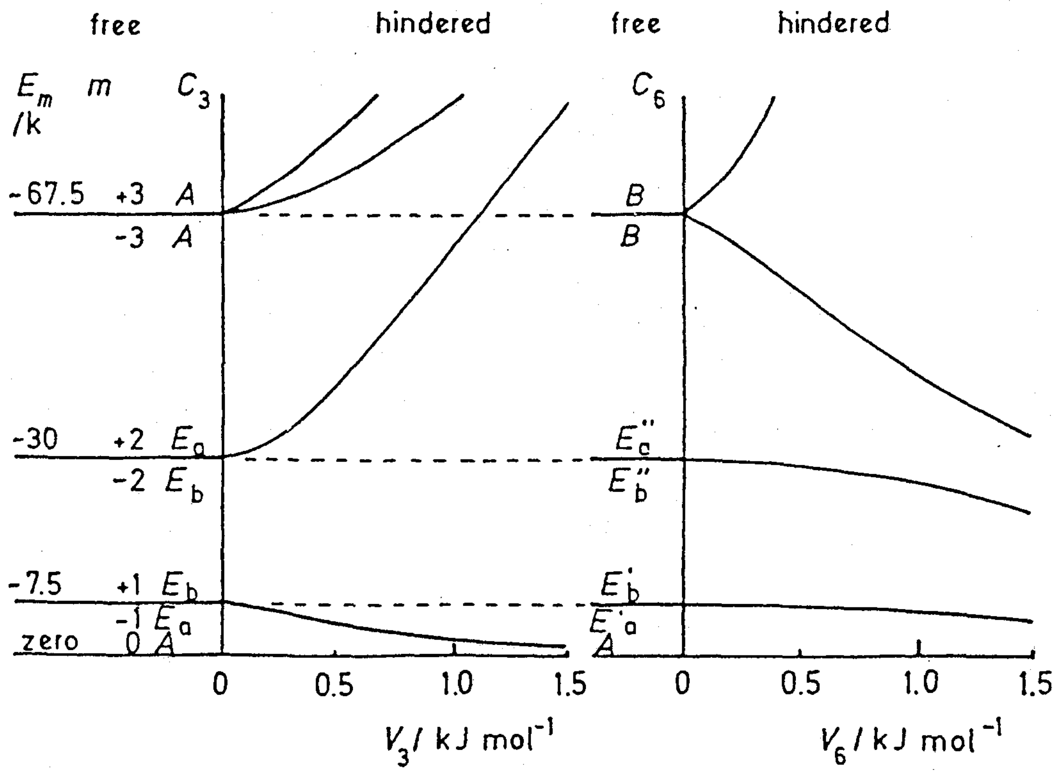

Classification of the free methyl rotor energy states under the symmetry groups C_3 and C_6. Also shown is how these states are perturbed in both cases by the growth of a hindering potential barrier. V_3 is the amplitude of a three-fold sinusoidal barrier whereas V_6 represents the amplitude of a six-fold sinusoid.

(after P.S. Allen)

Fig. 1

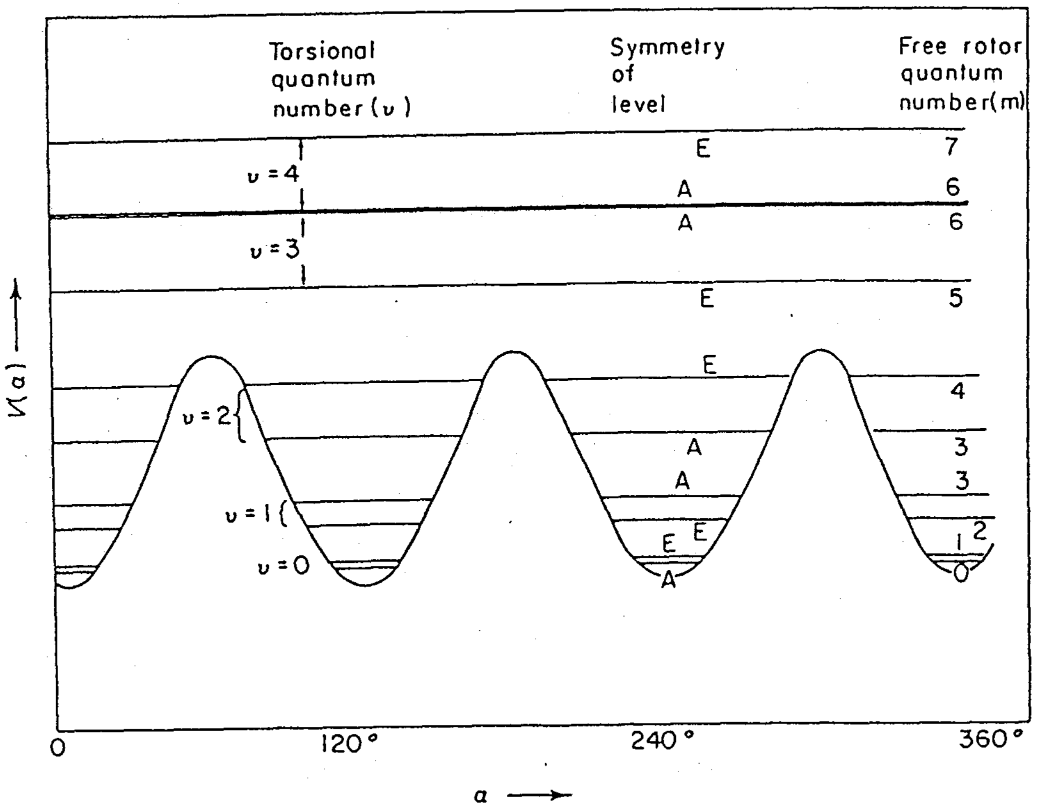

The potential function and torsional energy levels for a threefold symmetric rotor, showing the correlation between the hindered internal rotation quantum number (*v*) and the free internal rotation quantum number (*m*).

(Internal rotation and Inversion, 1978, D.G. Lister, et al.)

Fig. 2

1, 10-12). The eigen function can be described as follows,

$$\Phi_n^S = \frac{1}{\sqrt{2}} \sum_{m=-\infty}^{\infty} b_m^{nS} e^{i(3m + \ell^S)\theta} \tag{6}$$

where $\ell^S = 0$ for $S = A$, $\ell^S = 1$ for $S = E^a$, $\ell^S = 2$ for $S = E^b$ and b_m^{nS} are expansion coefficients,

$$\sum_{m=-\infty}^{\infty} |b_m^{nS}|^2 = 1 . \tag{7}$$

However, Φ_n^S belonging to the energy levels lying near the bottom of the potential well behave more or less as harmonic oscillator eigen fonctions. They can be expressed as follows[1,13)]

$$\Phi_n^S = \frac{1}{\sqrt{3}} \left\{ R_1^n(\theta) + \lambda R_2^n(\theta) + \lambda^* R_3^n(\theta) \right\} \tag{8}$$

where $\lambda = 1$, ε and ε^* ($\varepsilon = e^{2\pi i/3}$) for $S = A$, E^a and E^b respectively. $R_1^n(\theta)$, $R_2^n(\theta)$, and $R_3^n(\theta)$ are the normalized wave functions which describe that the methyl group is localized in the potential well 1, 2, and 3 respectively. $R_1^0(\theta)$, $R_2^0(\theta)$, and $R_3^0(\theta)$ denote the librational (torsional) ground state in the respective potential well and are shown schematically in Fig. 3. These potential wells 1, 2, and 3 correspond to the three orientations of a methyl group and these orientations are indistinguishable. The in-products $\langle R_1^n(\theta) | R_2^n(\theta) \rangle$, $\langle R_2^n(\theta) | R_3^n(\theta) \rangle$ and $\langle R_3^n(\theta) | R_1^n(\theta) \rangle$ are not completely zero due to a small overlap between the localized wave functions, which arises from the finite height of barrier. In the harmonic approximation which is valid for the high barrier and for the eigen states lying near the bottom of the potential well, the tunneling splitting Δ_n is described as[14)]

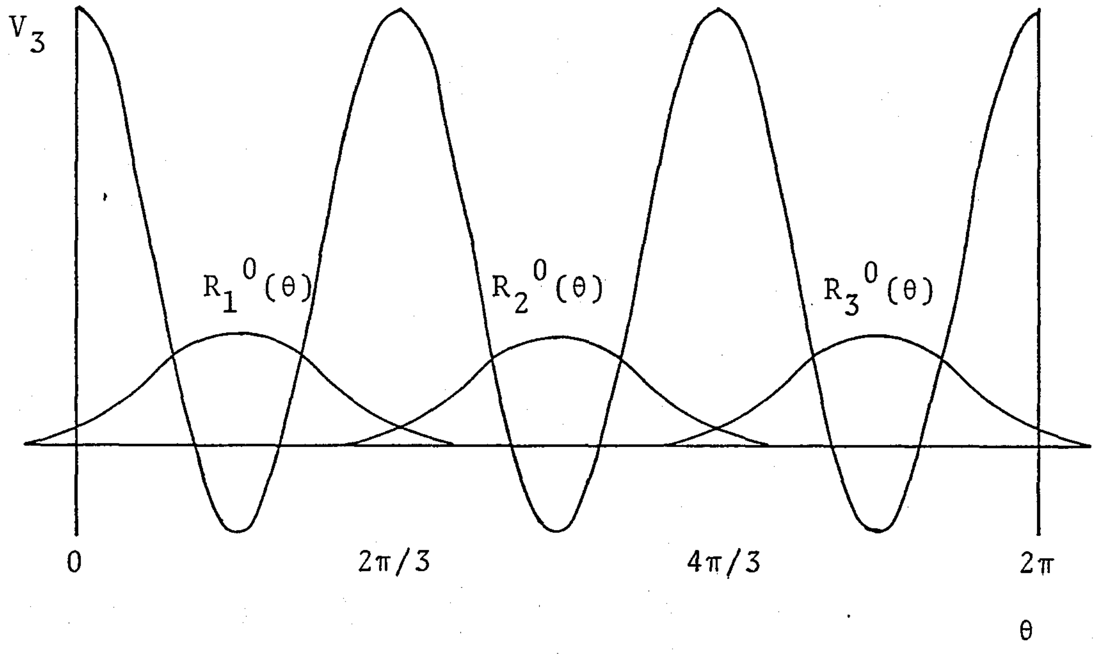

Fig. 3 Sketch of a three-fold potential and the three harmonic oscillator wave functions $R_1^0(\theta)$, $R_2^0(\theta)$, and $R_3^0(\theta)$.

$$\Delta_n = E_n^{E} - E_n^{A} = 3(D\ b - a), \qquad (9)$$

where

$$D_n = \langle R_1^n | H_R | R_1^n \rangle = \langle R_2^n | H_R | R_2^n \rangle = \langle R_3^n | H_R | R_3^n \rangle, \qquad (10)$$

$$a_n = \langle R_1^n | H_R | R_2^n \rangle = \langle R_2^n | H_R | R_3^n \rangle = \langle R_3^n | H_R | R_1^n \rangle << D \qquad (11)$$

and

$$b_n = \langle R_1^n | R_2^n \rangle = \langle R_2^n | R_3^n \rangle = \langle R_3^n | R_1^n \rangle << 1. \qquad (12)$$

The eigen function Φ_n^S (Eq. (6) or (8)) are the delocalized wave functions with which we can not visualize the "rotation" of a methyl group like in the case of classical treatment. Therefore, we will consider the rotation of a methyl group with the localized states $R_q^n(\theta)$ (q = 1, 2, and 3) for visualizing the jump- and tunneling-rotation of a methyl group in Section II. 1.4.

3) H_{RP}

H_{RP} includes the coordinate of a rotor and also that of a phonon$^{1,15)}$, which descdibes the coupling between a methyl rotor and phonon system (lattice vibration). H_{RP} induces the fluctuations of the potential barrier hindering the rotation of a methyl group due to lattice vibrations and the ensemble average of H_{RP} equals zero$^{15)}$. The height and also the phase of potential function fluctuate$^{15)}$. These fluctuations case the "non-magnetic transitions" among the various rotor levels$^{1,10)}$. Because the rotor states are coupled to the spin states by Pauli exclusion principle (see the expranation of the dipolar Hamiltonian), these transitions are therefore those between the rotor states of the same symmetry$^{1)}$ and the spin symmetry should not change by such transitions. The validity of this argument rests upon the rigidity of the rotor and the Born-Oppenheimer approximation$^{15)}$.

The main effects of the rotor-phonon coupling (H_{RP}) and therefore the main effects of "non-magnetic transitions" are two fold in the present consideration.

a) The fast non-magnetic transitions will establish the effective (thermal averaged) rotor system for each symmetry (A, E^a, E^b). By virtue of this situation, the temperature dependence of the observable tunneling frequency ω_t (not the same meaning as Δ_n) may be explained (see Section II. 2).

b) Because the dipole Hamiltonian H_D includes the coordinates of rotor system, the non-magnetic transitions modulates the dipole interaction (H_D), which cause the spin-lattice relaxation (see the discussion of H_D).

As described above, the effects of H_{RP} is very important for the dynamical behavior of the molecular groups in solid for the spin-lattice relaxation. However, to obtain the explicit expression for the H_{RP} is very difficult. Then the detailes of the H_{RP} is not considered but only the results of the effects H_{RP} are introduced in Section II. 1.4 and Section II. 2.

4) H_Z

H_z is the Zeeman Hamiltonian which is given by

$$H_z = -\hbar\omega_0 \sum_{n=0}^{3} I_{Zn} = -\hbar\omega_0\, I_Z \qquad (13)$$

This Hamiltonian represents the Zeeman coupling of the proton spins within a methyl group, I_{Z1}, I_{Z2}, and I_{Z3}, with the static magnetic field H_0 directed along the Z axis. $\omega_0 = \gamma H_0$, which is the Larmor frequency. γ is the proton gyromagnetic ratio. The spin states $\Psi_m^{S'}$ follow from the equation,

$$H_Z \Psi_m^{S'} = E_m^{S'} \Psi_m^{S'} \qquad (14)$$

with $E_m^S = - m \hbar\omega_0$. m is the Zeeman quantum number. The index S' represents A, E^a, or E^b and indicates that the spin states are expressed in term of the irreducible representations of the symmety group C_3 because the three spins within a methyl group are indistinguishable.

5) H_D

H_D represents the dipole interactions between the protons. When a methyl group undergoes the fast jump or tunneling rotation, H_D can be described by

$$H_D = \bar{H}_D^{intra} + H_D^{intra}(t) + \bar{H}_D^{inter} + H_D^{inter}(t), \qquad (15)$$

where "intra" or "inter" indicates whether the interacting protons belong to the same methyl group or to different groups. Both "intra" and "inter" interactions can be separated into the time-dependent part and the time-averaged part, the latter being indicated by a bar (—) in Eq. (15) The meaning and the role of these terms are as follows.

a) $\bar{H}_D^{intra}$

$\bar{H}_D^{intra}$ is considered as a small time-independent perturbation of H_Z and gives rise to a small static shift (d) of the Zeeman levels[16,17) (see Fig. 4). In the calculation of the magnetic transition probability, these shifts can be ignored.

b) $\bar{H}_D^{inter}$

$\bar{H}_D^{inter}$ containes the following two terms.

i) One is the term which causes the broadening of the Zeeman energy levels ($E_m^{S'}$ in Eq. (14)). The width of this broadning is indicated

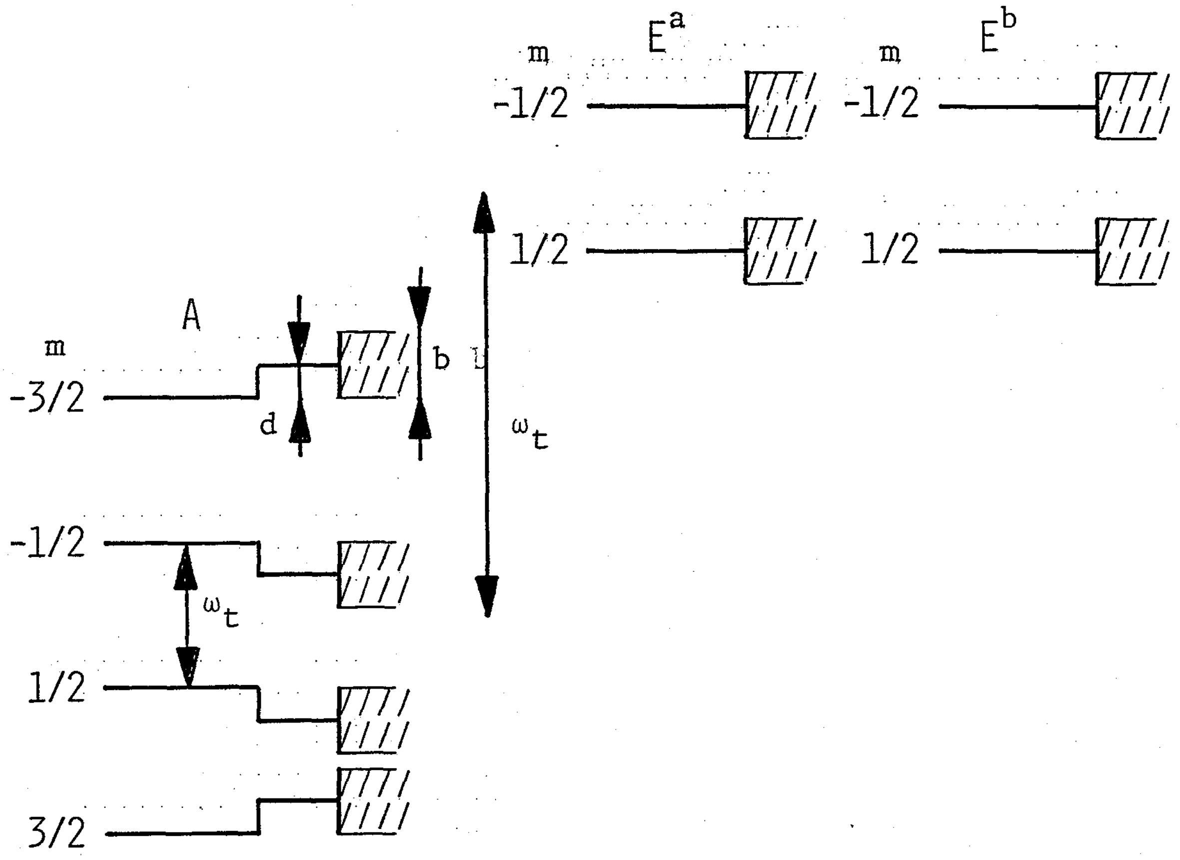

Fig. 4 The energy-level scheme of tunneling methyl groups. A, E^a, and E^b denote the symmetry of the eigen-states; m, magnetic quantum number; ω_0, Larmor frequency; ω_t, observable tunneling frequency; d, intramethyl dipolar shift; b, intermethyl broadning.

by b (in Fig. 4) which depends on the distance between a methyl proton and the surrownding protons,

ii) The other is the term which causes the spin diffusion process[18) between the spin states through so-called flip-flop transitions. This process may establish the internal thermal equilibrium among the spin states. Emid, et al.[16,17) have suggested that this flip-flop transition (spin diffusion) is restricted to between the different symmetry states. This means that we can not accept the traditional spin temperature theory (complete spin diffusion theory) indiscriminately. A more detailed discussion will be given in Section II. 1.3.

c) $H_D^{intra}(t)$

$H_D^{intra}(t)$ is randomly modulated by the motions of a methyl group and therefore causes the spin-lattice relaxation.

d) $H_D^{inter}(t)$

$H_D^{inter}(t)$ is also randomly modulated by the motion of a methyl group and contributes to the spin-lattice relaxation in a different manner from $H_D^{intra}(t)$[1,2,19). In the case of large tunneling splitting that $\omega_t >> \omega_0$, this relaxation mechanism is as impotant as H_D^{intra} (t)[19).

The intramethyl dipolar Hamiltonian H_D^{Intra} includes the spin and rotor operators, thereby describing the spin rotor coupling. The spin and rotor eigen states Ψ_m^S and Φ_n^S, respectively, can be classified according to $S = A$, E^a, and E^b. For a rigid rotor, the feasible operations are cyclic permutations. Therefoe, the Pauli exclusion principle requires that the product eigen functions $\Psi_m^S \Phi_n^S$ are of A symmetry[1,10-12). H_D^{intra} can be decomposed in a symmetry adapted form[1,12)

$$H_D^{intra} = \sum_S R(S)\, I(S), \quad S = A,\ E^a,\ E^b, \quad S \times S = A, \tag{16}$$

Where I(S) and R(S), respectively, contain spin and rotor operators.

II. 1.2 The transition probabilities between the eigen states.

An uncertainty of the rotor energy levels, which is caused by the rapid transitions due to H_{RP}, is taken into consideration. The transitions give rise to the fluctuation of H_D. The transition probability $W_{jj'}$ is given by [2,13)]

$$W_{jj'} = \frac{1}{\hbar^2} \int_{-\infty}^{\infty} \langle j | H_D^{intra}(t') | j' \rangle \langle j' | H_D^{intra}\ j \rangle \times \exp\left\{ i\omega_{jj'}(t' - t) \right\} d(t' - t), \tag{17}$$

with $\hbar\omega_{jj'} = E_{j'} - E_j$; j represents the eigen state $\Phi_n^S\ \Psi_m^{S'}$ (Section II. 1.1.5)). The correlation function is usually assumed to be an exponential function. In this case the transition probability becames

$$W_{jj'} = \frac{1}{\hbar^2} \overline{\left| \langle j | H_D^{intra} | j' \rangle \right|^2} \frac{\tau_c}{1 + \omega_{jj'}^2\ \tau_c^2} \tag{18}$$

where τ_c is the correation time of the dipole fluctuation.

The matrix element of $\langle j | H_D^{intra} | j' \rangle$ can be factorized (Eq.(16)),

$$\langle nm | R(S)\ I(S) | n'm' \rangle = \langle n | R(S) | n' \rangle \langle m | I(S) | m' \rangle . \tag{19}$$

The nonzero transition probability $W_{jj'}$ occurs when both matrix elements are nonzero.[2] $\langle n|R(S)|n'\rangle$ are all equal to δ which varies between 0 and 1. This vale depends on the shape and the hight of the potential barrier[1,2,4]. Therefore we can obatin some information about the potential function from δ[4]. The value δ^2, which is called the effective relaxation efficiency factor[4], was derived for a more general case in which not only the torsional ground state but also higher excited states are populated[4]. Johnson has derived this factor from a different starting point[21]. The factor δ^2 becomes unity in the limit of high barrier and about $\delta^2 \gtrsim 0.8$ for the methyl group which is hindered by the potential of $V_3 \gtrsim 4$ kJ mol^{-1} [21]. In this thesis we will consider the methyl group with $E_a = 5 \sim 8$ kJ mol^{-1} ($E_a = V(\theta) - E_0$). Therefore we assume that $\delta^2 = 1$. The non zero transition probabilities $W_{jj'}$ are listed in the literatures[1,20] for the case $\delta^2 = d_0^2$ [1] ($= |\langle n|R(S)|n'\rangle|^2$) or $\delta^2 = 1$[20]. The additional contributions occure when the intermethyl dipol interactions are taken into consideration. This provides the matrix elements of the same type as the intramethyl matrix elements. Furthermore the matrix elements between the states of the E^a and E^b symmetry also occur[2].

II.1.3 Symmetry restricted spin diffusion model by Emid, et al. and the behavior of the spin-lattice relaxation.

a) Relaxation equation.

The spin-lattice relaxation of an isolated methyl group which undergoes the fast jump- or tunneling-rotation (b = 0 in Fig. 4) is described by the transitions between the eight states with the transition probabilities $W_{jj'}$ (Eq. (19)). It is determined by the equation of motion.

$$\dot{\rho}_\alpha = - \sum_\beta W_{\alpha\beta} (\tilde{\rho}_\alpha - \tilde{\rho}_\beta), \tag{21}$$

where

$$\left.\begin{aligned} &\tilde{\rho} = \rho - \rho^{eq.}, \; \rho^{eq.} = 1 - \frac{\hbar}{kT_L}(-\omega_0 I_Z) \\ &\text{and} \\ &\rho_\alpha = \langle\alpha|\rho|\alpha\rangle \quad, \; W_{\alpha\beta} = W_{\beta\alpha}, \; \sum_\beta W_{\alpha\beta} = 0 \end{aligned}\right\} \tag{22}$$

where ρ_α is the diagonal part of the density matrix of the spin system, $\rho^{eq.}$ is its thermal equiliblium value, and T_L is the lattice temperature. α and β denote the eigen states (Fig. 4).

The eight-spin system has one constraint, i. e. the conservation of the number of particles (methyl groups) and therefore has the seven degrees of freedom. It thus is possible to express the occupation number operator ρ as a function of a complete set of seven mutually orthogonal, traceless, diagonal operators O_k and one unit operator[16,17].

$$\rho = 1 + \sum_{k=1}^{7} \alpha_k O_k$$

$$\mathrm{Tr}\, O_k = 0, \; \mathrm{Tr}\, O_k O_l = \delta_{kl}, \; \alpha_k = \mathrm{Tr}\, O_k \rho \tag{23}$$

where the high temperature approximation has been introduced, i.e. only the terms liner in α_k ~~have~~ been retained. The eigen values of the O_k's are given in Table 1. Two of them, denoted by O_1 and O_5, are physically of special interest, because they correspond to the "Zeeman system" and "dipolar system", respectively. Another two, denoted by O_4 and O_6, correspond to two other interesting systems, i.e. O_4 to the so-called "rotational polarization", being defind as

Table 1

		$A_{3/2}$	$A_{1/2}$	$A_{-1/2}$	$A_{-3/2}$	$E^{a}_{1/2}$	$E^{a}_{-1/2}$	$E^{b}_{1/2}$	$E^{b}_{-1/2}$
ZEEMAN	$\sqrt{6}\ O_1$	3/2	1/2	-1/2	-3/2	1/2	-1/2	1/2	-1/2
	$\sqrt{2}\ O_2$	1/2	-1/2	1/2	-1/2	-1/2	1/2	-1/2	1/2
	$\sqrt{3}\ O_3$	0	1	-1	0	-1/2	1/2	-1/2	1/2
ROT. POLA.	O_4	0	0	0	0	1/2	1/2	-1/2	-1/2
DIPOLE	O_5	1/2	-1/2	-1/2	1/2	0	0	0	0
TUNNEL	$\sqrt{2}\ O_6$	1/2	1/2	1/2	1/2	-1/2	-1/2	-1/2	-1/2
	O_7	0	0	0	0	1/2	-1/2	-1/2	1/2

The eigenvalues of the mutually orthogonal operators, $O_1, \cdots, O_7$, for the different spin eigen states.

the excess in population of E^a over E^b spin species and 0_6 to the "tunneling system", being defined as excess in population of A over the sum of E^a and E^b spin species. The remaing three operators 0_2, 0_3, and 0_7 have no simple physical meaning and are chosen in a manner which will prove to be most convenient for dicussing the effect of "spin- diffusion" on the spin-lattice relazation. Substituting equation(23) to equation (21) one obtains

$$\dot{\alpha} = - S (\alpha - \alpha^{eq.}), \tag{24}$$

where the colum-vector α has the components $\alpha_1, \cdots, \alpha_7$, each one of which has the equilibrium value $\alpha^{eq.}$; $\alpha_i^{eq.} = 0$ for $i = 2,3,4,7$ for $\omega_t = 0$ ($\alpha_6 = 0$ only for $\omega_t = 0$). The matrix S consists of the transition probanility $W_{jj'}$, and is listed in the literature[17)].
We note that the relaxation of the Zeenan system (see Table 1) which correspond to the recovery of the magnetization M_Z and is observed in the present measurements is dynamically coupled to other systems.

b) Spin diffusion.

Now,we consider the effects of spin diffusion due to $\bar{H}_D^{inter}$ on the spin-lattice ralaxation. The spin diffusion process, which is usually much faster than the spin-lattice relaxation in solids, should be taken into account.

If the three-spin systems (methyl group) are rigidly fixed in space, i.e. the "inter" part of the dipole interaction is time independent, each spin within a methyl group experiences a different local field from a neighbouring proton which is a single proton or one of the protons of other methyl groups. In this case, H_D^{inter} are of A, E^a, and E^b symmetry, and therefore A, E^a, and E^b spin states are mixed through spin diffusion (complete spin diffusion)$^{16)}$. In the time scale t, $b^{-1} \ll t \ll (\text{spin-lattice relaxation rate})^{-1}$, Eq. (23) becomes

$$\rho = 1 + {}_1 O_1 + {}_5 O_5 \tag{25}$$

This also the result of the traditional spin temperature theory$^{22,23)}$. The spin-lattice relaxations of α_1 and α_5 are mutually independent when the observable tunneling frequency ω_t is zero. α_1 and α_5 relax exponentially with the relaxation rates S_{11} and S_{55} in Eq. (24), respectively.

If, on the other hand, the methyl group is rapidly reorienting or tunneling (narrowing condition), H_D^{inter} can be divided into the time-averaged part and the fluctuation from it (Eq. (15)). Each of the three protons of a methyl group experiences the same averaged dipolar field from other protons. The averaged part $\overline{H}_D^{\text{inter}}$ which induces the flip-flop transitions is of A symmetry. We should note in this case that there are two restrictions for the spin diffusion process as follows.

i) Because $\overline{H}_D^{\text{inter}}$ is of A symmetry, the selection rule of the flip-flop transitions is described by

$$\langle S\ m \,|\, I_{\pm} \,|\, S'\ m' \rangle = C(S\ m,\ S'\ m')\ \delta_{m',m\pm 1}\ \delta_{S,S'}, \tag{26}$$

where S, S' = A, E^a, and E^b, C(S m, S' m') is a constant. The transitions between states of different symmetry is not possible in these systems.

ii) The other limitation is in terms of energy conservation. On condition that $b \ll 2|d|$ (see Fig. 4), which applies in spin-diluted solid, the energy levels become unequally spaced. The rapid spin diffusion occur only between the equally spaced levels (see Fig. 4) , because it satisfies the condition of energy conservation.

The spin diffusion process under the condition $b \gtrsim 2|d|$ and limitation i) in called "symmetry restricted spin diffusion" (S.R.S.D.). Under S.R.S.D. we have four degrees of freedom in the time domain t where $b^{-1} \ll t \ll T_1$ (spin-lattice relaxation time) and in this case Eq. (23) becomes

$$\rho = 1 + \alpha_1 O_1 + \alpha_4 O_4 + \alpha_5 O_5 + \alpha_6 O_6. \qquad (27)$$

The other systems in Eq. (23) relax as rapidly as spin diffusion takes place (at the rate b^{-1}).

The spin diffusion process with the limitations of i) and ii) is called "limited spin diffusion" process in this case Eq. (23) becomes

$$\rho = 1 + \alpha_1 O_1 + \alpha_2 O_2 + \alpha_4 O_4 + \alpha_5 O_5 + \alpha_6 O_6. \qquad (28)$$

For many cases of methyl groups in solid $b \gtrsim 2|d|$ will be satisfied and S.R.S.D. acceptable.

c) Relaxation behavior of Zeeman system.

In experiments we observe the time evolution of magnetization M_Z which corresponds to the Zeeman system. When the observable tunneling frequency (ω_t) is not zero, the Zeeman system is coupled to three other sytems (Eq. (27))$^{17)}$, i.e. dipolar system, rotational polarization system and tunneling system. However, when ω_t is zero, it is coupled only to the rotational polarization system[17]. The coupled relaxation equations for $\omega_t \neq 0$ for a powdered sample may be described by[24]

$$\frac{dZ}{dt} = - S_{ZZ}\,\tilde{Z} - S_{ZD}\,\tilde{D} - \sum_i S_{ZR}(\beta_i)\,\tilde{R}(\beta_i) - \sum_i S_{ZT}(\beta_i)\,\tilde{T}(\beta_i)$$

$$\frac{dD}{dt} = - S_{DZ}\,\tilde{Z} - S_{DD}\,\tilde{D} - \sum_i S_{DR}(\beta_i)\,\tilde{R}(\beta_i) - \sum_i S_{DT}(\beta_i)\,\tilde{T}(\beta_i)$$

$$\frac{dR(\beta_i)}{dt} = - S_{RZ}(\beta_i)\,\tilde{Z} - S_{RD}(\beta_i)\,\tilde{D} - S_{RR}(\beta_i)\,\tilde{R}(\beta_i) - S_{RT}(\beta_i)\,\tilde{T}(\beta_i)$$

(one equation for each orientation β_i)

$$\frac{dT(\beta_i)}{dt} = - S_{TZ}(\beta_i)\,\tilde{Z} - S_{TD}(\beta_i)\,\tilde{D} - S_{TR}(\beta_i)\,\tilde{R}(\beta_i) - S_{TT}(\beta_i)\,\tilde{T}(\beta_i)$$

(one equation for each orientation β_i). (29)

Z, D, $R(\beta_i)$, and $T(\beta_i)$ is the same meaning as α_1, α_5, α_4, and α_6, respectively. $\tilde{Z} = Z - Z^T$, $\tilde{D} = D - D^T$, $\tilde{R}(\alpha_i) = R(\alpha_i) - R(\alpha_i)^T$ and $\tilde{T}(\beta_i) = T(\beta_i) - T(\beta_i)^T$; the superscript T denotes the quantities at the thermal equilibrium. β_i describes the angle between the axis of methyl group and the static magnetic field. It is assumed that S.R.S.D. is effective throughout the sample. Then the Zeeman- and dipolar-spin-temperature are established over the whole sample, but not for α_4 and α_6 (see Eq. (26)). The powder averaging must be done with care since this is subject to the volume in which S.R.S.D. is effective[17,24]. The coupling terms (S_{ij} , $i \neq j$, in Eq. (29)) for the case of intramethyl relaxation are given in the reference (24). The Zeeman autorelaxation rate S_{ZZ} is described as

$$S_{ZZ} = \frac{9}{40} d^2 \left(J_{+1} + J_{-1} + 4J_{+2} + 4J_{-2} \right) \tag{30}$$

where

$$J_{\pm n} = J(\omega_t \pm n\omega_0), \; n = 1, 2, \qquad d^2 = \frac{\gamma^4 \hbar^2}{r^6},$$

and

$$J(\omega) = \tau_c/(1 + \omega^2\tau_c^2).$$

When ω_t equals zero, S_{ZZ} becomes the well known formula of B.P.P. function.

Because of the coupling, the Zeeman relaxation, after a perturbation is turned off, is generally described by the non-exponential recovery function and is dependent on the initial condition into which the firat 90° pulses bring the systems.[25] Such a behavior of Zeeman relaxation is different for different sets of conditions of τ_c, ω_t, and ω_0[26]. The experimental evidence and more detailed discussion will be given in Section VI.

II. 1.4 The meaning of the correlation time and the activation energy E_a for a reorienting or tunneling methyl group.

To explain the temperature dependence of the correlation time τ_c, a model which visualize the rotation of methyl group was proposed by Lightelm[4]. H_{RP} induces the non-magnetic transitions between the rotor levels having the same symmetry. He assumed that these transitions are described by the superposition of transitions between the states, Φ_0^S and Φ_n^S $(n > 0)$. The average time interval $\tau_c^S(0 \leftrightarrow n)$ that a methyl group remains in one of the three wells in relation to $0 \leftrightarrow n$ transition is described by

$$\tau_c{}^S(0\leftrightarrow n) = (\ \Delta\tau^S(0\ \ n) + \Delta\tau^S(n\ \ 0)\ )\ P_n{}^{-1} \tag{31}$$

and

$$\Delta\tau^S(0\ \ n) \simeq W_{0n}{}^{-1}\ ,\ \Delta\tau^S(n\ \ 0) \simeq W_{n0}{}^{-1}.$$

$\Delta\tau^S(0\ \ n)$ is the residence time between two excitations from $\Phi_0{}^S$ to $\Phi_n{}^S$ and $\Delta\tau^S(n\ \ 0)$ is the time interval that a methyl group remains in the state $\Phi_n{}^S$ after it has excited from the state $\Phi_0{}^S$. W_{0n} and W_{n0} are the transitition rate from $\Phi_0{}^S$ to $\Phi_n{}^S$ and vice versa, respectively. The ratio (W_{n0}/W_{0n}) is described as

$$\frac{W_{n0}}{W_{0n}} = \exp(E_n - E_0)/kT \tag{32}$$

If the transition takes place N times in a time interval, the rotation takes place N x P_n times from one well to another. For the states $\Phi_n{}^S$ $(n \gtrsim n')$, which lie above the top of the potential barrier, P_n is equal to unity. In the case of the potential barrier that assures the condition $\Delta\tau^S(n\ \ 0) \ll \Delta\tau^S(0\ \ n)$, the total averaged rotation frequency $(\tau_c{}^S)^{-1}$ from one well to another well is described by

$$\frac{1}{\tau_c{}^S} = \sum_{n=0}^{\infty} \tau_c{}^S(0\leftrightarrow n)^{-1} \approx \sum_{n=0}^{\infty} P_n/\ \tau^S(0\ \ n),$$

and therefore

$$\frac{1}{\tau_c{}^S} = \sum_{n=1}^{n'-1} W_{0n}{}^S\ P_n{}^S + \sum_{n=n'}^{\infty} W_{0n}{}^S. \tag{33}$$

where n' dwnotes the lowest state that lie avobe the top of the potential barrier. If one transition from $\Phi_0{}^S$ to $\Phi_n{}^S$ corresponds to once attacking the potential wall, P_n can be replaced by the transmission coefficient $T_n{}^S$ which describes the probability for a tunneling rotation to occur during the oscillation in the state Φ_n^S and only depends on the shape and height of the potential barrier. If W_{0n} is assumed to be described by

$$W_{0n}^S = a_n \exp\left\{- (E_n^S - E_0^S)/kT\right\}, \tag{34}$$

equation (33) becomes

$$\frac{1}{\tau_c^S} = \sum_{n=1}^{n'-1} a_n T_n^S \exp\left\{- (E_n^S - E_0^S)/kT\right\} + \sum_{n=n'}^{\infty} a_n \exp\left\{- (E_n^S - E_0^S)/kT\right\} \tag{35}$$

Assuming that the non-magnetic transitions within each symmetry are uncorrelated, equation (35) is applicable for $S = A, E$ (E^a and E^b). The correlation time in Eq. (19) is then described by

$$\tau_c^{-1} = (\tau_c^A)^{-1} + (\tau_c^E)^{-1}, \tag{36}$$

For the non-tunneling system, i.e. when $T_n^S = 0$ and $\tau_c^A = \tau_c^E$,

$$\frac{1}{\tau_c} = \sum_{n=n'}^{\infty} a_n \exp\left\{\frac{- (E_n^S - E_0^S)}{kT}\right\} \tag{37}$$

and the term of $n = n'$ in Eq. (37) makes the principal contribution to τ_c. Then the temperature dependence of τ_c becomes the well-known Arrhenius type

$$\tau_c^{-1} = a \exp\left\{- (V_0 - E_0)/kT\right\}, \tag{38}$$

where $V_0 - E_0 \simeq E_{n'} - E_0$.

At a sufficiently low temperature for the tunneling system ($T_n^S \neq 0$), i.e. if only the torsional ground and first excited states are populated, the activation energy is given by ($E_1 - E_0$). This result was also obtained by Wallach, et al.$^{27)}$ and Haupt$^{1)}$ in a different approach. Equation (35) described that the apparent activation energy becomes larger from $E_1 - E_0$ to $E_{n'} - E_0$ with increasing temperature.

II. 2 The temperature dependence of the observable tunneling frequency ω_t.

The tunneling splitting Δ_n (Eq. (9)) is determined by the potential barrier uniquely and Δ_n is not a function of temperature for an isolated methyl group. However, several experiments have demonstrated the decreasing tunneling frequency with increasing temperature$^{28-32)}$. The effort has been payed by several authors$^{17,33-37)}$ to explain this behavior by considering that the rotating molecular group in solid is coupled to lattice modes (phonon). Other mechanisms have also been proposed.$^{38,39)}$ However, the model of coupling to phonon is acceptable for many molecular groups in solid. The coupling effect was taken into account in two different ways as follows.

II. 2.1 The model of thermal averaging.

The rapid non-magnetic transitions due to H_{RP} establish the thermal equilibrium between the same symmetry rotor levels. The temperature T of the A symmetry-and E symmetry-system is the same as that of the phonon system. The free energy for M^S methyl groups with symetry S (S = A, E^a, or E^b) is described by[4)]

$$F^S = - kT \ln\{Z^S\}^{M^S} \tag{39}$$

Z^S is the partition function of a single methyl group and given by

$$Z^S = \sum_{n=0}^{\infty} \exp(- E_n{}^S/kT). \tag{40}$$

We consider the case that $M^A = M^{E^a} = M^{E^b} = M$. The averaged tunneling energy is

$$\hbar\omega_t = \frac{F^{E^a} - F^A}{M} = \frac{F^{E^b} - F^A}{M}$$

$$= - kT \ln \frac{\sum_{n=0}^{\infty} \exp(- E_n{}^E/kT)}{\sum_{n=0}^{\infty} \exp(- E_n{}^A/kT)} \tag{41}$$

Noting that the A-E sequence of the ground and excited torsional levels alternates, i.e. $E_n{}^E - E_n{}^A = (-1)^n \hbar\Delta_n$, and assuming $\hbar\Delta_n/kT \ll 1$ equation (41) becomes[17)]

$$\omega_t = \frac{\sum_{n=0}^{\infty} (-1)^n \Delta_n \exp(- E_n/kT)}{\sum_{n=0}^{\infty} \exp(- E_n/kT)} \tag{42}$$

where $E_n + \hbar\Delta_n = E_n{}^E$.

If only the ground and first excited states are populated, equation (42) becomes

$$\omega_t = \frac{\Delta_0 - \Delta_1 \exp(- E_1/kT)}{1 + \exp(- E_1/kT)} . \qquad (43)$$

Equation (43), which describes the temperature variation of the peak frequency, is equivalent to the results of Allen's model[33]. His model also express the width of the tunneling spectrum. However his model is based on the improbable concept that transition between $\Phi_0{}^E$ and $\Phi_n{}^E$ is completly correlated with that between $\Phi_0{}^A$ and $\Phi_n{}^A$. Therefore we accept the model of uncorrelated transition (Eq. (41) or Eq. (42)).

II. 2.2 A direct effect of coupling between methyl-rotor and the lattice modes.

Another mechanism of this coupling was proposed by Huller[37]. This effect may partially cancell the overlap of the wave functions and diminish the tunneling splitting $\hbar\Delta_n$ itself by successive excitation of the coupled lattice mode with increasing temperature. In the case of small coupling to a phonon in the Einstein mode, the temperature dependence of the tunneling splitting is described by

$$\Delta_0(\bar{n}) = \Delta_0(0) \; (1 - 2\bar{n} \, Q^2) \qquad (44)$$

where

$$\bar{n} = 1/(e^{\hbar\omega/kT} - 1).$$

$\bar{n}$ is the occupation number of the Einstein mode and ω is its frequency. Q is propotinal to the strength of the coupling. For the small coupling with Debye phonon, Δ_0 is

$$\Delta_0(T) = \Delta_0(0) \left\{ 1 - \frac{\pi^6}{45} g^2 \frac{\hbar\omega_D}{B} \left(\frac{kT}{\hbar\omega_D}\right)^4 \right\} , \qquad (45)$$

where B is the rotational constant of a methyl group, ω_D is the Debye cut off frequency and g is proportional to the strength of the coupling. This model due to Huller is not in contradiction to the model of thermal averaging. The main contribution to the temperature dependence of observable tunneling frequency is probably due to thermal averaging effect.

References

1) J. Haupt, Z. Naturforsch., 26a (1971) 1578.

2) W. Muller-Warmuth, R. Schuler, M. Prager, and A. Kollmar J. Chem. Phys., 69 (1978) 2382.

3) A.E. Zweers and H.B. Brom, Physica, 85B (1977) 223.

4) D.J. Ligthelm, Thesis (1981), Technische Hogeschool, Delft, The Netherlands.

5) P.S. Allen, Faraday Symposia Chem. Soc., No13 (1978) 133.

6) J.E. Wollrab, "Rotational Spectra and Moleculer Structure", (1967) Academic Press.

7) D. Smith, J. Chem. Phys., 72 (1980) 1408.

8) D. Smith, AIP document No. PAPS JCPSA-72-1408-19 pagrs of tables, Physics Auxiliary Publication Service, 335 East 45th Street, New york, N.Y. 10017.

9) Y. Numasawa, H. Kitaguchi, and T. Watanabe, J. Phys. Soc. Japan, 38 (1975) 1415.

10) J.H. Freed, J. Chem. Phys., 43 (1965) 1710.

11) P.S. Allen, J. Chem. Phys., 48 (1968) 3031.

12) F. Apaydin and S. Clough, J. Phys., C1 (1968) 932.

13) M. Punkkinen and S. Clough, J. Phys., C7 (1974) 3403.

14) A. Huller, Z. Physik, B36 (1980) 215.

15) S. Emid, Chem. Phys. Lett., 72 (1980) 189.

16) S. Emid, R.J. Baarda, J. Smidt, and R.A. Wind, Physica, 93B (1978) 327.

17) S. Emid and R.A. Wind, Chem. Phys. Lett., 33 (1975) 269.

18) A. Abragam, "The principles of Nuclear Magnetism", (1961) Oxford.

19) W. Muller-Warmuth, R. Schuler, M. Prager, and A. Kollmar, J. Mag. Reson., 34 (1979) 83,

20) M. Punkkinen, L.P. Ingman, D.G. Tatlor, and P.S. Allen, J. Phys., C8 (1975) 2159,

21) C.S. Johnson, Jr, J. Mag. Reson., 24 (1976) 63.

22) M. Goldman, "Spin Temperature and Nuclear Magnetic Resonance in Solids", Oxford Univ. Press., Oxford (1970).

23) J. Jeener, Advan. Magn. Reson., Vol.3 (1968) 205, Ed. by J.S. Waugh.

24) D.J. Ligthelm, R.A. Wind, and J. Smidt, Physica, 100 (1980) 175.

25) R.A. Wind, S. Emid, J.F.J.M. Pourquie, and J.Smidt, J. Chem. Phys., 67 (1977) 2436.

26) D.J. Ligthelm, R.A. Wind, and J. Smidt, Physica, 104 (1981) 397.

27) D. Wallach and W.A. Steele, J. Chem. Phys., 52 (1970) 2534.

28) M. Punkkinen, J.F. Tuohi, and E.E. Ylinen, Chem. Phys. Lett., 36 (1975) 393.

29) S. Clough, A. Heideman, and M. Paley, J. Phys., C14 (1981) 1001.

30) S. Clough and J.R. Hill, J. Phys., C7 (1974) L20.

31) C.S. Johnson, Jr, and C. Mottley, Chem. Phys. Lett., 22 (1973) 430.

32) M. Prager, W. Press, B. Alefeld, and A. Huller, J. Chem. Phys., 67 (1977) 5126.

33) P.S. Allen, J. Phys., C7 (1974) L22.

34) S. Clough, J. Phys., C9 (1976) L523.

35) I. Svare, J. Phys., C12 (1979) 3907.

36) S. Clough and A. Heideman, J. Phys., C12 (1979) 761.

37) A. Huller, Z. Physik, B36 (1980) 215.

38) M. Punkkinen, J. Phys., C11 (1978) 3039.

39) M. Punkkinen, Phys. Rev., B21 (1980) 54.

III The effect of coupling between some equivalent methyl groups on the rotor level scheme and on the spin-lattice relaxation.

In the case that two equivalent methyl groups are situated closely with each other, the hindering potential of a methyl group is affected by the orientation of the neigbouring methyl group. In this situation there is coupling between the two methyl groups and the rotations of these groups are not independent but mutually correlated. This is so-called "geared motion" of methyl groups in the classical sense. The rotation of these methyl groups should be described by the "nomal mode". These features are also the same in case of more than two methyl groups. This coupling effect will alter the energy scheme of the methyl rotor from that of a singl rotor (Section II.1.1), therefore the feature of the tunneling rotation will be different from that of a single methyl group.

In this Section we will consider the difference of the energy scheme between coupled methyl groups and a singl one and its effect to the spin-lattice relaxation. Furthermore, it will be considered whether we can get the evidence of the coupling both in the classical and quantummechanical sense by the N.M.R. methods.

III. 1 Energy scheme of two coupled methyl-rotor system.

The Hamiltonian of two-rotor molecules with the symmetry $C_{3v}(r)$ $-C_{2v}(f)-C_{3v}(r)$ is described by$^{1-5)}$

$$H = F(P_1^2 + P_2^2) + F'(P_1P_2 + P_2P_1) + V(\phi_1, \phi_2) \qquad (1)$$

where P_1 and P_2 are the angular momenta associated with two internal rotation angles ϕ_1 and ϕ_2 (see Fig. 1). r and f indicate the methyl rotor and the frame, respectively. And the coefficients F and F' are described by[4)]

$$
\begin{aligned}
F &= \hbar^2/(4I_{CH_3})(r_z^{-1} + r_x^{-1}) \\
F' &= \hbar^2/(4I_{CH_3})(r_z^{-1} + r_x^{-1}) \\
r_z &= 1 - 2\lambda_z^2 I_{CH_3}/I_z \\
r_x &= 1 - 2\lambda_x^2 I_{CH_3}/I_x
\end{aligned}
\qquad (2)
$$

λ_x and λ_z are the cosine of the angle between the axes of the internal rotors with the x and z axes. I_x and I_z are the moment of inertia of the molecule about the x and z axes. For the molecules which have sufficiently large moment of inertia (I_x and I_z) than that of methyl groups (I_{CH_3}), r_z and r_x become unity. In this case coupling term of the kinetic energy is zero, i.e. F' = 0. Therefore, the coupling between these two rotors is described by only the potential energy term $V(\phi_1,\phi_2)$ in Eq. (1). The potential function, in the most simple case, is described by[2,3)]

$$
\begin{aligned}
V(\phi_1,\phi_2) = {} & (V_3/2)(2 - \cos 3\phi_1 - \cos 3\phi_2) \\
& + V_{12}\cos 3\phi_1 \cos 3\phi_2 + V_{12}'\sin 3\phi_1 \sin 3\phi_2 .
\end{aligned}
\qquad (3)
$$

where $V_{12}\cos 3\phi_1 \cos 3\phi_2$ and $V_{12}'\sin 3\phi_1 \sin 3\phi_2$ are the coupling terms between the two rotors. In general, higher terms are included in Eq. (3)[1)]. Now we can introduce the symmetry coordinate,

$$
\alpha_1 = (\phi_1 + \phi_2)/2, \quad \alpha_2 = (\phi_1 - \phi_2)/2 \qquad (4)
$$

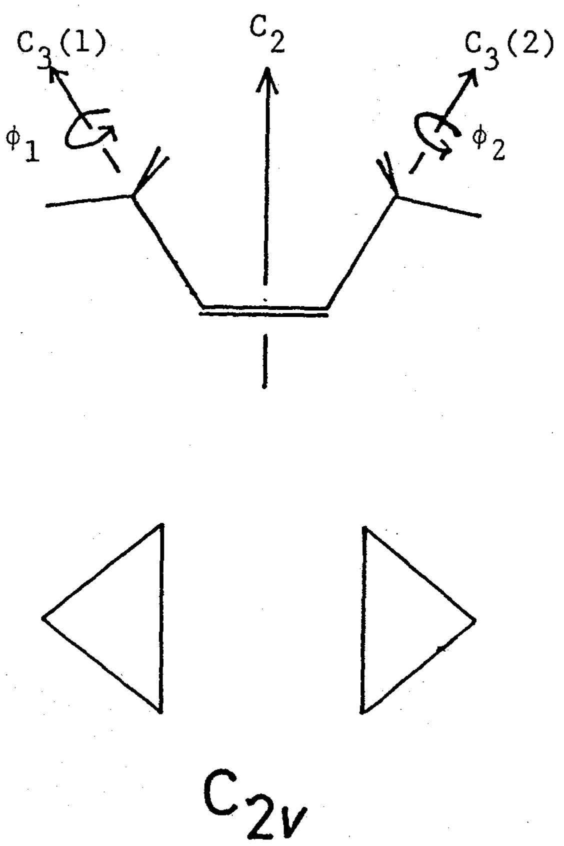

Fig. 1 Sketch of two-rotor system with C_{2v} symmetry. $C_3(1)$ and $C_3(2)$ indicate the symmetry axes of the methyl groups (1) and (2). ϕ_1 and ϕ_2 indicate the rotation angles of the methyl groups.

The coordinate α_1 is symmetrical and α_2 is antisymmetrical with C_2 operation. By substituting Eq. (4) to Eq. (3), we obtain

$$\begin{aligned} V(\phi_1,\phi_2) &= V(\alpha_1,\alpha_2) \\ &= V_3(1 - \cos3\alpha_1 \cos3\alpha_2) + V_{12}\cos6\alpha_2 \end{aligned} \tag{5}$$

for $V_{12} = V_{12}'$. Ofcause the situation that $V_{12} = V_{12}'$ is the assumption. In this case the difference between the symmetric mode α_1 and antisymmetric mode α_2 is clearly described. The first term in right hand side of Eq. (5) is equivalent for the α_1 and α_2 modes but the second term which is the coupling term is inequivalent. This coupling term, in which V_{12} is the strength of the coupling, causes the energy difference between α_1 and α_2 modes (see Fig. 2). The schematic view of the potential surface of the two coupled totors is shown in Fig. 3. The vertical section along the line indicated by ϕ_1 or ϕ_2 show the V_3 potential curve (similar to Fig. 3 in Section II). The section of α_1 is differ from the section of α_2 due to the coupling term in Eq. (5).

III. 2 Energy scheme of four coupled methyl groups with T_d symmetry.

The energy scheme of the torsional levels for the four coupled methyl rotors with T_d symmetry$^{6)}$ is shown in Fig. 4. The torsional first excited state splits due to the coupling between the methyl groups into two sublevels which are of A_2 and F_1 (T_1) symmetry. The degeneracies of A_2 and F_1 states are 1 and 3, respectively.

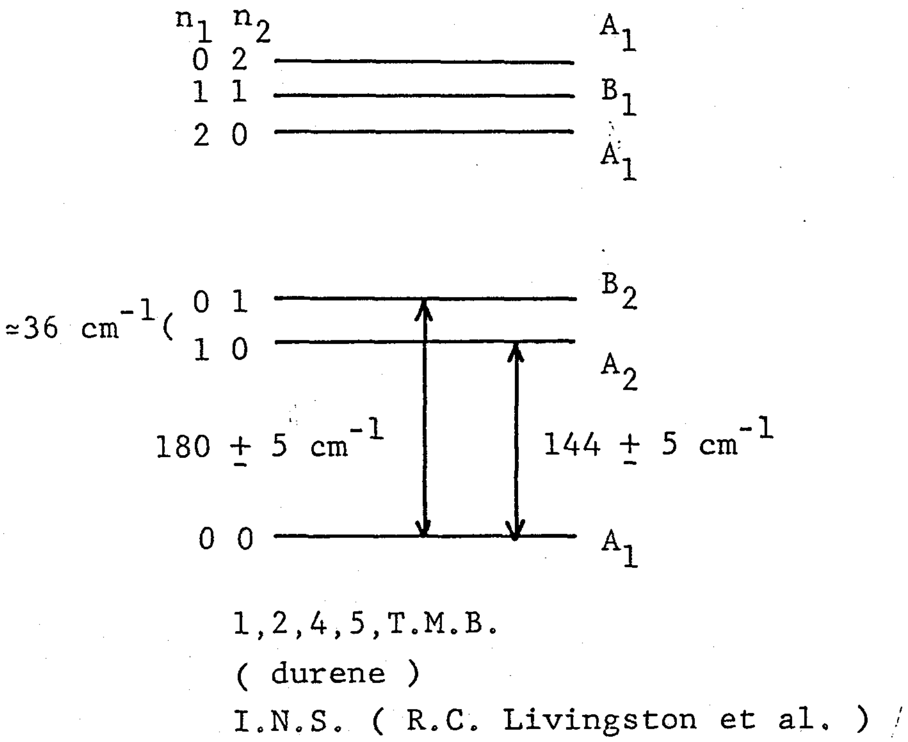

Fig. 2 The torsional energy scheme of 1,2,4,5-tetramethylbenzene (durene). n_1 and n_2 are the torsional quantum numbers of the methyl groups and $n_1 + n_2$ is the quantum number of the two-rotor system. A_1, A_2, B_1, and B_2 are the irreducible representations. The torsional energies indicated by arrows are determined by inelastic neutron scattering experiment$^{3)}$.

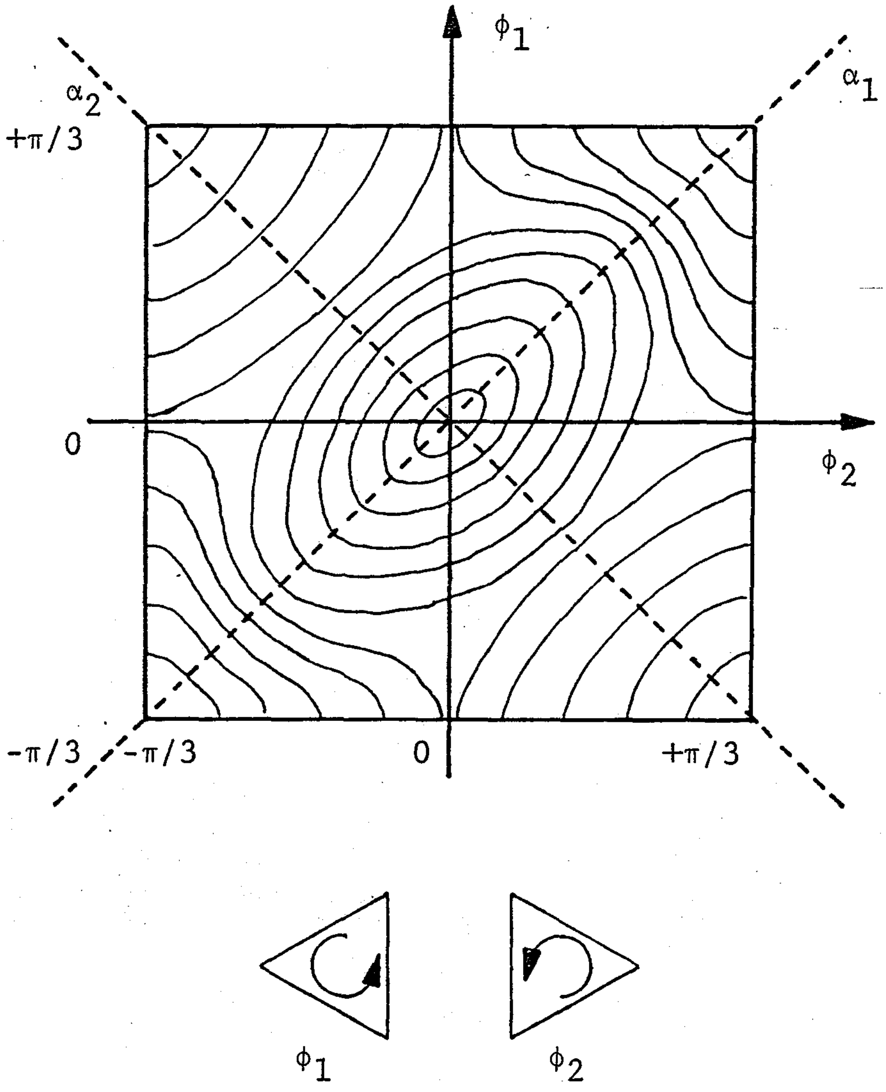

Fig. 3 Schematic view of the potential surface of two coupled methyl groups. The center of the square is a bottom of the potential and four vertexes are the tops of the potential.

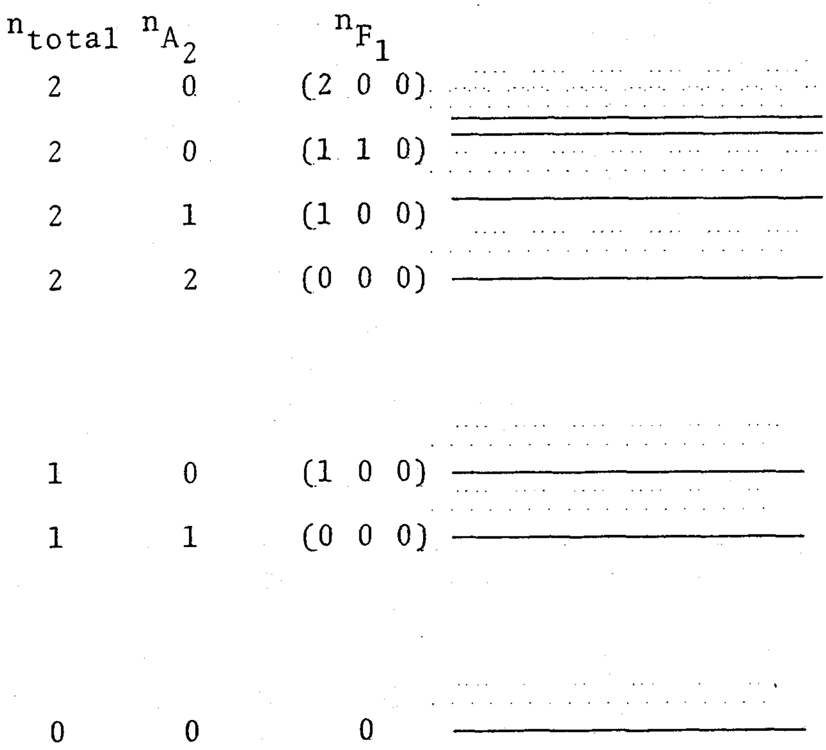

Fig. 4 Torsional energy scheme of four methyl groups with T_d symmetry. n_{total}, n_{A_2}, and n_{F_1} are the librational quantum number. The first excited state split into two sublevels with different symmetries. (after D.M. Grant, et al.)

The rotation angles ϕ_i (i = 1,2,3,and 4) of the methyl groups are symmetrized under T_d symmetry[7)]

$$\begin{aligned}\alpha_1 &= (\phi_1 + \phi_2 + \phi_3 + \phi_4)/2\\ \alpha_2 &= (3\phi_1 - \phi_2 - \phi_3 - \phi_4)/\ 12\\ \alpha_3 &= (2\phi_2 - \phi_3 - \phi_4)/\ 6\\ \alpha_4 &= (\phi_3 - \phi_4)/\ 2. \end{aligned} \qquad (6)$$

The kinetic energy is

$$2T = 3P^2/I + p_1{}^2/\ I_A + (p_2{}^2 + p_3{}^2 + p_4{}^2)/I_F. \qquad (7)$$

Here I is the moment of inertia of the spherical molecule with overall angular momentum P, and p_i is the momentum conjugated to the ϕ_i. In the assumption that the coupling between internal and overall rotation can be neglected[7)], the moment of intertia I_A and I_F equal I_{CH_3}. The potential of internal rotation can be expressed as

$$\begin{aligned}2V = V_0 &- V_1 \sum_i \cos3\phi_i - V_2 \sum_{i\ j} \cos3\phi_i \cos3\phi_j\\ &- V_3 \sum_{i\neq j\neq k} \cos3\phi_i \cos3\phi_j \cos3\phi_k - V_4 \sum_i \cos3\phi_i\\ &+ V_5 \sum_{i\ j} \sin3\phi_i \sin3\phi_j + V_6 \sum_i \sin3\phi_i\\ &+ V_7 \sum_{i\neq j\neq k} \cos3\phi_i \sin3\phi_j \sin3\phi_k\\ &+ V_8 \sum_{i\neq j\neq k\neq l} \cos3\phi_i \cos3\phi_j \sin3\phi_k \sin3\phi_l \end{aligned} \qquad (8)$$

The cross terms in Eq. (8) express the coupling effects between the four methyl groups. To visualize which term is impotant for splitting of the torsional first excited state due to coupling, we can use the harmonic approximation. Then the potential energy equation becomes

$$2V = K \sum_{i} \phi_i^{2} + 2L \sum_{i\,j} \phi_i \phi_j \qquad (9)$$

where

$$K = (9/2)(V_1 + 3V_2 + 3V_3 + V_4), \quad L = (9/2)(V_5 + 3V_7 + V_7).$$

Symmetrization of this expression gives

$$2V = (K + 3L)\alpha_1^{2} + (K-L)(\alpha_2^{2} + \alpha_3^{2} + \alpha_4^{2}).$$

The frequencies are given by

$$\nu_{A_2} = [2G_{A_2}(K + 3L)]^{1/2}, \quad \nu_{F_1} = [2G_{F_1}(K - L)]^{1/2}$$

where $G_{A_2} = \hbar^2/2I_{A_2}$ and $G_{F_1} = \hbar^2/2I_{F_1}$, which are approximated by $\hbar^2/2I_{CH_3}$.

Further splittings of torsional ground and excited states due to tunneling effect have not been studied.

III. 3 Energy scheme of six coupled methyl groups with D_{3d} symmetry.

We consider the case of hexamethylbenzene, which has six methyl groups with D_{3d} symmetry[8)]. The splittings of the torsional first excited state due to the coupling effect are shown in Fig. 5. The

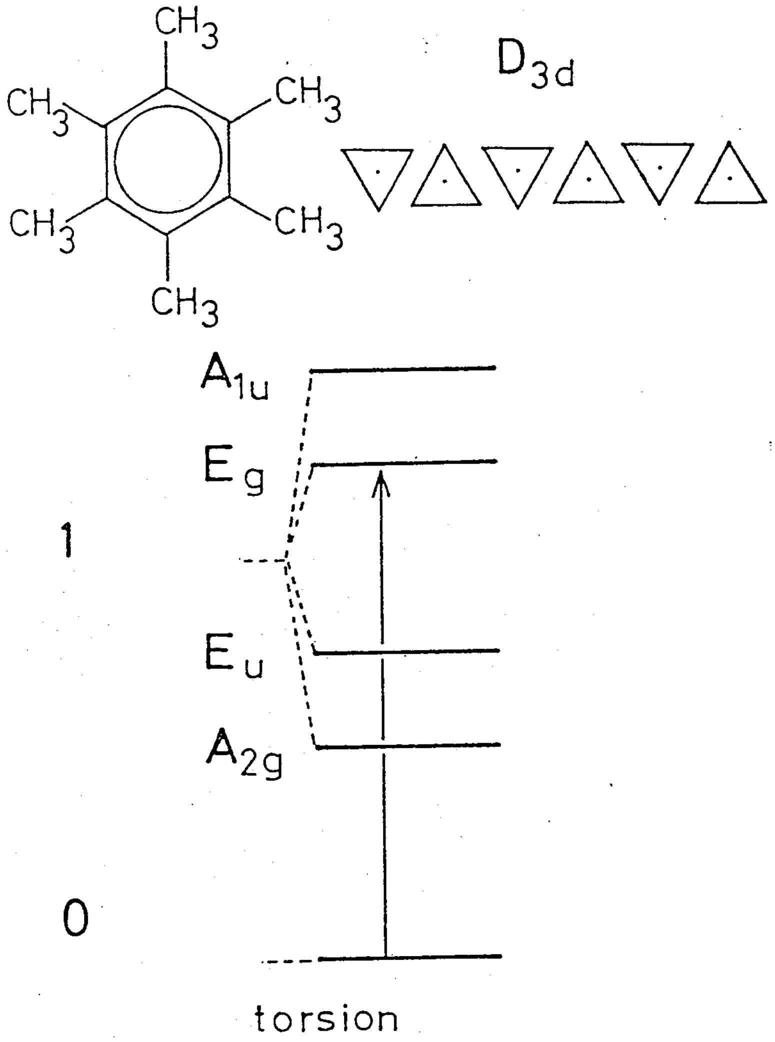

Fig. 5 Torsional energy scheme of six methyl groups with D_{3d} symmetry (hexamethylbenzene). The first excited dtate splits into four sublevels with different symmetries, A_{2g}, E_u, E_g, and A_{1u}. The transition indicated by arrow was observed by Raman sca scattering experiment to be 170 cm^{-1} at 20 K.

torsional first excited state splits into the four sublevels of different symmetries, A_{2g}, E_u, E_g, and A_{1u}.

III. 4 The effect of correlated motion (coupling) of two methyl groups on the spin-lattice relaxation rate in the classical limit.

An attempt will be made to develop the effect of correlated motion of two equivalent methyl groups. It will be assumed that the spin-system can be described classically for non-tunneling system. In general "cross correlation" of different dipole-dipole interaction should be taken into account for treating a methyl group correctly [13.14]. However, as will be discussed in the next Subsection III.4.1, we can safely use the pairwise additivity of the magnetic dipole dipole interactions without concideration of "cross correlation" for describing the autorelaxation rate of Zeeman system (S_{ZZ} in Eq. (29) in Section II.1.3) of non-tunneling methyl group[20].

III. 4.1 Method.

It has been discussed by Hilt and Hubbard (H.H.)[13] and Runnels (R.)[14] that the "cross correlation" of different dipole-dipole interactions are to be taken into account for describing the spin-lattice relaxation of a methyl group correctry. The relaxation equation of the Zeeman system (longitudinal magnetization, y_4 by H.H.) is generally described by four exponential functions and if "cross correlations" are ignored, it is described by a single exponential function. In order to make the physical background of this relaxation behavior more transparent, Mehring and Raber (M.R.)[15] presented a simple explanation on the basis of transitions among the energy levels of the three-spin system. H.H. and M.R. discussed the same problem from different starting points but their results were the same. Indeed the non-exponential relaxation equation obtained by M.R. is the same as that obtained by H.H.[15)] for a special case of $\beta = 0$, where β is an angle between the C_3 symmetry axis of a methyl group and the direction of external magnetic field. H.H. and R. showed that the "cross correlation" is important for describing the methyl group correctly in the classical manner. However, the theory by H.H. and slso the theory by M.R. was not complete for a methyl group in solid because they ignored the "spin-diffusion" process which plays an impotant role for spin relaxation in solids. Emid, et al. have further discussed the relaxation behavior of a methyl group in solid in the framework of symmetry restricted spin diffusion (S.R.S.D.) theory[16)]. If we omit the "spin diffusion" process, the relaxation of the Zeeman system (longitudinal magnetization, O_1) becomes coupled to three other degrees of freedom (O_2, O_3, and O_4) and is described by four exponential functions for a non-tunneling methyl group ($\omega_t = 0$)[16)]. When we compare the two theories of which one is based on the semiclassical treatment (H.H.) and the other is based on the quantum-mechanical treatment (M.R. and Emid, et al.), it is clear that the inclusion of the "cross correlation" is to couple the Zeeman system (y_4 by H.H.) to the other three degrees of freedom.

For a satisfactory treatment of the spin-lattice relaxation in solid state, we must take the "spin diffusion" into consideration. If we do so we can neglect the two degrees of freedom, i.e. O_2 and O_3, in the time domain of t, where (spin diffusion rate)$^{-1}$ << t << (spin-lattice relaxation rate)$^{-1}$ [16)]. This situation may be realized in the S.R.S.D. model as discussed by Emid, et al.[16)] in the following way. Under S.R.S.D. the Zeeman system is only coupled to the rotational polarization system and the relaxation of the Zeeman system is generally described by two exponential functions.

Further decoupling of the Zeeman system from the rotational polarization system is possible in one of the two ways. One is to rotate the sample about an axis perpendicular to the H_0 field with an angular velocity at least about three times larger than T_1^{-1} 17). The other is through the condition that the autorelaxation rate of the rotational polarization system is much faster than that of the Zeeman system, the condition that can be satisfied when $\omega_0\tau_c >> 1$18). Under such conditions, the magnetization recovery becomes single exponential and is independent on the pulse sequence applied. The observable time constant is the autorelaxation rate of the Zeeman system (S_{ZZ}). Such a behavior of relaxation is not in conflict with the S.R.S.D. theory but represents a special case of the S.R.S.D. model. Once the Zeeman system is decoupled from the rest, we can adopt the pairwise additivity omitting "cross correlation", and the traditional spin-temperature theory is applicable to the spin-lattice ralaxation rate (S_{ZZ}).

Even when the Zeeman system couples to the other system O_4 (rotational polarization system), we can obtain the autorelaxation rate of the Zeeman system(S_{ZZ}) as the time constant of the fast recovering component of magnetization19,20), which can be obtained by the pulse sequence B (see in Section V. 2).

The formalism which we will apply to the present problem is based on an equation of motion of stocastic probability which governs the jumping rate of a proton-proton vector (p-p vector) among several allowed orientations. The stochastic jumping of the p-p vector induce the spin-lattice relaxation. The formulation of the correlation function is based on the matrix formarism.[20-23)].

The total relaxation rate T_1^{-1} consists of sum of the intramethyl relaxation rate T_1^{-1}(intra) and the intermethyl relaxation rate T_1^{-1}(inter).

$$T_1^{-1} = T_1^{-1}(\text{intra}) + T_1^{-1}(\text{inter}) \tag{10}$$

The intramethyl and intermethyl relaxation rates are due to the dipole-dipole interactions within a methyl group and between the two methyl groups, respectively.

III. 4.2 Intramethyl relaxation rate, T_1^{-1}(intra).

We consider a molecule which contains the two equivalent methyl groups. The type of the motion (elementary process of the motion) in consideration is only the reorientation of a methyl group with the jumping rate ω_3 about its there fold symmetry axis.

T_1^{-1}(intra) is described as

$$T_1^{-1}(\text{intra}) = 2 \times \frac{9}{40} \frac{\gamma^4 \hbar^2}{r^6} B(\lambda, \omega) \tag{11}$$

where

$$\lambda = 3\,\omega_3 \quad , \quad B(\lambda, \omega) = \frac{\lambda}{\lambda^2 + \omega^2} + \frac{4\lambda}{\lambda^2 + 4\omega^2} \tag{12}$$

This equation represents the autorelaxation rate of Zeeman system (S_{ZZ}; Section II.1.3) for classical reorientation of a metyl group.

T_1^{-1}(intra) depends only on the dipole-dipole interaction within a methyl group, therefore this value is of the problem about a single methyl group in principle. T_1^{-1}(intra) does not depend on whether the reorientation of two methyl groups are completly correlated or completly indipendent.

III. 4.3 Intermethyl relaxation rate, T_1^{-1}(inter).

To calculate the intermethyl relaxation rate T_1^{-1}(inter), we need to write down the transition matrix D which describes the jumping of the intermethyl p-p vectors (internuclear vectors).11,12,20,21) A p-p vector may jump among the nine orientations (see Fig.6).

i) In the case that two methyl groups reorient independently with the jumping rate of ω_3 .

The transition matrix D is given by

$$D = \omega_3 \begin{bmatrix} A & 1(3) & 1(3) \\ 1(3) & A & 1(3) \\ 1(3) & 1(3) & A \end{bmatrix} , \qquad (13)$$

where 1(3) denotes the unit matrix in three demension and A represents

$$A = \begin{bmatrix} -4 & 1 & 1 \\ 1 & -4 & 1 \\ 1 & 1 & -4 \end{bmatrix} , \qquad (14)$$

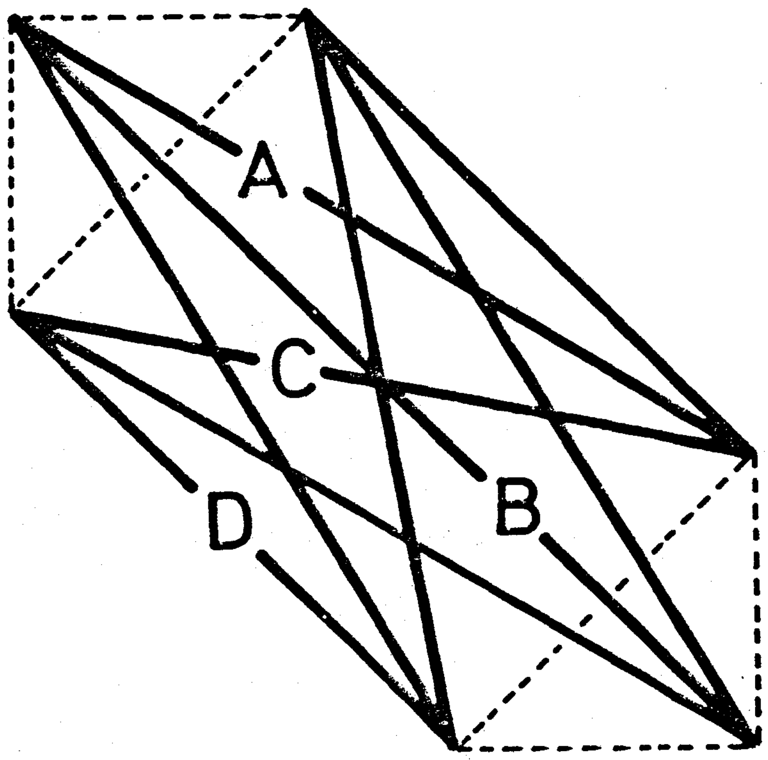

Fig. 6 The orientations or the sites of intermethyl p-p vector which are classified in four different length A, B, C, and D. The triangles shown by broken line indicate the methyl groups.

Matrix D is diagonalized by the direct product of matrix T, where

$$T = (1/\sqrt{3}) \begin{pmatrix} 1 & 1 & 1 \\ 1 & \varepsilon & \varepsilon^* \\ 1 & \varepsilon^* & \varepsilon \end{pmatrix} , \quad \varepsilon = \exp(2\pi i/3) \qquad (15)$$

i.e. $DU = U\Lambda$, $U = T \times T$.

Λ is the diagonal matrix with the element λ_i, where λ_i is

$$\begin{aligned} \lambda_1 &= 0 \\ \lambda_2 = \lambda_3 = \lambda_4 = \lambda_7 &= 3\omega_3 = \Lambda(3) \\ \lambda_5 = \lambda_6 = \lambda_8 = \lambda_9 &= 6\omega_3 = \Lambda(6) \end{aligned} \qquad (16)$$

T^{-1}(inter) is described as

$$T_1^{-1}(\text{inter}) = 3 \times \frac{9}{4} \gamma^4 \hbar^2 \quad (K_2 + K_3 + K_4 + K_7)\, B(\tau_c(3),\ \omega) + (K_5 + K_6 + K_8 + K_9)\, B(\tau_c(6),\ \omega) \ , \qquad (17)$$

where

$$\tau_c(3) = \Lambda(3)^{-1}, \quad \tau_c(6) = \Lambda(6)^{-1}$$

and

$$B(\tau_c\ ,\ \omega) = \frac{\tau_c}{1+\tau_c^2\ \omega^2} + \frac{4\tau_c}{1 + 4\tau_c^2\ \omega^2} \ .$$

K_i $(i = 2,\cdots,9)$ is the coefficient which only depends on the structure of the two-mehtyl system. For the special case of ethane molecul, the coefficients of T_1^{-1}(inter) in Eq. (17) are in complete agreement with the results by Woessner[9,10].

ii) In the case that the reorientation of two methyl groups are completely correlated.

The correlated reorientations of two methyl groups are classified into two different natures which are symmetric and antisymmetric reorientations with respect to the C_2 operation (see Section III. 1). The transition matrix D for the "symmetric" reorientation is given by

$$D_s = \omega_3 \begin{pmatrix} 2\ 1(3) & B & A \\ A & 2\ 1(3) & B \\ B & A & 2\ 1(3) \end{pmatrix} \qquad (18)$$

where

$$A = \begin{pmatrix} 0 & 0 & 1 \\ 1 & 0 & 0 \\ 0 & 1 & 0 \end{pmatrix} , \quad B = \tilde{A} = \begin{pmatrix} 0 & 1 & 0 \\ 0 & 0 & 1 \\ 1 & 0 & 0 \end{pmatrix} .$$

The transition matrix D for the "antisymmetric" reorientation is given by

$$D_a = \tilde{D}_s = \omega_3 \begin{pmatrix} 2\ 1(3) & A & B \\ B & 2\ 1(3) & A \\ A & B & 2\ 1(3) \end{pmatrix} \qquad (19)$$

where matrices A and B are the same as those in Eq. (18). Both D_s and D_a are diagonalized by matrix U in Eq. (16). The eigen values λ_i's are

$$\begin{aligned} \lambda_1 &= \lambda_6 = \lambda_8 = 0 \\ \lambda_2 &= \lambda_3 = \lambda_4 = \lambda_5 = \lambda_7 = \lambda_9 = 3\omega_3 \end{aligned} \qquad (20)$$

for the "symmetric" reorientation, and

$$\lambda_1 = \lambda_5 = \lambda_9 = 0$$
$$\lambda_2 = \lambda_3 = \lambda_4 = \lambda_6 = \lambda_7 = \lambda_8 = 3\omega_3 \qquad (21)$$

for the "antisymmetric" reorientation. T_1^{-1}(inter) is described as

$$T_1^{-1}(\text{inter, s}) = 3 \times \frac{9}{4}\gamma^4 \hbar^2 \Big\{(K_2 + K_3 + K_4 + K_5 + K_7 + K_9)\Big\} B(\tau_c(3),\omega\ ) \qquad (22)$$

for "symmetric" reorientation, and

$$T_1^{-1}(\text{inter, a}) = 3 \times \frac{9}{4}\gamma^4 \hbar^2 \Big\{(K_2 + K_3 + K_4 + K_6 + K_7 + K_8)\Big\} B(\tau_c(3),\omega\ ) \qquad (23)$$

for "antisymmetric" reorientation.

The calculation of the coefficient K_i was done numerically for the case of tetramethylpyrazine molecule. The bond distances, 1.38 Å, 1.51 Å, and 1.10 Å were used, respectively, for C=C. C-C$\Big\langle$, and C-H. The tetrahedral angle was assumed for a methyl group and an equilateral hexagon was assumed for the pyrazine ring. The coefficients $K_2 + K_3 + K_4 + K_7$ and $K_5 + K_6 + K_8 + K_9$ in Eq. (17) are 1.074×10^{-5} Å^{-6} and 2.335×10^{-6} Å^{-6} respectively. $K_2 + K_3 + K_4 + K_5 + K_7 + K_9$ in Eq. (22) and $K_2 + K_3 + K_4 + K_6 + K_7 + K_8$ in Eq. (23) are 1.271×10^{-5} Å^{-6} and 1.099×10^{-5} Å^{-6}, respectively. The differencies of Eqs. (17), (22), and (23) are shown in Fig. 7, where the activation process is assumed for ω_3 [22]. The difference between the independent reorientation and correlated reorientation appears in the low temperaturr branch of T_1^{-1}(inter) curve and in the efficiency of T_1^{-1}(inter). However, because the contribution

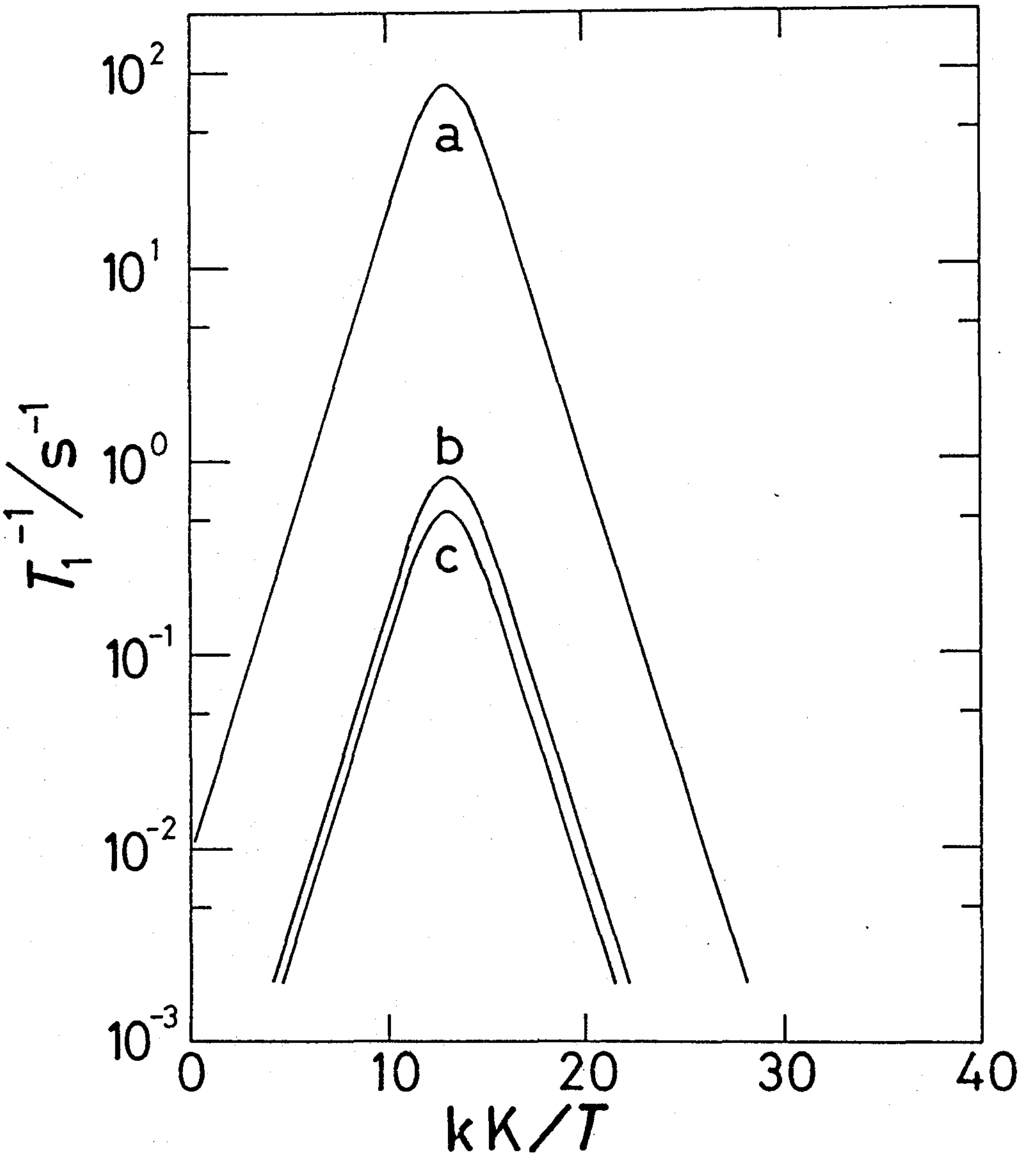

Fig. 7 The calculated spin-lattice relaxation rate. The activation process (Eq. (11) in Section VI. 3) was used. The curve a indicates the T_1^{-1}(intra) calculated with Eq. (11). The curves b and c show the T_1^{-1}(inter), b corresponds to the completely independent reorientation (Eq. (17)), c corresponds to the completely correlated "symmetric" reorientation (Eq. (22)). T_1^{-1}(inter) curve for "antisymmetric" reorientation is not shown. It nearly falls on the curve c.

of T_1^{-1}(inter) is rather smaller than T_1^{-1}(intra), it is difficult for us to determine whether the correlated reorientation or independent reorientation takes place from the observed T_1^{-1} value. The useful experiment for this purpose is to measure the spin-lattice relaxation rate of the partially deuterated material, i.e. two protons in a methyl group is replaced by deuteron and furthermore it is diluted by the copletely deuterated one. In this case the obsevable relaxation rate is only due to the intermethyl dipole interaction and relaxation equations (17), (22), and (23) must be divided by the facter of 3.

III. 5. The effect of coupling on the spin-lattice relaxation rate in the tunneling system.

In Section III. 4, we discussed the coupling effect (correlated reorientation) on the spin-lattice relaxation rate in the classical limit. The classical treatment dose not contain the term of torsional energy of the rotor system. The energy term is included only as the activation energy (see the reference 22 in this Section). On the other hand, the torsional energy scheme is included in the equation of the spin-lattice relaxation in the framework of the quantum-mechanical treatment of tunneling methyl groups (see Section II. 1.1 and Section II.1.2 for a single methyl group). From this fact, we can clearly identify the evidence of the coupling between the methyl groups by N.M.R. relaxation method. The transition probability between the eigen states $j = |S\ m\rangle$ and $j' = |S'\ m'\rangle$ is generally described by

$$W_{jj'} = \frac{1}{\hbar^2} \int_{-\infty}^{\infty} \langle j \mid H_D(t') \mid j' \rangle \langle j' \mid H_D(t) \mid j \rangle$$

$$\times \exp\left\{ i\, \omega_{jj'} (t' - t) \right\} d(t' - t). \qquad (24)$$

The eigen state $| S\ m \rangle$ denotes that this state is included in S symmetry species and its magnetic quantum number is m. Equation (24) is valid even for the coupled methyl system and becomes

$$W_{jj'} = \frac{1}{\hbar^2} \overline{|\langle j \mid H_D \mid j' \rangle|^2} \frac{\tau_c}{1 + \omega_{jj'}\, \tau_c^2} \qquad (25)$$

where $\hbar\omega_{jj'} = E_{j'} - E_j$ or $\omega_{jj'} = \omega_t(SS') + n\omega_0$. $\omega_t(SS')$ is the tunneling splitting between the symmetry species S and S' and ω_0 is the Larmor frequency. Equation (25) has maxma when the condition that $\omega_t(SS') + n\omega_0 = 0$ is satisfied, which induces so-called tunneling assisted minimum in the spin-lattice relaxation time (see Section II. 1.3) and enables us to observe the tunneling spectra $\omega_t(SS')$ by N.M.R. ralaxation method.

References

1) P. Groner and J.R. Durig, J. Chem. Phys., 66 (1977) 1856.

2) D.M. Grant, R.J. Pugmire, and R.C. Livingston, J. Chem. Phys., 52 (1970) 4424.

3) R.C. Livingston, D.M. Grant, and R.J. Pugmire, K.A. Strong, and R.M. Brugger, J. Chem. Phys., 58 (1973) 1438.

4) D. Smith, J. Chem. Phys., 73 (1980) 3947.

5) J.E. Wollab, "Rotational Spectra and Molecular Structure", (1967), Academic Press,(Physical Chemistry, A series of monographs No.13. Ed. by E.M. Loebl)

6) D.M. Grant, K.A. Strong, and R.M. Brugger, Phys. Rev. Lett., 20 (1968) 983.

7) J.R. Durig, S.M. Craven, and J. Bragin, J. Chem. Phys., 52 (1970) 2046, and the references cited therein.

8) W. Hamilton, J.W. Edmonds, A. Tippe, and J.J. Rush, Diss. Faraday Soc., 48 (1969) 192.

9) D.E. Woessner, J. Chem. Phys., 42 (1965) 1855.

10) G. Soda, private communication.

11) G. Soda, Kagaku no Ryoiki, 28 (1974) 799.

12) G. Soda and H. Chihara, unpublished work.

13) R.L. Hilt and R.S. Hubbard, Phys. Rev., 134 (1964) A329.

14) L.A. Lunnels, Phys. Rev., 134 (1964) A28.

15) M. Mehring and H. Raber, J. Chem. Phys., 59 (1973) 1116.

16) S. Emid, R.J. Baarda, J. Smidt, and R.A. Wind, Physica, 93B (1978) 327, and the references cited therein.

17) D.J. Ligthelm, R.A. Wind, and J. Smidt, Physica, 104B (1981) 397.

18) R.A. Wind, S. Emid, J.F.J.M. Pourquie, and J. Smidt, J. Chem. Phys., 67 (1977) 2436.

19) R.A. Wind, W.M.M.J. Boyee, J.C.F. Kupers, and J. Smidt, Z. Naturforsh., 34a (1979) 631.

20) S. Takeda, G. Soda, and H. Chihara, submitted to Mol. Phys..

21) T. Yamamoto, Thesis (1980), Osaka University.

22) Generally the activation energy for symmetric correlated reorientation is different from thst for the antisymmetric correlated reorientation. But we assumed that the activation energy is the same for both cases.

IV. Direct measurement of tunneling frequency of molecular groups in solid.

IV. 1 Various methods for determining the tunneling frequency.

In recent years, the rotational tunneling frequency of highly symmetrical molecular groups (CH_3-, NH_4^+, and CH_4, etc.) in solid has been observed by the several methods. Examples of such methods are as follows.

1) inelastic neutron scattering.$^{1-14)}$
2) electron spin reasonance (line shape)$^{15-17)}$
3) electron - nuclear double relaxation method. $^{18-19)}$
4) nuclear magnetic resonance.
    i) relaxation method$^{23-29)}$
    ii) adiabatic magnetization method (level crossing)$^{30)}$
    iii) line shape.$^{20,21)}$
    iv) nuclear magnetization time evolution in the rotating frame$^{22)}$

To measure the complicated tunneling spectrum, the methods using line shape, 2) and 4)-iii), and 4)-ii) are not appropreate, because these methods are insensitive to such a situation. The methods, in which the electron spin is used as a probe, is applicable only limited materials. The sample should contain the electron spin or it must be irradiated by high energy beam, e.g. γ-ray, to produce the free-radical in a material.

Each method is appropreate for a limited frequency range. The frequency range, in which each method is useful, is shown in Fig.1.

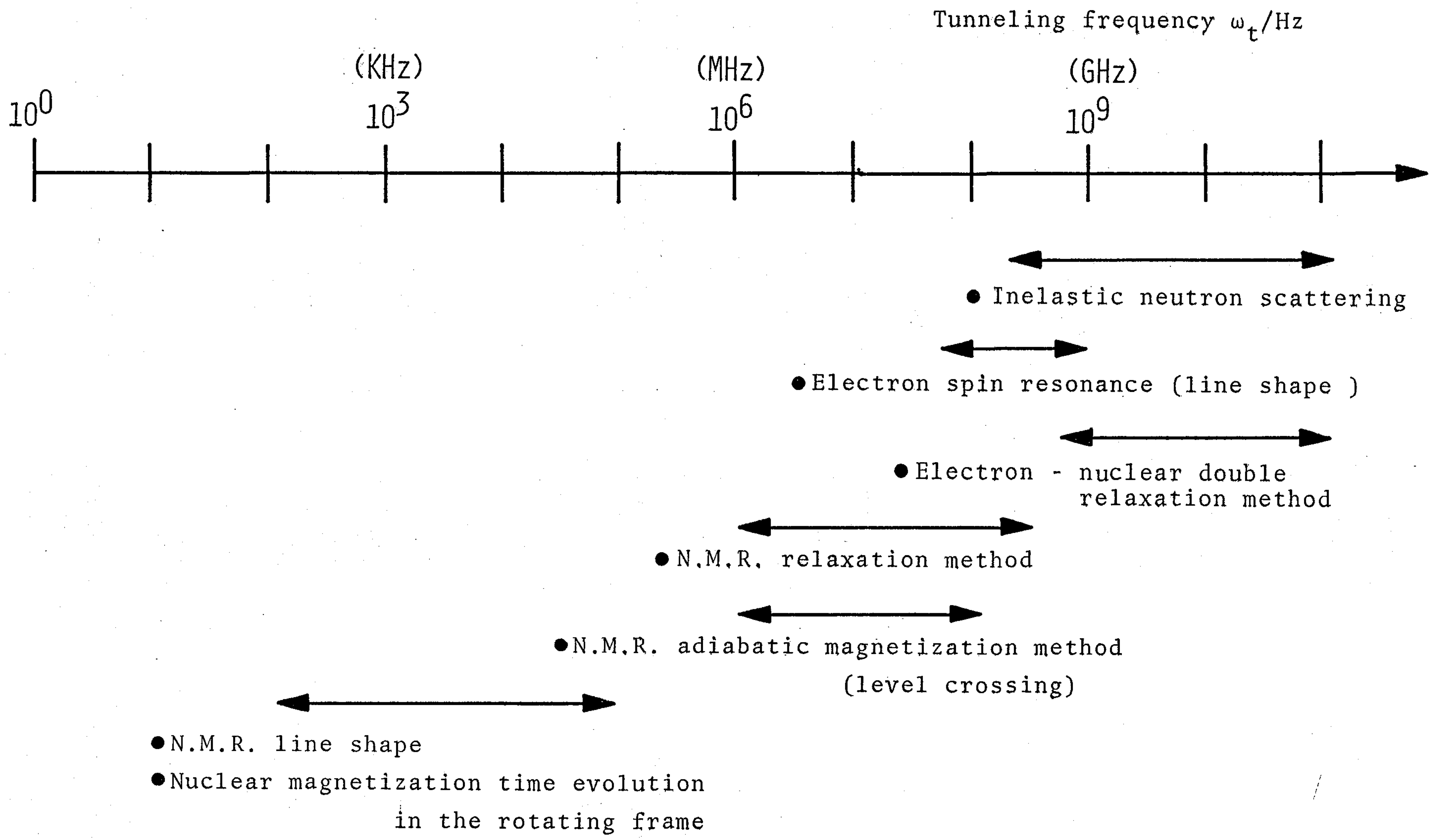

Fig. 1 Various method for determing the tunneling frequency in solids

One of the our purposes in this thesis is to investigate the coupling effect between the methyl groups on the tunneling state. When the methyl groups are situated so closely with each other as the coupling effect is observable, the hindering barrier to rotation of a methyl group is probably not so small, i.e. the tunneling splitting is not so large. Therefore we chose N.M.R. relaxation method in this thesis. The two techniques, which belong to N.M.R. relaxation method, were employed. One of them is to measure the T_1 curve v.s. temperature at several different Larmor frequencies. If the tunneling frequency is temperature dependent (see equation (41) in Section II.2), the condition that $\omega_t + n\omega_0 = 0$ is satisfied at appropriate Larmor frequency ω_0. The so-called tunneling assisted minimum will be observed (see Section III.5).[23,28,29] The otehr method is the field cycling technique [25-28] which is equivalent to the method described above and is more eloquent and easy, especially for the case of very long spin-lattice relaxation time. The principle of this method will be detailed in the next Section.

IV. 2 The principle and general procedures of N.M.R. field cycling technique.

The field cycling technique employed here was first used by P. Van Hecke et al.[25], and similar method (electron-nuclear double relaxation method) was used by S. Clough, et al..[18,19] In the field cycling experiments, what we observe is the nuclear spin magnetization at time τ, $M_z(\tau)$, which is related to spin-lattice relaxation time T_1 through the formula,

$$M_z(\tau) = \chi H_0 \left[1 - \sum_i a_i \exp(-\tau/T_{1i})\right] \qquad (1)$$

where the second term in the brackets represents the apparent non-exponential behavior due to relaxation of coupled "systems" (see Section II.1.3). a_i is the weight of the component i that corresponds to the time constant T_{1i}.

The sequence of events in the field cycling experiment was as follows (Fig.2). The proton magnetization is saturated by train of radio frequency ($\omega_0 = \gamma H_{0a}$) 90° pulses in the static magnetic field H_{0a} at resonance. The value of H_{0a} will be chosen appropriately for each sample. The magnetic field is then brought "adiabatically" to another value H_{0b}, in about 7 s irrespective of the value of H_{0b}, where the nuclear magnetization is allowed to relax for a time τ. A time τ should be chosen to be shorter than the relaxation time T_1. The magnetic field is then brought back "adiabatically" to the resonance value H_{0a}, where after about 3 s a 90° pulse is applied to determine the magnitude of partially relaxed proton magnetization $M_z(\tau)$. The interval of 3 s is taken to stabilize the magnetic field H_{0a} completely. This cycle is then repeated for different values of static magnetic field H_{0b} at a constant temperature.

H_{0b} should be chosen to cover the tunneling spectrum of the material in investigation. Then the maxima of $M_z(\tau)$, which correspond to tunneling assisted maxima of relaxation rate at the situation that $\omega_t + n\omega_0 = 0$, will be observed. The external magnetic field H_0 should be swept adiabatically. The meaning of adiabatic condition is as follows. The populations of eigenstates should not change in the time of

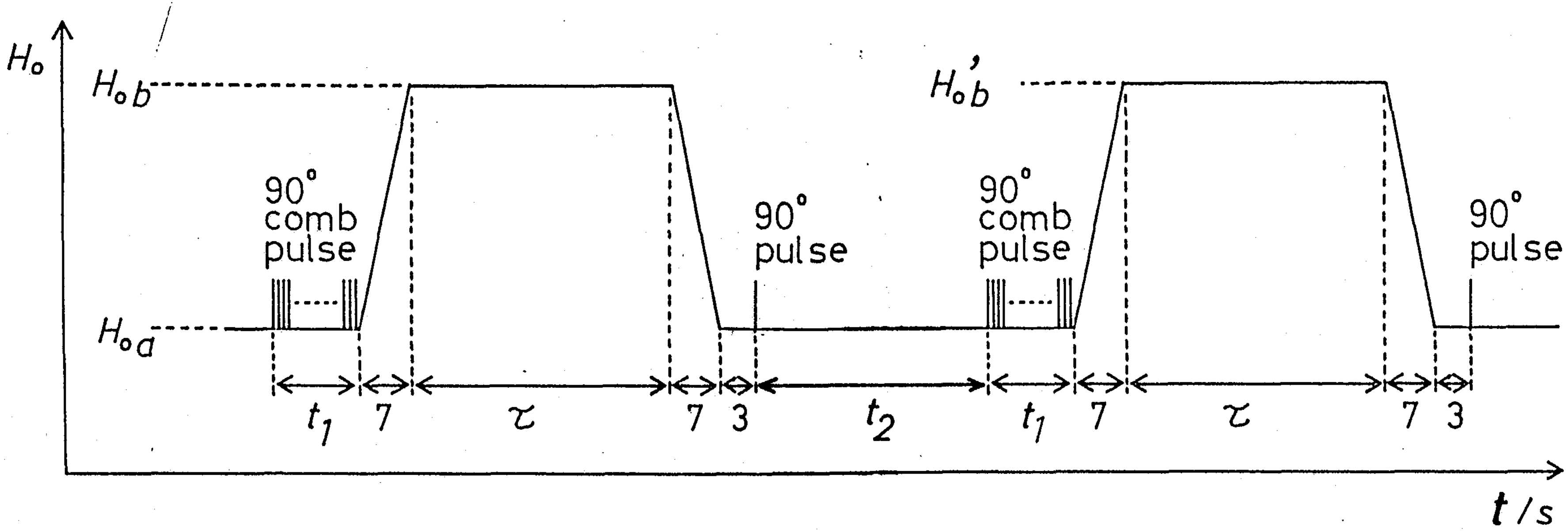

Fig. 2 The sequence of events in the successive field cycling runs. H_{0a}, H_{0b}, and H_{0b}' are the magnitude of the external magnetic field. The value of H_{0b} can be chosen larger and smaller than the reference field H_{0a}.

sweep, i.e. the spin energy does not flow to the lattice within this time interval. This situation is satisfied, when we chose the sweep-time to be much shorter than the spin-lattice relaxation time. Of course, it should not become as short that the Zeeman state of nuclear spins are not defined.

We will show the schematic view of the expected result of field cycling runs for a single methyl group. The energy shceme of a single methyl group is shown in Fig.3. The torsional ground state splits into two sublevels due to tunneling effect, where ω_t is the tunneling splitting. Each sublevel further splitts into the Zeeman levels by appling the external magnetic field. We note that the level crossing occurs between the levels of A and E symmetry at the condition that $\omega_t + n\omega_0 = 0$ (n=-1,-2) and the relaxation rate has maxima If the tunnel splitting is zero (ω_t=0), equation (1) becomes[31)]

$$M_z(\tau) = \chi H_0 \left[1 - \exp(-\tau/T_1)\right] . \qquad (2)$$

T_1 is proportional to ω_0^2 for the low temperature side of T_1 minimum,

$$T_1 \propto \omega_0^2 \quad \text{or} \quad T_1 \propto H_0^2. \qquad (3)$$

The magnetization $M_z(\tau)$ (τ is constant) v.s. external field H_0 is shown in Fig.3 by solid line. $M_z(\tau)$ is proportional to H_0 in the low field limit and $M_z(\tau)$ is proportional to H_0^{-1} in the high field limit. When ω_t is the order of ω_0, $M_z(\tau)$ in Eq.(1) show maxima at the condition that $\omega_t + n\omega_0 = 0$ (n=-1,-2) as shown in

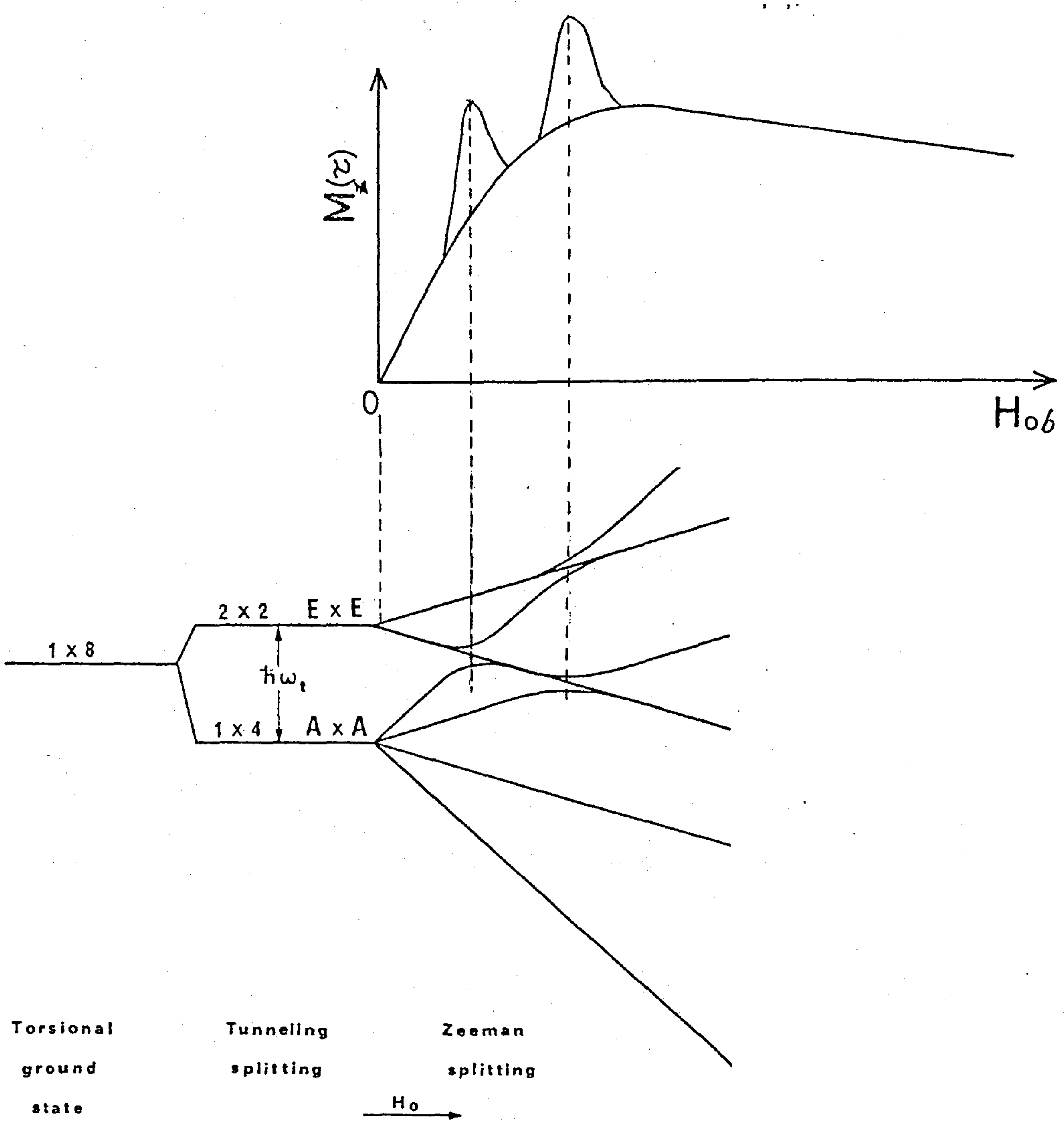

Fig. 3 Energy diagram of a sigle methyl group and the expected field cycling spectrum of a single methyl group. $\hbar\omega_t$ indicates the tunneling splitting of the torsional ground state. Two peaks of magnetization are to be observed in the field cycling experiment, corresponding to the positions of "level crossing".

Fig.3. We can determin the splitting ω_t from the magnitude of external field H_0 at which $M_z(\tau)$ show two peaks. The frequencies of the peaks are in the ratio 1:2 , corresponding to the situations, $\omega_0 = \omega_t/2$ and $\omega_0 = \omega_t$.

References

1) B. Alefeld, A. Kollmar, and B.A. Dasannacharya, J. Chem. Phys., 63 (1975) 4415.

2) W. Muller-Warmuth, R. Shuler, M. Prager, and A. Kollmar, J. Chem. Phys., 69 (1978) 2382.

3) S. Clough, A. Heideman, M. Paley, and C. Vettier, J. Phys. C12 (1979) L781.

4) S. Clough, A. Heideman, and M. Paley, J. Phys., C14 (1981) 1001.

5) S. Clough, A. Heideman, M.N.J. Paley, and J-B. Suck, J. Phys., C13 (1980) 6599.

6) S. Clough and A. Heideman, J. Phys., C12 (1979) 761.

7) S. Clough, A.J. Horsewell, and A. Heideman, Chem. Phys. Lett., 82 (1981) 264.

8) S. Clough, A. Heideman, and M. Paley, J. Phys., C13 (1980) 4009.

9) S.F. Trevino and W.H. Rymes, J. Chem. Phys., 76 (1980) 3001.

10) W. Press and A. Kollmar, Solid State Commun., 17 (1975) 405.

11) M. Prager, W. Press, B. Alefeld, and A. Huller, J. Chem. Phys., 67 (1977) 5126.

12) A. Heideman, W. Press, K.J. Lushington, and J.A. Morrison, J. Chem. Phys., 75 (1981) 4003.

13) K.J. Lushington, K. Maki, J.A. Morrison, A. Heideman, and W. Press, J. Chem. Phys., 75 (1981) 4010.

14) M. Prager, W. Press, and A. Heideman, J. Chem. Phys., 75 (1981) 1442.

15) S. Clough and J.R. Hill, J. Phys., C7 (1974) L20.

16) S. Clough, J.R. Hill, and M. Punkkinen, J. Phys., C7 (1974) 3413.

17) K. Toriyama, M. Iwasaki, K. nunome, and H. Muto, J. Chem. Phys., 75 (1981) 1633.

18) S. Clough and B.J. Mulady, Phys. Rev. Lett., 30 (1973) 161.

19) P. Beckman and S. Clough, J. Phys., C11 (1978) 4055.

20) C.S. Johnson, Jr and C. Mottley, Chem. Phys. Lett., 22 (1973) 430.

21) T. Yamamoto, G. soda, N. Nakamura, nad H. Chihara, J. Phys. Soc. Japan, 50 (1981) 2014.

22) D.W. Nicoll and M.M. Pinter, Phys. Rev., B23 (1981) 1064.

23) M. Punkkinen, J.E. Tuohi, and E.E. Ylinen, Chem. Phys. Lett., 36 (1975) 393.

24) Z.T. Lalowicz, M. Punkkinen, and E.E. Ylinen, J. Phys., C12 (1979) 4051.

25) P. Van Hecke and G. Janssens, Phys. Rev., B17 (1978) 2124.

26) S. Takeda, G. Soda, and H. Chihara, Solid State Commun.,36 (1980) 445.

27) B. Gabrys and L. van Gerven, Chem. Phys. Lett., 82 (1981) 260.

28) S. Takeda and H. Chihara, J. Phys. Soc. Jaoan, 51 (1982) in press.

29) D.J. Ligthelm, R.A. Wind, and J. Smidt, Physica, 100B (1980) 175.

30) E.P. Jones and M. Bloom, Phys. Rev. Lett., 28 (1972)1239.

31) For the non-tunneling system, Zeeman system couples to the rotational polarization system (see Subsection II.1.3). The autorelaxation rate of rotational polarization system is much larger than that of Zeeman system , when the condition that $\omega_0\tau_c$ 1 is satisfied, where τ_c is the correlation time of the rotation of a methyl group about it C_3 symmetry axsis.

Then the coupling between them can be ignored and Zeeman system relaxes exponentially.

V. Experimental details

V.1. Materials

To investigate the evidence of the mechanical coupling between the methyl groups, the five materials, which have different number of methyl groups with considerably good symmetry, were studied. These are as follws.

i) Trichloromethylsilane

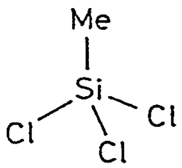

ii) a) Tetramethylpyrazine

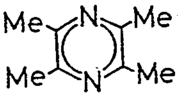

b) 1,2,4,5-tetramethylbenzene (durene)

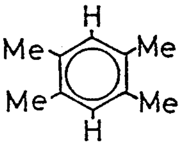

iii) Tetramethylsilane

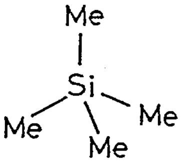

iv) Hexamethylbenzene

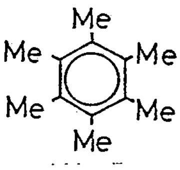

V.1.1 Properties and preparation of the samples.

i) Trichloromethylsilane

The specimen of CH_3SiCl_3 used in this study was obtained from Wako Pure Chemical Industries, LTD. It was twice distilled under dry air. The specimen was dried over Molecular Sieve 4A in vacuo and further purified by repeated vacuum distillation. The distillate was degassed by means of freeze-pump-thaw cycles and then it was sealed into an N.M.R. glass tube with helium gas (about 10 Torr) for heat exchange. The melting point of the specimen used in this experiment was examined to be 196. 2± 0.1 K by differential thermal analysis (D.T.A.) and any other anomaly was not found between 80K and the melting point.

ii) Tetramethylpyrazine (T.M.P.) and durene.

T.M.P. used in this study was obtained from Aldrich Chemical Company, Inc. Durene which was purified by Zoon melting refinement was obtained from Nakarai Chemical, LTD. These samples were further purified by several times of vacuum sublimation and degassed in a N.M.R. glass ample which was sealed with 20 (T.M.P.) and 12 (durene) Torr of helium gas for heat exchange. These samples were melted and cooled for experiments.

The melting points of these specimens used in this study were examined by D.T.A. to be 356.0 ± 0.7 K (T.M.P.) and 352.5 ± 0.8 K (durene), respectively. The gas-chromatographic analysis was also performed for durene. Any other impurity was not detectable.

iii) Tetramethylsilane (T.M.S.)

The specimen of $Si(CH_3)_4$ used in this study was the one for the N.M.R. standard (E. Merck Co.). It was dried over Molecular Sieve 4A in vacuo and purified by repeated vacuum distillation. The distillate, after degassing by means of freeze-pump-thaw cycles, was sealed into an N.M.R. glass tube (12^{ϕ})with helium gas (about

17 Torr) for heat exchange.

Since there are three solid phases α, β, and γ, of $Si(CH_3)_4$ at ordinary pressure1) (there is yet another phase above 20 MPa)2) and the β and γ phases are very similar to each other thermodynamically and otherwise, one has to take extreme precautions as to identification of which phase he is dealing with. In fact, there have been confusing and mutually conflicting reports with regard to the solid state properties owing to such polymorphic complications. Even after the phase relations were established,1) reports have appeared in which the solid phase or phases were not clearly identified.3)

We used two thermocouples in the N.M.R. cryostat, (see Section V.5) one attached to the specimen tube and the other to the shielding can that enclosed the specimen tube. The two thermocouples served to run the cryostat in the form of differential thermal analysis1,4) through which it was possible to assign unambiguously which phase we were looking at. Unlike the case of thermodynamic studies,1) the β Phase was stable all the way down to 4.2 K.

The melting points of the α, β, and γ phases of the specimen used in this experiment were 167.9 ± 0.2 K, 170.5 ± 0.2 K, and 174.0 ± 0.2 K, respectively. These values determined by D.T.A. were in good agreement with the established values.1)

iv) Hexamethylbenzene (H.M.B.)

The specimen of H.M.B. used in this study was obtained from Tokyo Chemical Industries Co, LTD. It was purified by several times of vacuum sublimation and degassed in a glass ample which was sealed with 10 Torr of helium gas for heat exchange. This sample was melted and cooled for experiments. Hexamethylhenzene undergoes the successive phase transitions. The two transition points and melting point of the specimen were examined by D.T.A. to be 117.0 ± 0.7 K (phase III → phase II), 380.6 ± 0.6 K (phase II → phase I), and 433.4 ± 0.4 K (melting), respectively. The gas-chromatographic analysis was also performed. Any other impurity was not detectable.

V. 2. Measurement of the spin-lattice ralaxation times.

V. 2.1. Apparatus

The spin-lattice relaxation time was measured with the pulse spectrometers one of which was a variable frequency type (7MHz ~ 50 MHz)[5] and the other was fixed frequency type (10 MHz).[6] Some improvements were performed to shorten the dead time of the receiver amplifier of a variable frequency type spectometer. The two types of limiter circiuts were employed. One of them is a passive type. It is very simple turned limiter.[7] This is shown in Fig. 1.a. The other is an active one which consists of double balanced mixer and a trapezoid wave generator[8], (see in Fig. 1. b). These devices prevent overload of the reciver amplifier due to the high-power Rf pulse and thereby allow the fast recovery of the amplifier. The block diagram of the spectrometer with these limiters is shown in Fig. 2. The typical free induction decay which was obtained with these devices is shown in Fig. 3. The trangent of high-power Rf-pulse is smaller than the signal (F.I.D.).

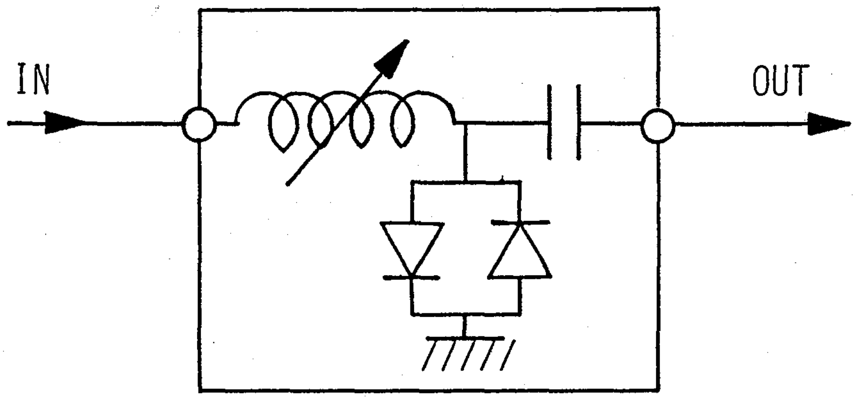

Fig. 1.a Passive limiter. For large input (V_{in}), the crossed diodes to ground limit the Rf-amplitude between the inductor and capacitor to a voltage V_d(diode level). V_{out} is limited to ωRCV_d, where R is the imput resistance of preamp. and ω is Rf-frequency. The condition that $\omega R \ll 1$ was assumed. A factor ωRC is better than cross diode alone. 7)

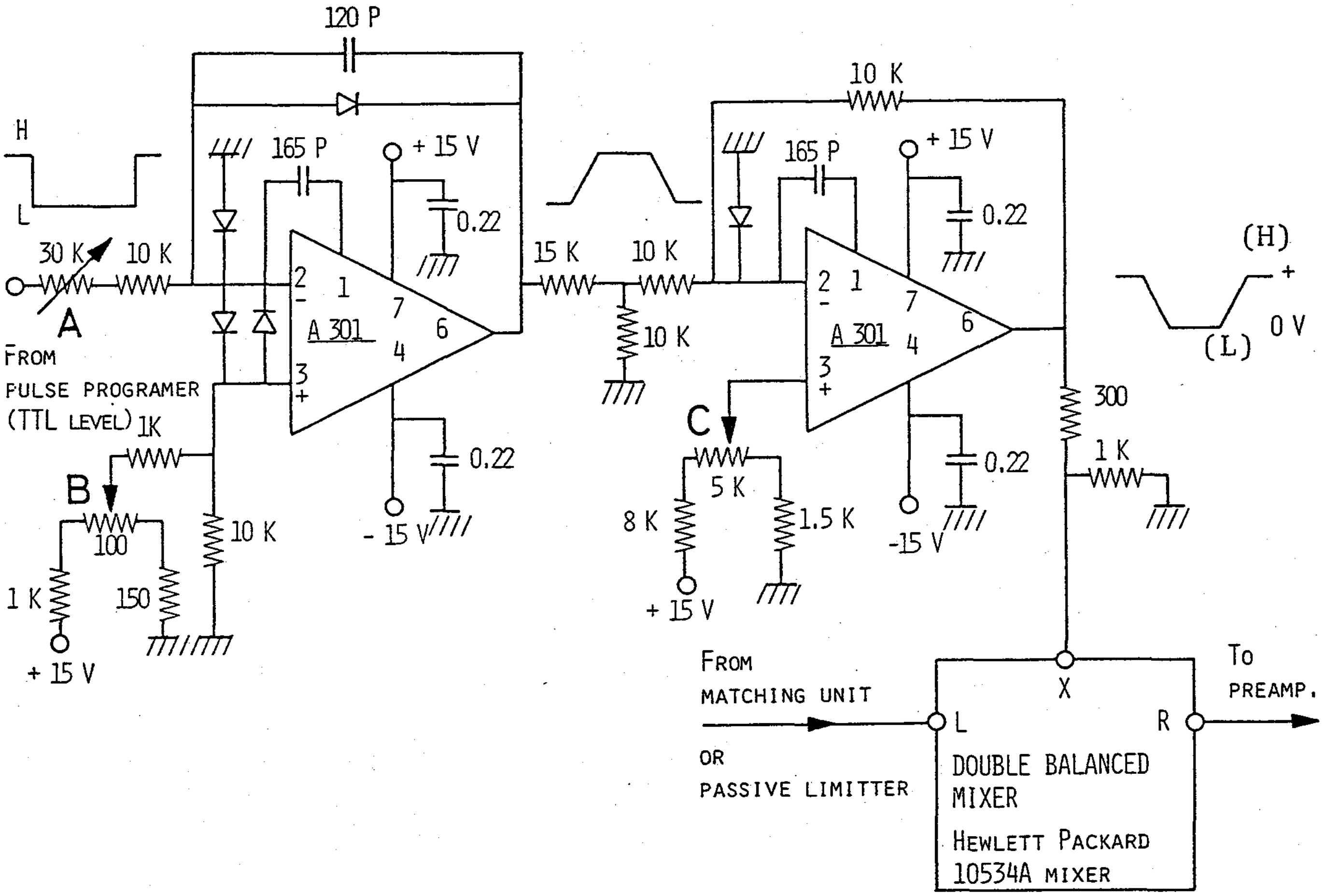

Fig. 1.b Active limiter used in the present experiments. Variable resistance A determines the slope of the side line of the trapezoid wave. The value of B determines the asymmetry of the trapezoid wave and the value of C shifts the out-put level (indicated by L in the figure) near 0V. Double balanced mixer works as Rf-gate.

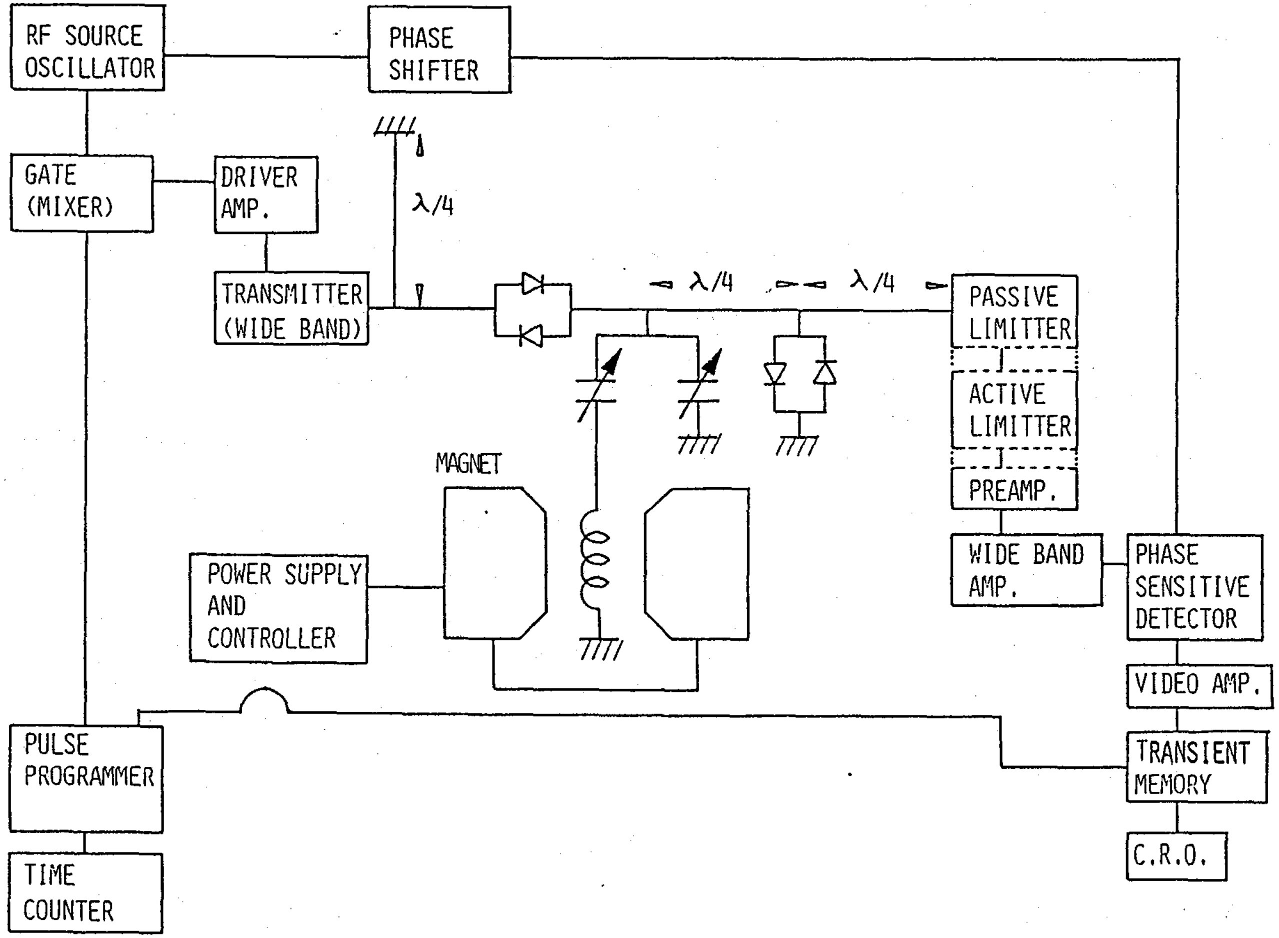

Fig. 2 Block diagram of pulse N.M.R. spectrometer with limiter circuits. The spectrometer is a wide band type[6)].

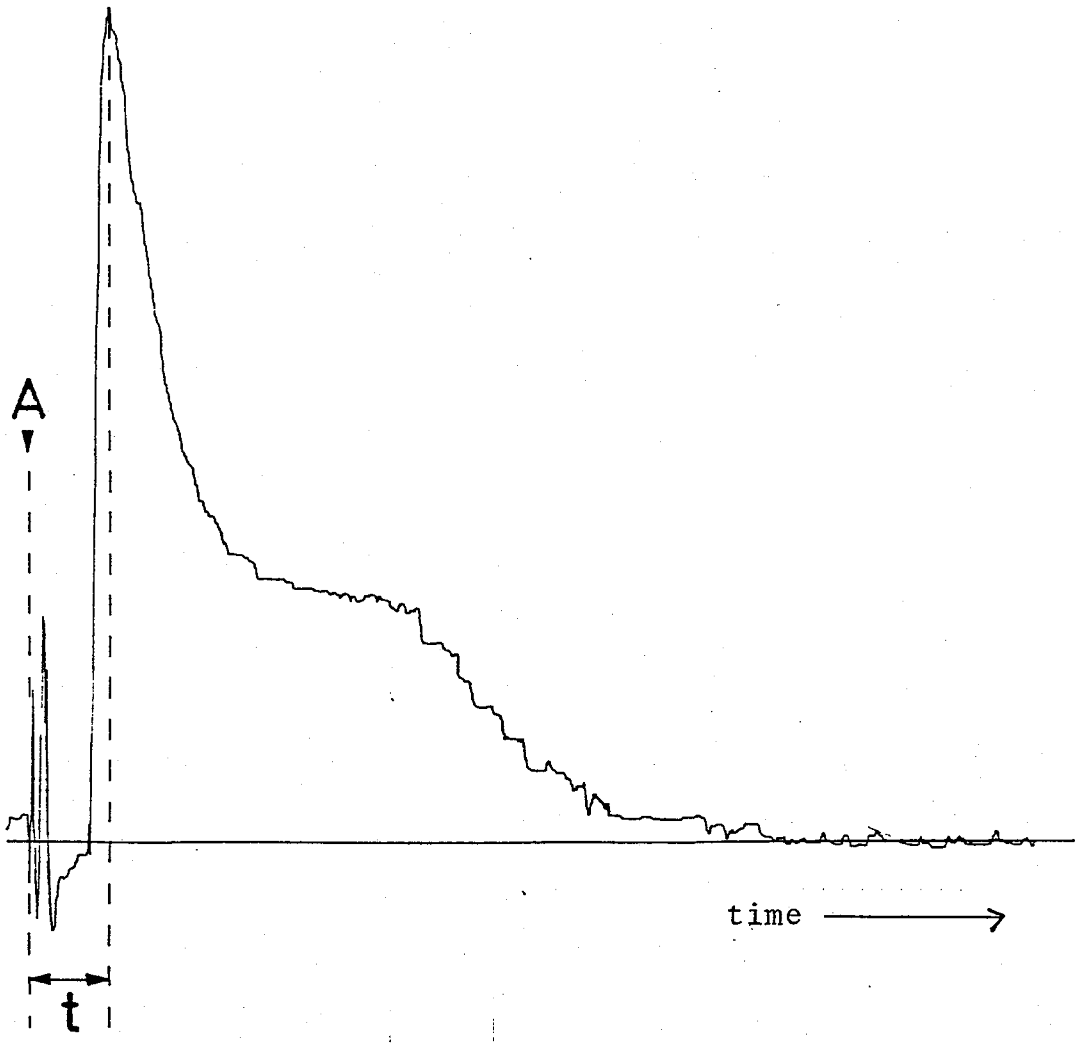

Fig. 3 A typical free induction decay (F.I.D.) of CH_3SiCl_3 which was obtained with the apparatus shown in Fig. 2. The working frequency was 29.9 MHz. A is the start point of the high-power Rf-pulse. The trangent of this pulse is seen in the time duration of t. The time duration, t, is dead time and is 11 μs which includes the width of the 90° pulse.

F.I.D. shows the structure which Corresponds to the observed line shape (Fig. 10 in Section VI)

V. 2.2. Pulse sequences for reliable measurements.

As will be demonstrated and discussed in Section VI. 1, the magnetization recovery curve depends on the method of measurement. Therefore, we discriminately used the two kinds of H_1 pulse arrengements, A and B.

A; Long train of 90° pulse.

The train of pulses continues during a time spane longer than or at least comparable to the relaxation time and it not only saturates the Zeeman system but also bring the three other systems (see Section II. 1,3) out of thermal equilibrium[9)]

B; Short train of 90° pulses - τ - single 90° pulse.

The short train continues during a time much shorter than the relaxation times. In actual experimental set up, we used four 90° pulse at interval of 200 μs except for CH_3SiCl_3 (the nuclear signal, F.I.D., after each 90° pulse decayed with a half-life of about 7 μs except for CH_3SiCl_3. For CH_3SiCl_3 the time interval of 500 μs was chosen, corresponding to the long life of F.I.D. which is not a simple exponential decay but has a structure corresponding to the line shape (see Section VI). With the short train, only the Zeeman system is saturated, the other systems remaining at the thermal equilibrium states.[9)] The pulse sequence B is equivalent to the conventional 90° - τ - 90° pulse sequence and also similar to 180° - τ - 90° pulse sequence[9)] but it can eliminate the unfavorable effect of deviation from 90° which causes a considerable error in the spin-lattice relaxation time, especially in the fast relaxing component. We also used these conventional methods as we used pulse sequence B and compared the recovery curves of magnetization. For the sequence B, to be able to lead to a well-defined T_1 value, one must start this sequence from the spin state of complete thermal equilibrium, whereas such initial conditions is not necessary for the pulse sequence A.

V. 3 Field cycling experiment

To perform the field cycling experiment the aparatus, which swept the external magnetic field H_0 as shown in Fig. 2 in Section VI. 2, was constructed.

V. 3.1 Apparatus

The block diagram of the apparatus for the field cycling experiment is shown in Fig. 4. This is almost the same as that for T_1 measurement (Fig. 2) except for the field sweeper. This field sweeper generates the trapezoide wave ($\pm$5V) of which the voltage was used as the reference for the field controller to sweep and to stabilize the current of the electric magnet. The circuit of the trapezoid wave generator is shown in Fig. 5. The preliminary circuit was shown in M.S. thesis.[10] One of the important problem is to stabilize the reference field H_{0a} (Fig. 2 in Section IV. 2) completely to eliminate the deformation of F.I.D. due to fluctuating magnetic field. For this purpose the "analog switch" was used to stabilize the out-put voltage. The H_{0b} value can be kept constant to within $\pm$0.02% in all the runs.

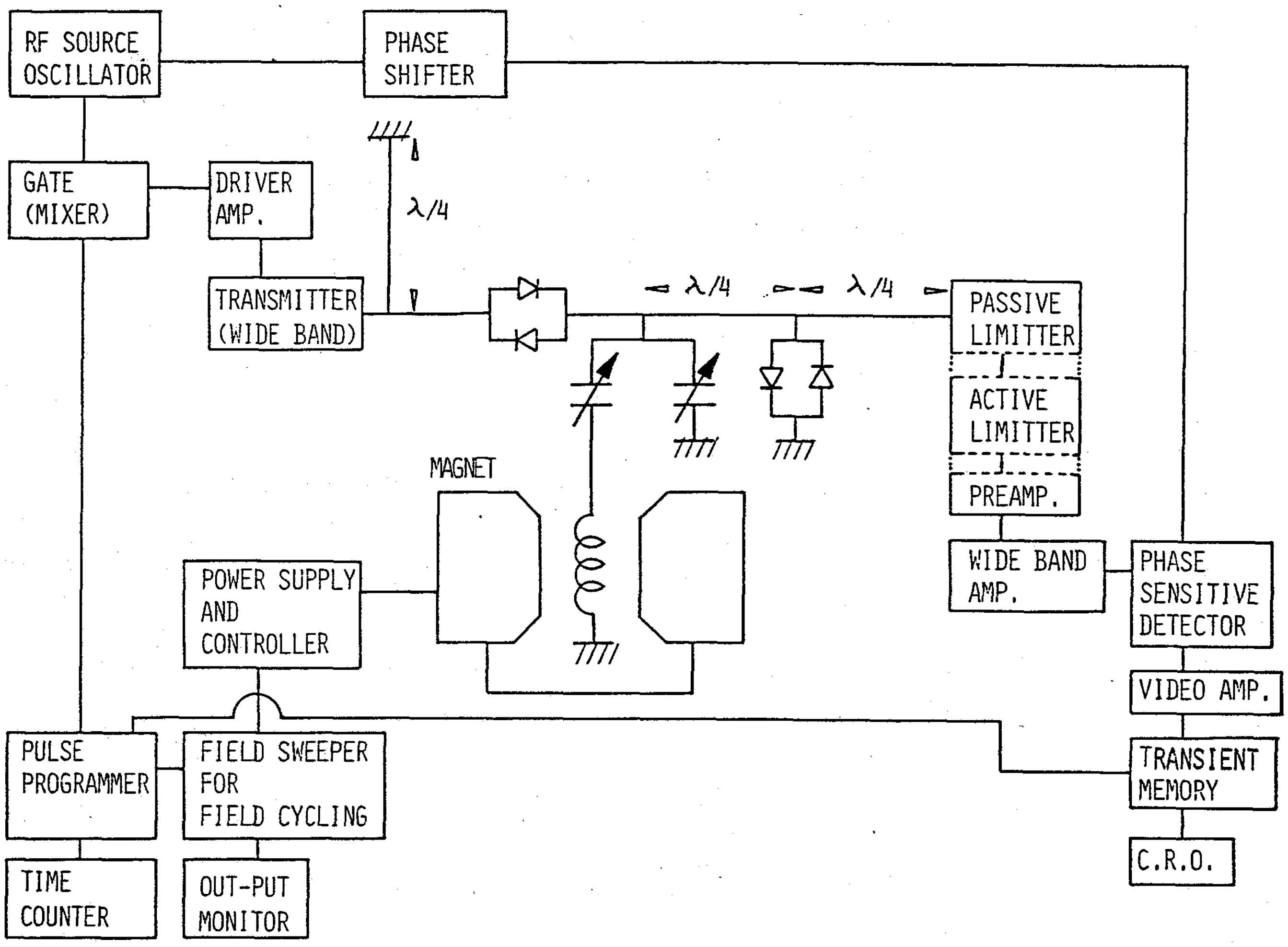

Fig. 4 Block diagram of the apparatus for field cycling experiments. Except for field sweeper conected to pulse programer, the apparatus is the same as that in Fig. 2.

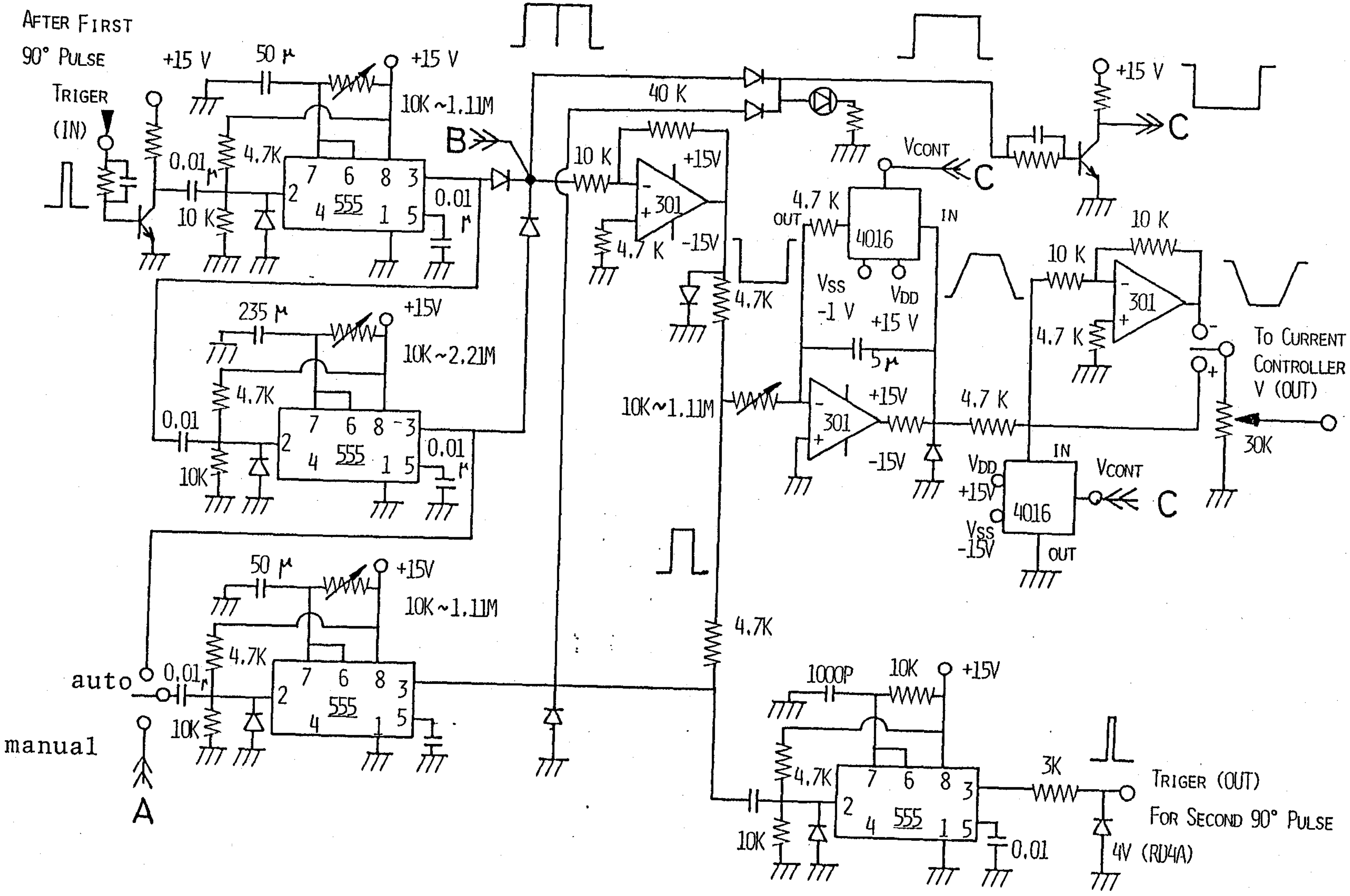

Fig. 5 Trapezoid wave generator for field cycling.

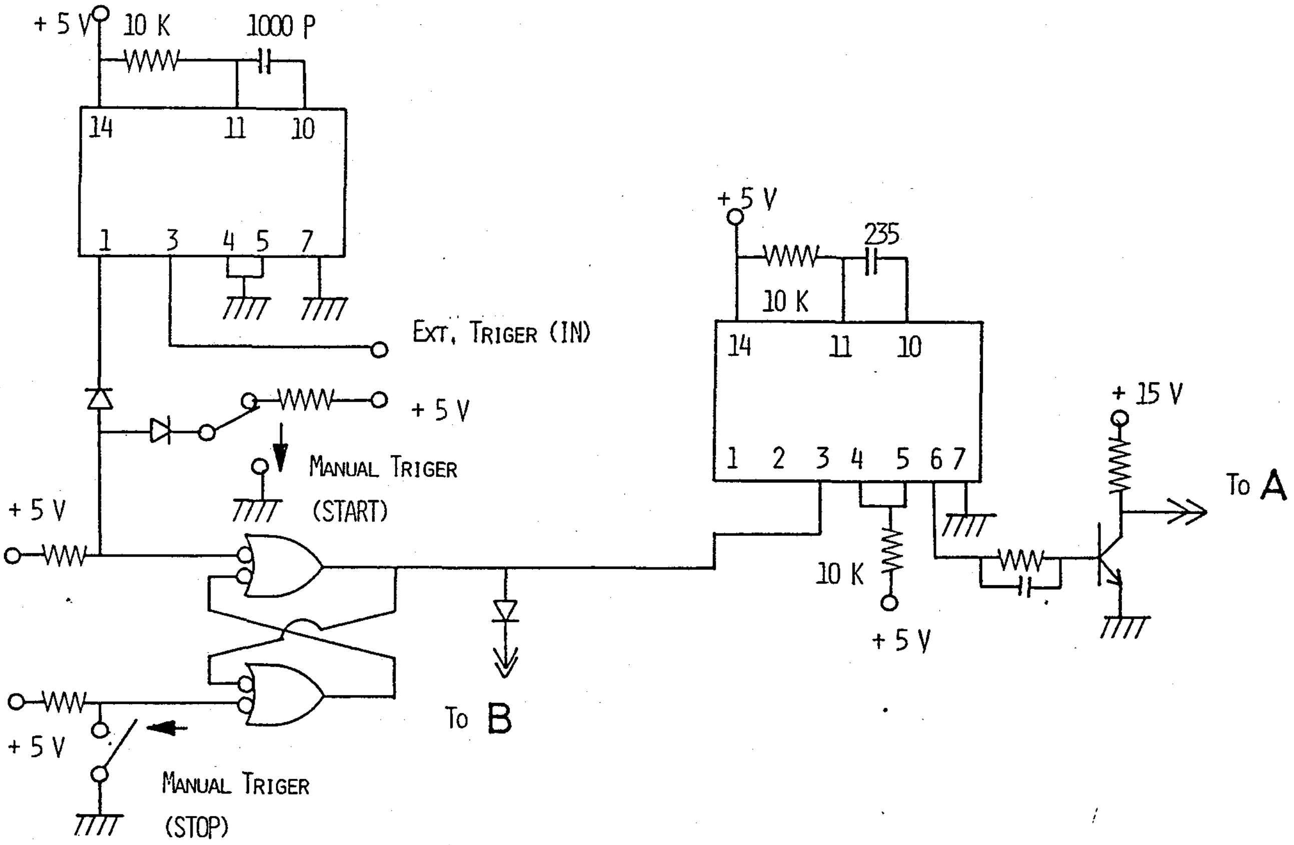

Fig. 5 (continued)
Maximum out-put voltage is ± 15 V. The time duration of trapezoid wave is determined by timer IC 555. The base line (0 V level) is stabilized by using analog switch 4016. The stability of 0 V level determines the stability of the reference field H_{0a} (see in the text).

V. 3.2 Calibration of the field sweep.

The field sweep by the apparatus described above was calibrated by the N.M.R. signal of tetramethylsilane at about 80K for several H_{0a} values. The relation between the strength of the magnetic field H_{0b} and the out-put voltage (V) of the trapezoid wave generator was determined. In the experiments, the out-put voltage of the trapezoid wave generator was monitored by digital voltage meter and then the value of H_{0b} was known. The external magnetic field H_{0b} v.s. out-put valtage V was almost described by linear function. When we use the explicit linear function, the maximum error is within ± 1 % of the value of H_{0b} for ± 0.5 T sweep-width. This error did not affect the results of tunneling splittings, because the observable peaks of magnetization are not so sharp.

V. 3.3 The detailed condition of field cycling experiments

The pulse sequence B (Section V. 2.6) should be used for the field cycling experiments to obtaine the maximum enhancement of the magnetization. As we shall discuss in Section VI we cannot obtaine the tunneling spectrum under the condition of complete saturation of spin system, i.e. by the method A. Therefore we used the short train (pulse sequence B) for the field cycling experiments. We should then start each field cycle run from the state of complete thermal equilibrium of the spin system to obtain the maximum enhancement of the magnetization at the condition of $\omega_t+n\omega_0=0$. However, because the relaxation time at low temperature is extremely long ($10^3 \sim 10^5$s) for the materials studied in this thesis, it was not practical to wait for the whole spin-system to come to complete thermal equilibrium before starting each field cycle run. We thus made a compromise between very long experimental time and diminished intensity of the peaks in the field cycle spectrum which depends on the fraction of fast-recovery component (see in Section VI.1). It was ascertained that the positions of the peaks of magnetization at $\omega_t+n\omega_0=0$ did not depend on such experimental conditions within the width of the peak by doing a separate experiment for γ phase of $Si(CH_3)_4$ at 26.7K (T_{1s}=560 s). Therefore, we will pay attention only to the positions of the peaks of magnetization. The field cycle runs were conducted with a constant interval (t_2= constant; see Fig. 2 in Section IV. 2) and from the low to high field

of H_{0b} for any materials and at any temperature.

V. 4. Continuous wave N.M.R. measurement.

The proton N.M.R. line shapes were observed by the continuous wave (c.w.) method by using a Robinson type spectrometer[11)] and bridge circuit with hybrid junction.[11)] The field moduration method was used for both systems and its frequency was 33 Hz. The width of the moduration, $2H_m$, and the sweep of external magnetic field were calibrated by a N.M.R. signal of Cu^{2+} doped H_2O at room temperature. The Robinson type spectrometer used in this study worked at about 7～13 MH_z[12)]. A bridge circuit with hybrid junction was constructed to observe the line shape at high Larmor frequency (～60MHz). The block diagram of the bridge circuit system is shown in Fig.6. The appropriate character of this bridge circuit are as follows.

i) Rf-power can be controled easily. Furthermore even at very low Rf-power the spectrometer works with good stability.

ii) The working frequency can be chosen widely and easily.

V.5. Cryostat for the N.M.R. measurements between 2K and room temperature.13)

To perform the N.M.R. measurements at wide temperature range, an appropriate cryostat was constructed. The schematic view of this cryostat is shown in Fig. 5. The capacity for reserving the liquid helium under the shielding can is about 250 cm^3. The temperature was controled automatically by the apparatus13) which keeps the temperature-difference between the reference point (U) and the shielding can (Q) constant by the two kinds of heaters E and T. When the liquid helium is not used the temperature of the sample is controled against the ice-point (reference point). The temperature could be stabilized within ± 0.1K for 8 ~10 hours between 4.2K and about 100K by using the coolant of liquid helium. Above 80K the stability of temperature was better than ± 0.1K by using the coolant of liquid nitrogen which was reserved in the out-side dewer (R). In this case we can keep the temperature constant as very long time as desired. The temperature was measured with a Chromel-P-Constantan thermocouple above 15K and with a gold/iron-Chromel thermocouple or a germanium thermometer below 15K.

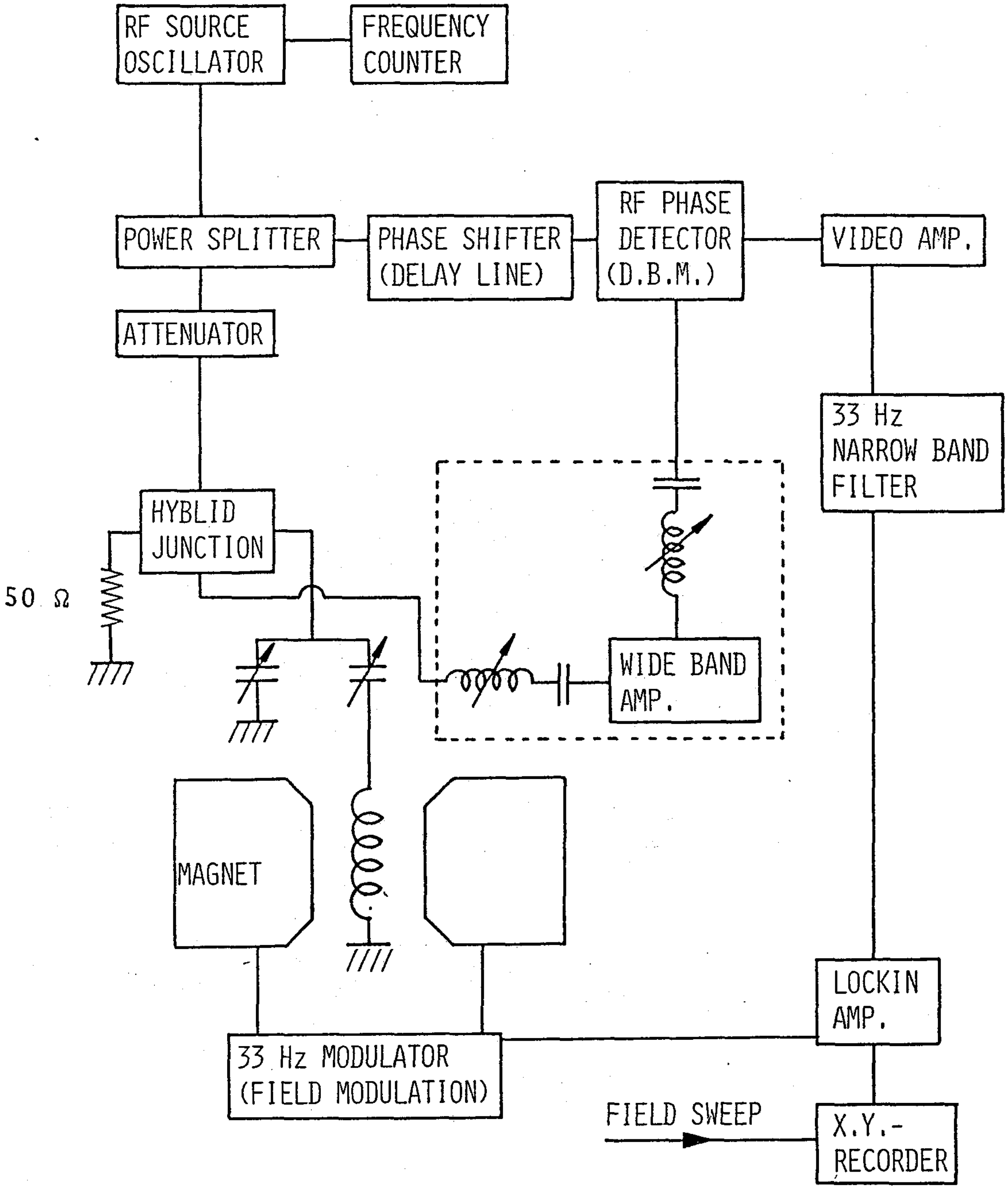

Fig. 6 Block diagram of a bridge type N.M.R. spectrometer (continuous wave). The working frequency can be chosen widely. In the present experiments, 59.82 MHz was chosen.

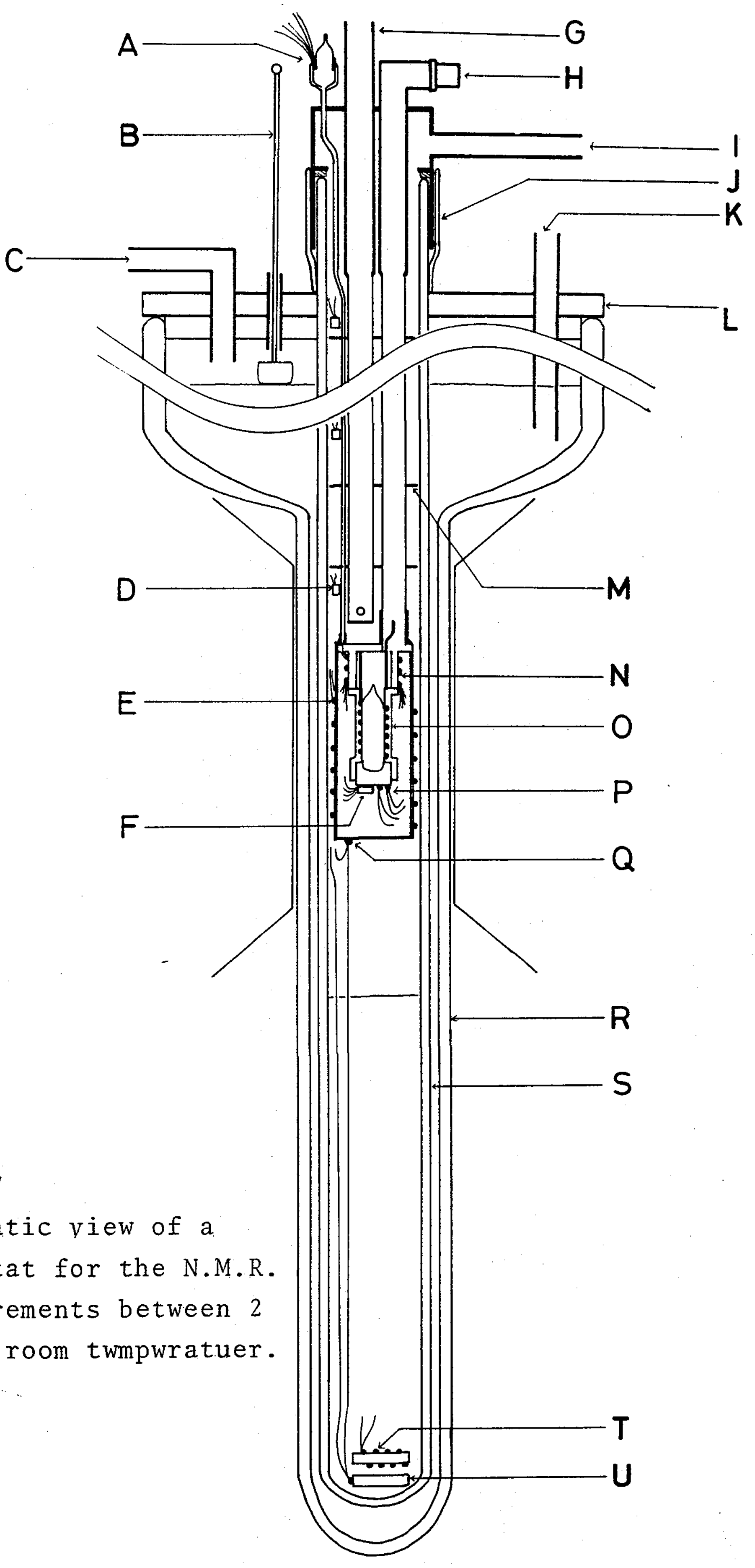

Fig. 7
Schematic view of a
cryostat for the N.M.R.
measurements between 2
K and room twmpwratuer.

Fig. 7 (caption)

A; outlet of the lead wiers and thermocouples,
B; level indicator for liquid nitrogen,
C; outlet of nitorgen gas,
D; level indicator for liquid helium, carbon resisters (250Ω, 1/8 W) were used,
E; heater for temperature control,
F; germanium thermometer,
G; inlet of liquid helium,
H; Rf-conector,
I; outlet of helium gas,
J; rubber tube to ensure vacuum,
K; inlet of liquid nitrogen,
L; cap of the out-side vessel,
M; radiation shield,
N; thermal ancher for heat exchange between the lead wiers (thermocouples) and the shied can,
O; Rf-coil (sample coil),
P; thermocouples,
Q; Au(Fe)-thermocouple for temperature control, reference point is liquid helium temperature (U),
R; out-side vessel,
S; in-side vessel,
T; heater to evapolate the liquid helium,
U; reference point of Q

References

1) M. Harada, T. Atake, and H. Chhara, J. Chem. Thermodynamics, 9 (1977) 523.

2) T. Atake and H. Chihara, Chem. Phys. Lett., 56 (1978) 330.

3) D.J. Ligthelm, Thesis (1981), Technische Hogeschool, Delft, The Netherlands.

4) T. Hasebe, G. Soda, and H. Chihara, Proc. Jaoan Acad. 51 (1975) 168.

5) K. Ichimura, private communication.

6) K. Ichimura and K. Sasaki, private communication.

7) H.T. Stokes, Rev. Sci. Instrum. 49 (1978) 1011.

8) T. Terao, private communication.

9) R.A. Wind, S. Emid, J.F.J.M. Pourquie, and J. Smidt, J. Chem. Phys., 67 (1977) 2436.

10) S. Takeda, M.S. Thesis (1979), Osaka University.

11) "Techniques of Metals Reserch" (Ed. by r.f. Bunshah) Vol.VI, "Measurement of Physical Properties, Pt.2, Magnetic properties and Mossbauer Effect" (Ed. by E Passaglia, John Wiley & Sons, 1973).

12) K. Koda, private communication.

13) This cryostat has already been described in M.S. Thesis (reference 10).

VI. Experimental results and discussions.

In this Section the experimental results about three problems will be demonstrated and discussed. Firstly the characteristic behaviors of the Zeeman relaxation due to the quantummechanical tunneling and/or classical jump-reorientation of a methyl group about its C_3 symmetry axis was examined (Subsection VI.1). The nonexponential magnetization recovery was observed in the low and high temperature branch of the T_1 curve. This nonexponentiality was dependent on the experimental method employed. Secondly the tunneling spectra of the sets of some different numbers of methyl groups were obtained by "N.M.R. field cycling technique" for the five materials; CH_3SiCl_3 containing a single methyl group in a molecule (Subsection VI. 2), durene and T.M.P. containing two pairs of two adjacent methyl groups in a molecule (Subsection VI.3), $Si(CH_3)_4$ containing the four adjacent methyl groups in a molecule (Subsection VI.4), and H.M.B. containing adjacent six methyl groups which are placed like as a ring in a molecule (Subsection VI.5). The temperature dependence of the tunneling spectra (frequencies) was observed directly for $Si(CH_3)_4$ and H.M.B.. For CH_3SiCl_3, durene and T.M.P., the indirect evidences of the temperature dependence of the tunneling frequencies were obtained. Thirdly the small reduction of the line width was observed at low temperature (30 ∿ 60 K) for CH_3SiCl_3, T.M.P. and $Si(CH_3)_4$[1)] (Subsection VI.7). This behavior is not expected for the intramethyl dipole-dipole interaction[2-5)].

VI.1 The behavior of the Zeeman relaxation or the recovery of the longitudinal magnetization.

Typical magnetization recovery curves from the different initial conditions of the spin states are shown in Figs. 1,2,3, and 4, respectively, for CH_3SiCl_3, durene, T.M.P., and $Si(CH_3)_4$. The initial condition was prepared either by the pulse sequence A (long train of first pulse) or the sequence B (short train or single pulse of first pulse; see Section V.1). The magnetization recovery was nonexponential irrespective of the method (A or B) above the temperature of T_1 (min.) due to methyl rotation about its C_3 symmetry axis, whereas it was exponential for the method A and nonexponential for the method B below that temperature. When the recovery was nonexponential, it was decomposed into the fast-recovering component (T_{1f}) and the slowly - recovering component (T_{1s}). T_{1f} is shorter than T_{1s} by two or four orders below the T_1(min.) temperature. The decomposition was performed and two components at these temperatures are also illustrated in Fig.1 - Fig.4. Above the T_1(min.) temperature the two components ($T_{1f}$and T_{1s}) were not so different as that below that temperature. The decomposition was performed by least squre refinment [6)] and the typical examples for T.M.P. and CH_3SiCl_3 are shown in Fig.5.

The temperature dependence of the spin-lattice relaxation time of T.M.P. measured at 20.5 MHz is shown in Fig.6. In the low temperature branch ($(kK/T) \gtrsim 13.5$ or $T \lesssim 75$ K) the

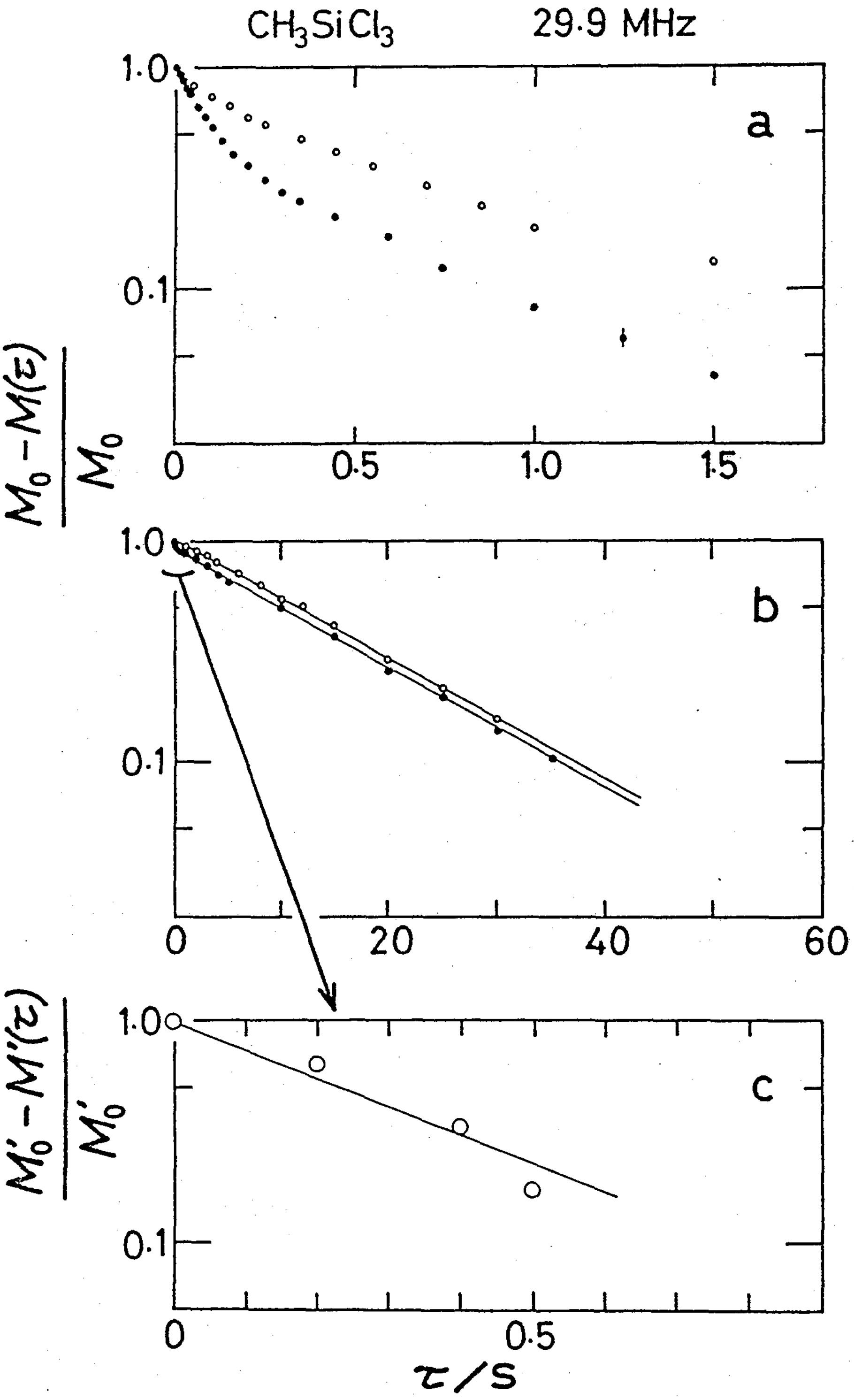

Fig. 1 The typical magnetization recovery at different temperatuers for CH_3SiCl_3. a: above the temperature of T_1 minimum, ○ by the method A (long train), ● by the method B (short train). b: below the T_1 minimum temperature, ○ by the method A, ● by the method B. c is the portion of fast-recovering component of magnetization obtained by the method B.

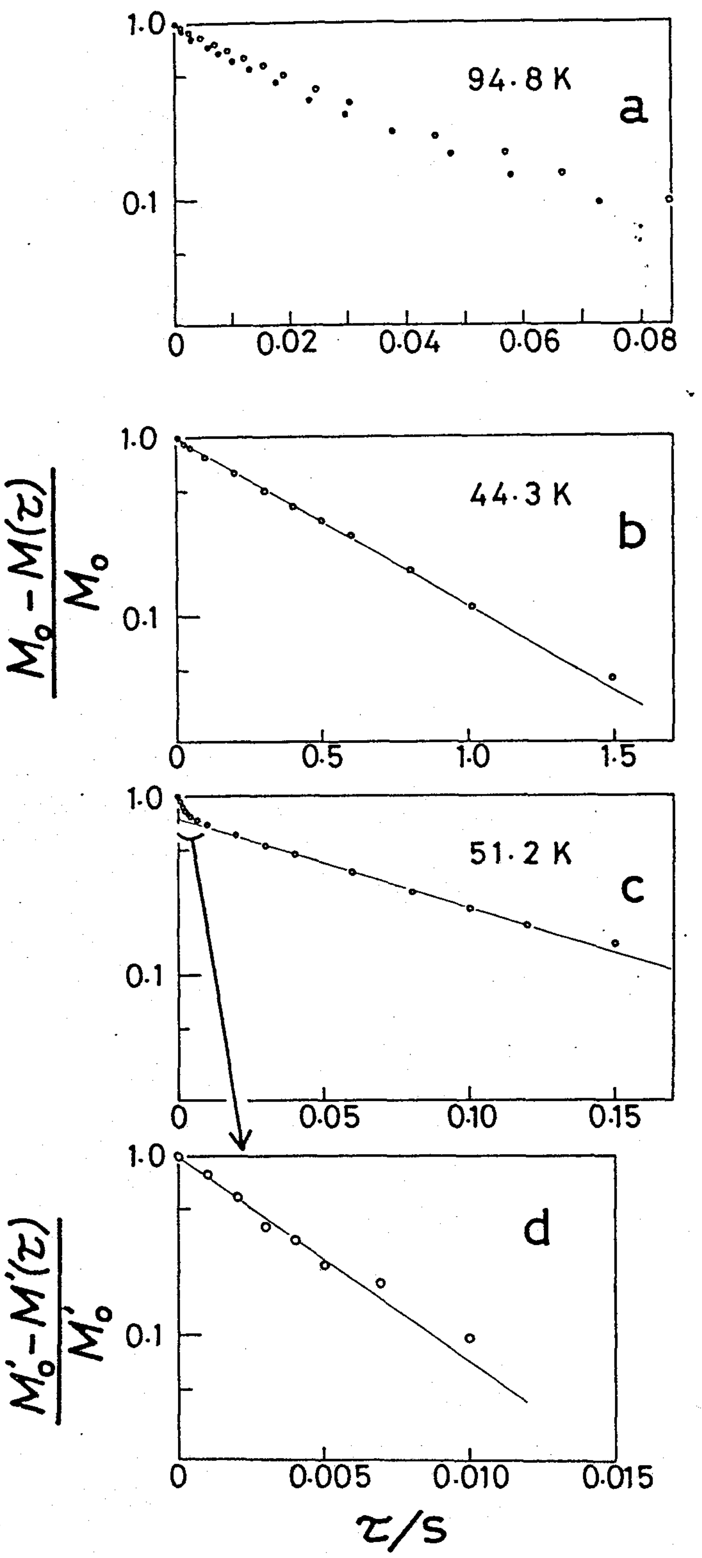

Fig. 2 The typical magnetization recovery at different temperatures for the β phase of $Si(CH_3)_4$. a: above the temperature of T_1 minimum, ○ by the method A (long train), ● by the method B (short train). b,c: below the T_1 minimum temperatures. b is obtained by the method A while c by the method B. d is the portion of fast-recovering component of c. A similar results were observed in the γ phase.

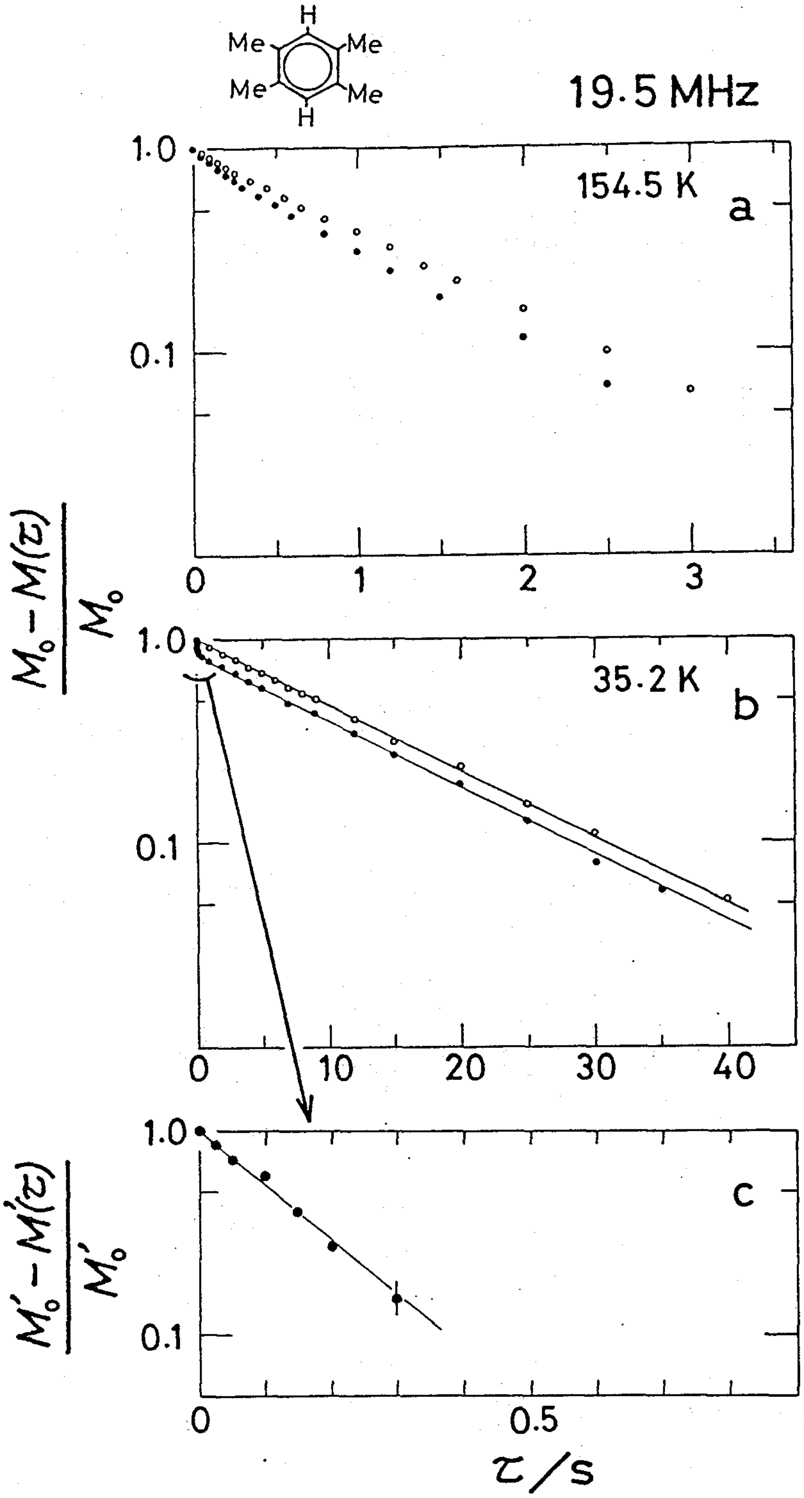

Fig. 3 The typical magnetization recovery at different temperatures for durene. a: above the temperature of T_1 minimum, ○ by the method A (long train), ● by the method B (short train). b: below the T_1 minimum temperature, ○ by the method A, ● by the method B. c is the portion of fast-recovering component of magnetization obtained by the method B.

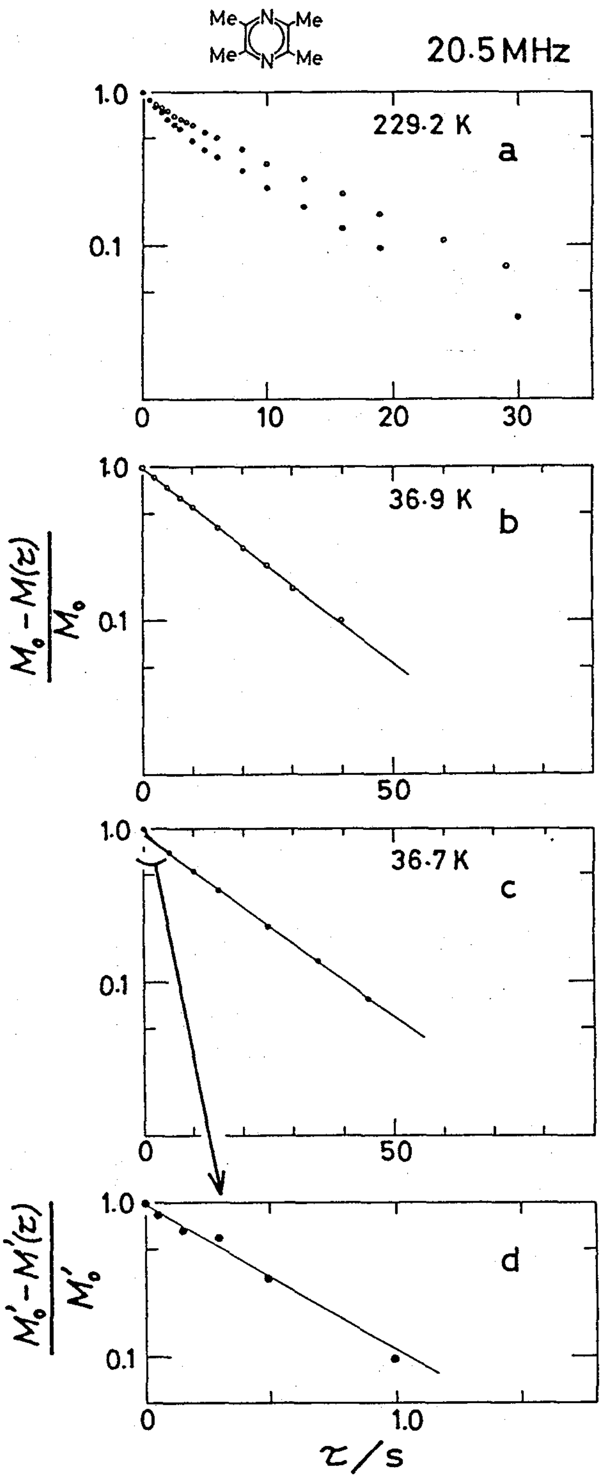

Fig. 4 The typical magnetization recovery at different temperatures for tetramethylpyzazine, a: above the temperature of T_1 minimum, ○ by the method A (long train), ● by the method B (short train). b,c: bel-w the T_1 minimum temperatures. b is obtained by the method A while c by the method B. d is the portion of fast-ralaxing componentof c.

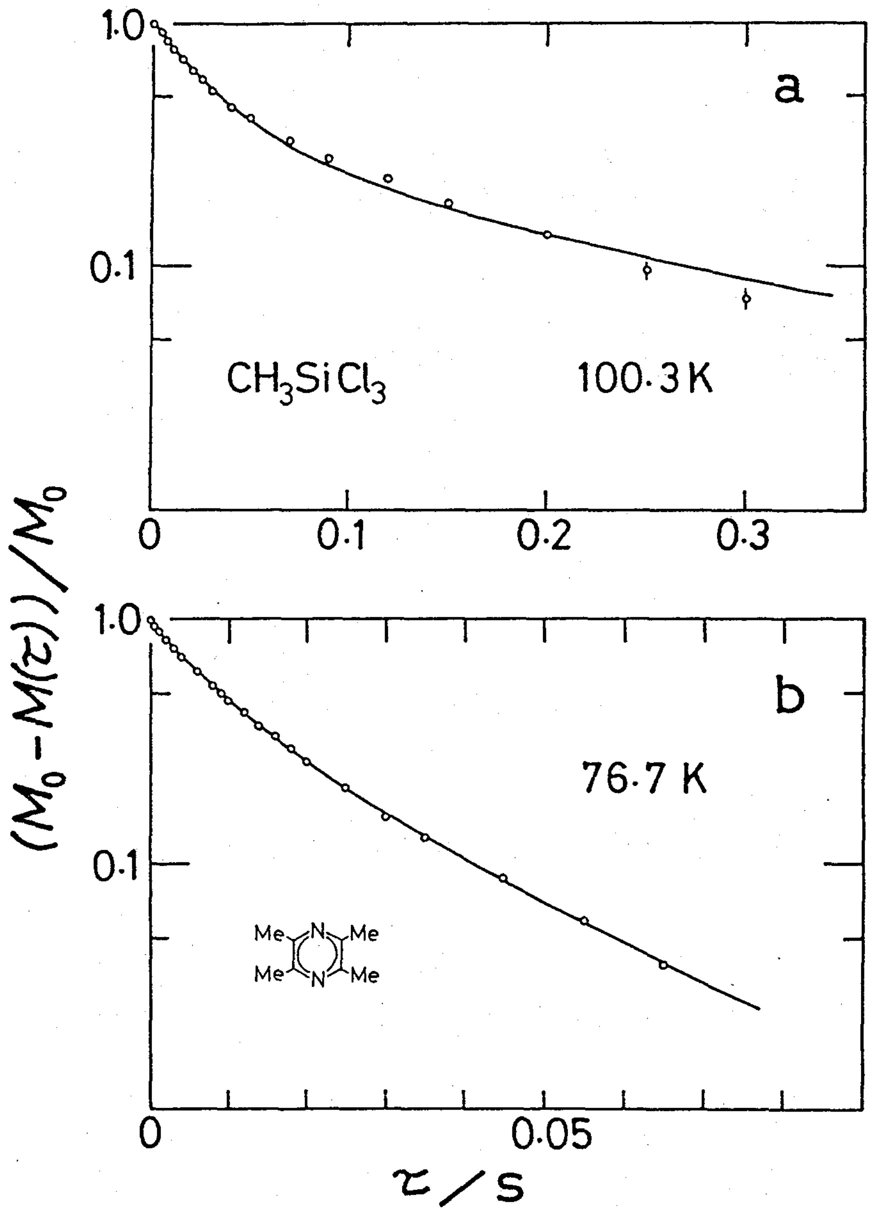

Fig. 5 The magnetization recovery curves of trichloromethylsilane (a) and tetramethylpyrazine (b). a and b are obtained avobe the respective T_1 mimimum temperatures. The solid curves show the fitted values using the formurae,

$$M(\tau) = M_0[1 - 0.66 \exp(- 3.12 \times 10^{-2} \text{ s}/\tau) - 0.34 \exp(- 2.25 \times 10^{-1} \text{ s}/\tau)]$$

and

$$M(\tau) = M_0[1 - 0.61 \exp(- 9.50 \times 10^{-3} \text{ s}/\tau) -0.39 \exp (- 2.93 \times 10^{-2} \text{ s}/\tau)] ,$$

respectively, for CH_3SiCl_3 and tetramethylpyrazine.

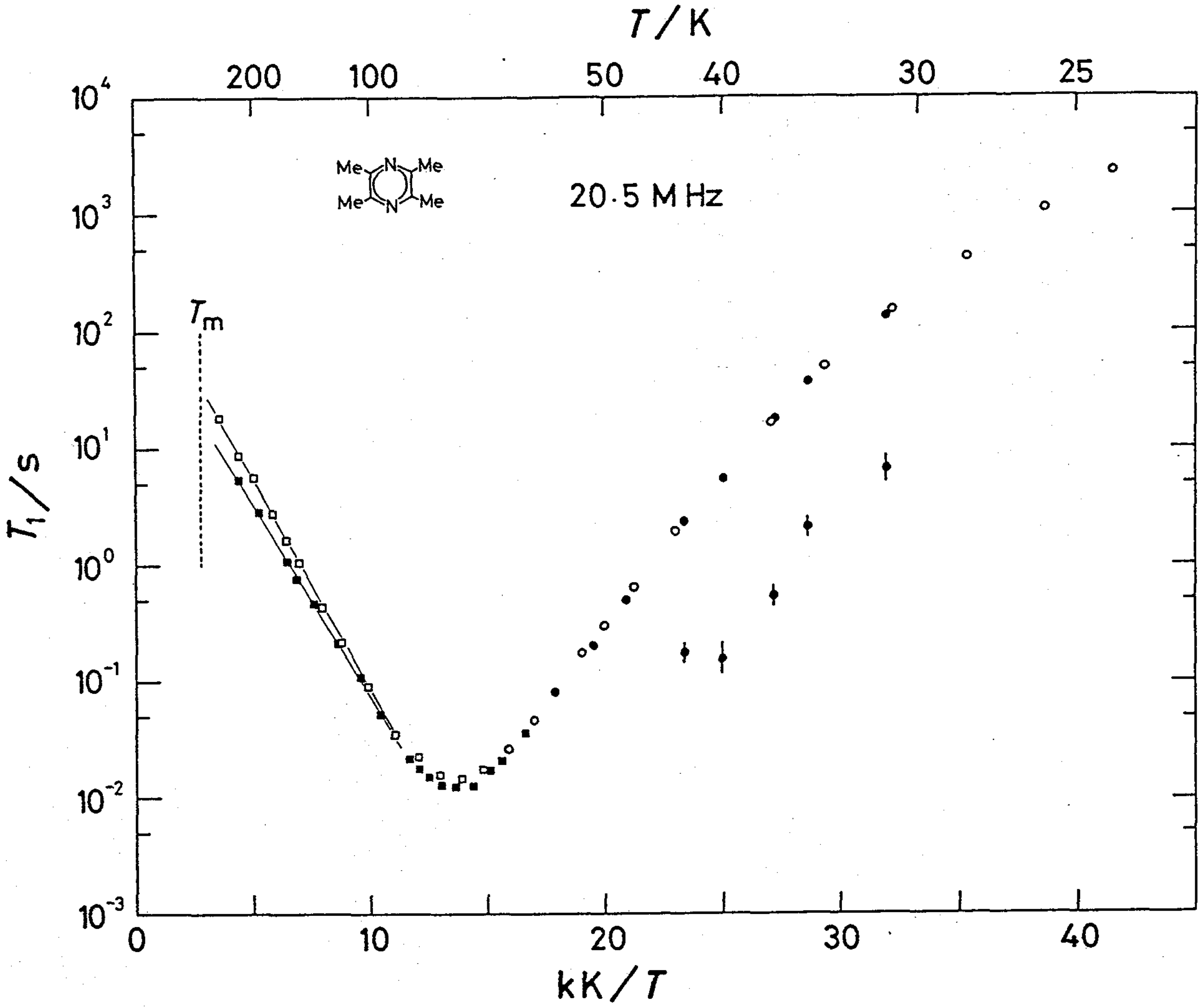

Fig. 6 Temperature dependence of the spin-lattice relaxation time of tetramethylpyrazine at 20.5 MHz. □ (■) was determined from $(\ln 2)^{-1}\tau_{1/2}$ where $\tau_{1/2}$ is the half recovery time of magnetization. □ (○) was obtained by method A (long train) while ■(●) was obtained by method B (short train or a single 90° pulse). ● shows the fast and also slow components (T_{1f} and T_{1s}) of the relaxation.

relaxation time measured by the method A was in good agreement with the slow component T_{1s} by the method B. The weight of T_{1f} component by the method B became small with increasing temperature and the magnetization recovery became single exponential function just below the T_1(min.) temperature. These behaviors are also the same for CH_3SiCl_3, durene, and $Si(CH_3)_4$ and are understood by the symmetry restricted spin diffusion theory (S.R.S.D. theory) by Emid, et al.[7,8] (see in Subsection II.1.3)

As will be dexcribed in Subsection VI.2 - VI.5 the tunneling frequencies of methyl groups in the materials studied in this thesis are comparable order ($10^0 \sim 10^2$ Hz) with the Larmor frequency. At this condition the relaxation of Zeeman system is coupled with the tunneling system, dipolar system and rotational polarization system in general under S.R.S.D. theory.[8] However it was examined by Ligthelm, et al.[10] that the coupling with the tunneling system is most effective on the non-exponential behavior of the Zeeman relaxation at the condition that $\omega_t \approx \omega_0$ (the same order). Therefore we will now consider only the two system, i.e. Zeeman system and tunneling system in the low temperature branch of T_1 curve. By this simplification we can schematically illustrate the non-exponentiality and the dependence of the Zeeman relaxation on the method employed as shown in Fig.7. The origin 0 indicates the complete thermal equilibrium state of the spin system. The abscissa describes the Zeeman system, M_z-M_0; population difference from the thermal equilibrium. The ordinate indicates the tunnel system, N_{AE}-N_{AE0}; the deviation of the population difference between A and

E spin species from the thermal equilibrium value. We can experimentally observe only the longitudinal magnetization M_z which corresponds to the value along the abscissa in Fig.7. Because the relaxation of Zeeman system is coupled to the tunneling system, the relaxation equations are coupled to one another.

$$\frac{d}{dt}(M_z - M_0) = a_1(M_z - M_0) + b_1(N_{AE} - N_{AE0})$$

$$\frac{d}{dt}(N_{AE} - N_{AE0}) = a_2(M_z - M_0) + b_2(N_{AE} - N_{AE0})$$

The solution of eq.(1) is

$$\begin{pmatrix} M_z - M_0 \\ N_{AE} - N_{AE0} \end{pmatrix} = \begin{pmatrix} A_1 & B_1 \\ A_2 & B_2 \end{pmatrix} \begin{pmatrix} \exp(-R_1 t) \\ \mathrm{ex}(-R_2 t) \end{pmatrix} ,$$

Therefore the abscissa $(M_z - M_0)$ and ordinate $(N_{AE} - N_{AE0})$ both containe the two kinds of rate constants, R_1 and R_2. Equation (2) can be decomposed mathematically with regard to the rate constants by a simple rotation of the coordinate axes in the Zeeman -tunnel plane in Fig.7. We obtain

$$\begin{pmatrix} \exp(-R_1 t) \\ \exp(-R_2 t) \end{pmatrix} = \begin{pmatrix} A_1 & B_1 \\ A_2 & B_2 \end{pmatrix}^{-1} \begin{pmatrix} M_z - M_0 \\ N_{AE} - N_{AE0} \end{pmatrix}$$

and then we obtain new coordinate axes I and II as shown in Fig.7. Each of these axes, I and II, contains a single rate

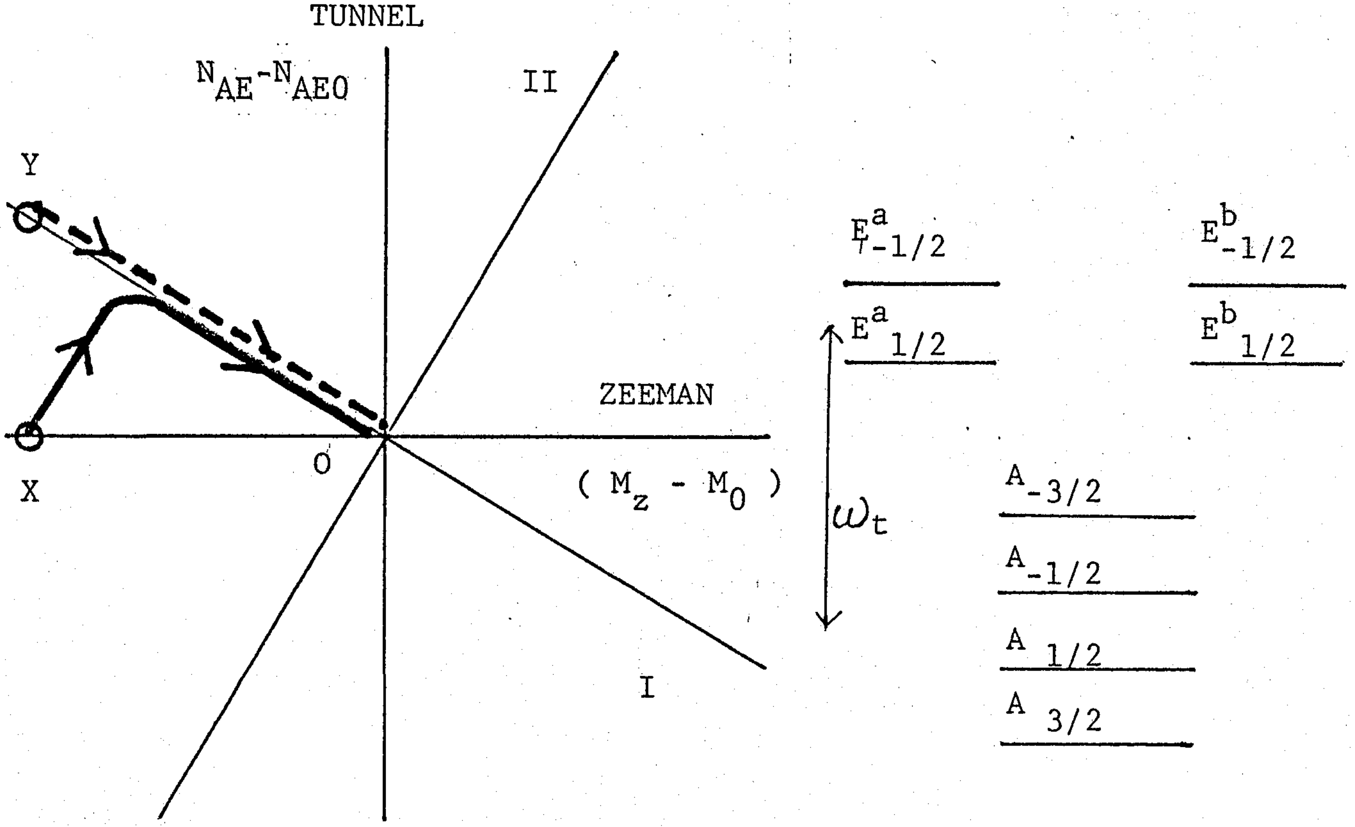

Fig. 7 Schematic view of the spin-lattice relaxation processes of a tunneling methyl group from the different initial conditions of the spin systems, each of wich is prepared by the long train (method A) or the short train (or a single 90° pulse, method B). The right hand side of the figure showes the energy sheme of torsional ground state of a methyl gtoup.

constant R_1 or R_2. This transformation of the coordinate axes do not correspond with the physical operation but only has the mathematical meaning.

A single 90° pulse or a short train of 90° pulse brings the spin system from the point O to the point X. The relaxation occurs firstly along the axis II with large relaxation rate and secondly along the axis I with small rate (as indicated by solid line as in Fig.7). On the other hand, a long train of 90° pulses brings the system from O to Y and the relaxation takes place along the axis I as indicated by the broken line with only one rate constant. Experimentally we observe their projections to the abscissa.

When the tunneling frequency ω_t equals zero or the condition that $(\omega_t + n\omega_0)\tau_c \ll 1$ is satisfied, Zeeman system is coupled only to the rotational polarization system 7,8). The similar concept as that described above is acceptable9).

It was observed that below the T_1(min.) temperature the weight of T_{1f} component by the method B became small with increasing temperature. This fact corresponds with the result that the tunneling frequencies $\omega_t^{SS'}$ decrease when the temperature increases as will be examined in the following Subsections.

Thus the behaviour of the Zeeman relaxation due to the rotation of methyl groups is not contradiction to the S.R.S.D. theory.

VI. 2 Methyltrichlorosilane, CH_3SiCl_3

VI. 2.1 Tunneling spectrum and the potential barrier hindering the rotation of a methyl group.

Figure 8 shows the results of field cycling experiment for CH_3SiCl_3 at 11.7 and 20.5 K. The results at both temperatures show two small peaks indicated by arrows and a large enhancement of the magnetization below 0.55 T. This enhancement below 0.55 T was attributed to the cross relaxation effect between the protons and the chlorine nuclea, i.e. ^{35}Cl and ^{37}Cl. The effect of cross relaxation is to shorten the spin-lattice relaxation time of proton. The relaxation of spin energy of the chlorine nucleus is induced by the nuclear quadrupole interaction[11] and the energy exchange between the proton and chlorine nucleus is performed by the dipole-dipole interactions.[12] When the spin lattice relaxation time of chlorine nucleus is much shorter than that of proton, the spin energy of the proton flows to the lattice through the chlorine spin system.

The nuclear spin of ^{35}Cl (or ^{37}Cl) is 3/2 and therefore they have a finite quadrupole moment Q. The interaction of the quadrupole moment of a nucleus with the electric field gradient at its position due to surrounding charges induce the energy separation of the spin states. In absence of external magnetic field H_0 there are two doubly degenerate energy levels $E_{|m|}$ ($m = \pm 1/2, \pm 3/2$). The Zeeman field removes this degeneracy

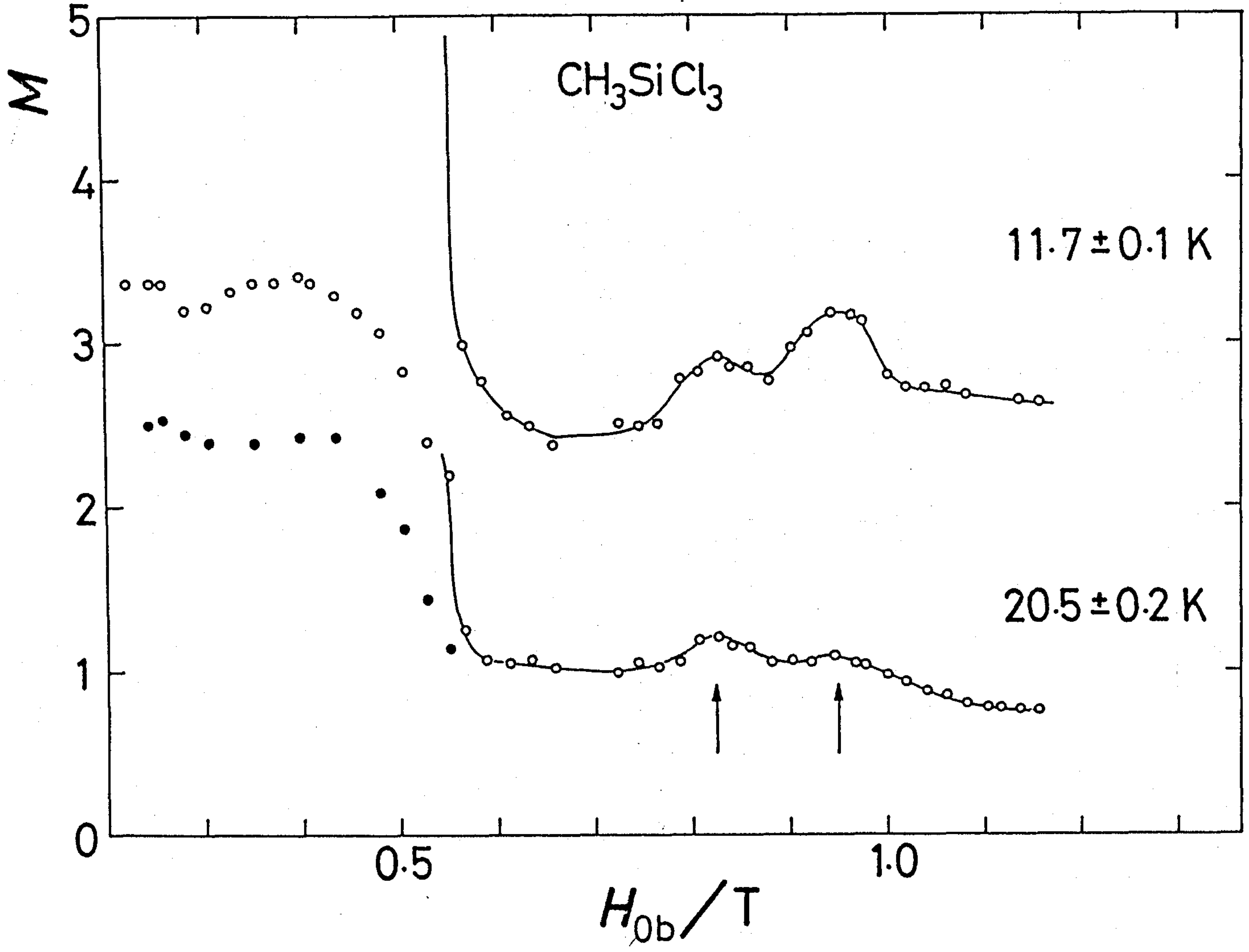

Fig. 8 Results of field cycling runs for trichloromethylsilane (CH_3SiCl_3). The magnetization M is plotted in arbitrary scale against the external magnetic field H_{0b}. The reference field H_{0a} is 0.70 T (29.9 MHz). The time τ was chosen as 467 ± 3 s (11.7 K) and 245 ± 2 s (20.5 K). ● show the observed points at 11.7 K, which were divided by the factor of 5.

and for $|m| = 3/2$ there are two energy levels,

$$E_m = A\left[3m^2 - I(I+1)\right] - m\hbar\Omega\cos\theta. \qquad (4)$$

The case of the states $m=\pm1/2$ is somewhat special[12]. The mixing between the states $|+1/2\rangle$ and $|-1/2\rangle$ occurs to form new states $|+\rangle$ and $|-\rangle$ with energies given by,

$$E_\pm = A\left[3/4 - I(I+1)\right] \mp (f/2)\hbar\Omega\cos\theta \qquad (5)$$

$$f = \left[1 + (I+1/2)^2 \tan^2\theta\right]^{1/2}$$

This energy scheme is obtained for the axially symmetric field gradient ($\eta = 0$) and the magnetic field is considered to be rather weak, i.e. $\hbar\Omega << e^2qQ$. The energy scheme is shown in Fig. 9. For CH_3SiCl_3 the asymmetry parameter η is probably finite and the magnetic field is not so weak in the present case of the field cycling experiments. However, we can estimate the frequencies between the spin states (Fig.9) with sufficient accuracy for our purpose by using Eq. (4) and (5). Three kinds of pure quadrupole frequencies of CH_3SiCl_3 were observed by Hooper and Bray[14), which are 18.955, 19.020 and 19.155 MHz at 77 K. The maximum frequency of chlorine nucleus in the magnetic field corresponds with the transition indicated by arrow in Fig.9. The separation between $|-3/2\rangle$ and $|+\rangle$ with the condition that $\cos\theta=1$ is 22.3 MHz (0.52 T) at 0.55 T of external magnetic field. Blow 0.55 T the effect of "cross relaxation" is to be observed, because the separations smaller than 22.3 MHz exist

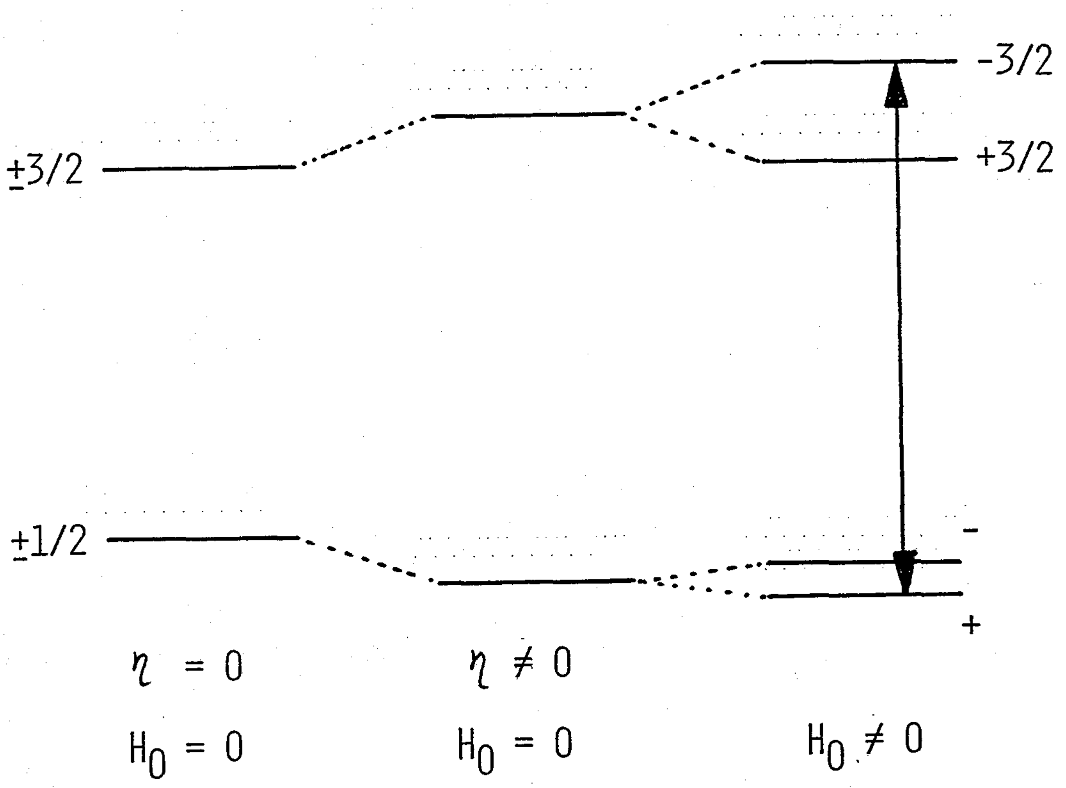

Fig. 9 The energy scheme of ^{35}Cl nucleus (I = 3/2). η is the asymmetry parameter and H_0 is the external magnetic field.

for ^{35}Cl and do so for ^{37}Cl of which the quadrupole moment Q is smaller than that of ^{35}Cl by the factor of 0.78. This fact is in good agreement with the experimental result that the large enhancement of the proton magnetization was observed below 0.55 T. Above 0.55 T the effect of "cross relaxation" is not expected.

The two peaks of magnetization indicated by arrows in Fig.8 is the tunnel spectrum of a methyl group. The frequencies of these peaks are 34.6 ± 0.5 and 40.4 ± 0.5 MHz. The two peaks are attributed to the different kinds of methyl groups which are hindered by slightly different potential barriers in the crystal. Because the crystal structure of CH_3SiCl_3 has been not known, we cannot obtain the complete informations about the surroundings of a methyl group. But we can obtain an information about the averaged distance between the methyl groups from the second moment value. The observed line shape is a typical one which is expected for a rapidly reorienting[2,15)] or tunneling[3,4,16)] methyl group about its C_3 symmetry axis (Figs.10 and 11). We note that the portion of intermethyl broading is very small and the shift due to intramethyl dipole interaction was distinguishable (Fig.11). The second moment at 83.3 K is 6.6 ± 0.1 G^2, which is larger than that reported by Rochow, et al.[17)] (3.55 G^2 at 77 K). The discrepancy of these values is due to the missing tails of the experimental curve by Rochow, et al. This is not due to other modes of molecular motion but probably due to instrumental problem. Indeed any other mode of molecular motion in CH_3SiCl_3 crystal was not detected by our measurement of line shape up to 120 K (Fig.12) and also by our spin-lattice

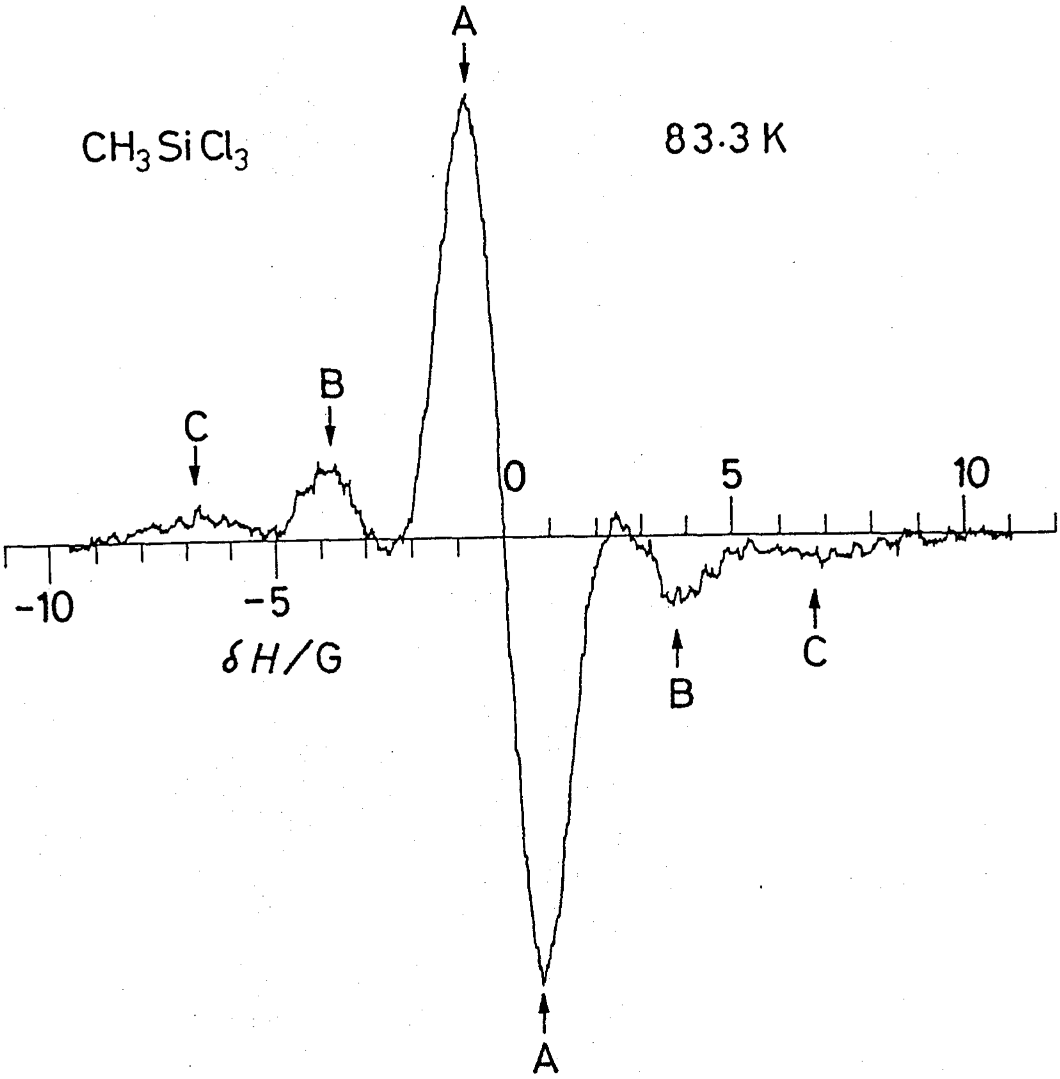

Fig. 10 Typical differential absorption line of trichloromethylsilane (CH_3SiCl_3).

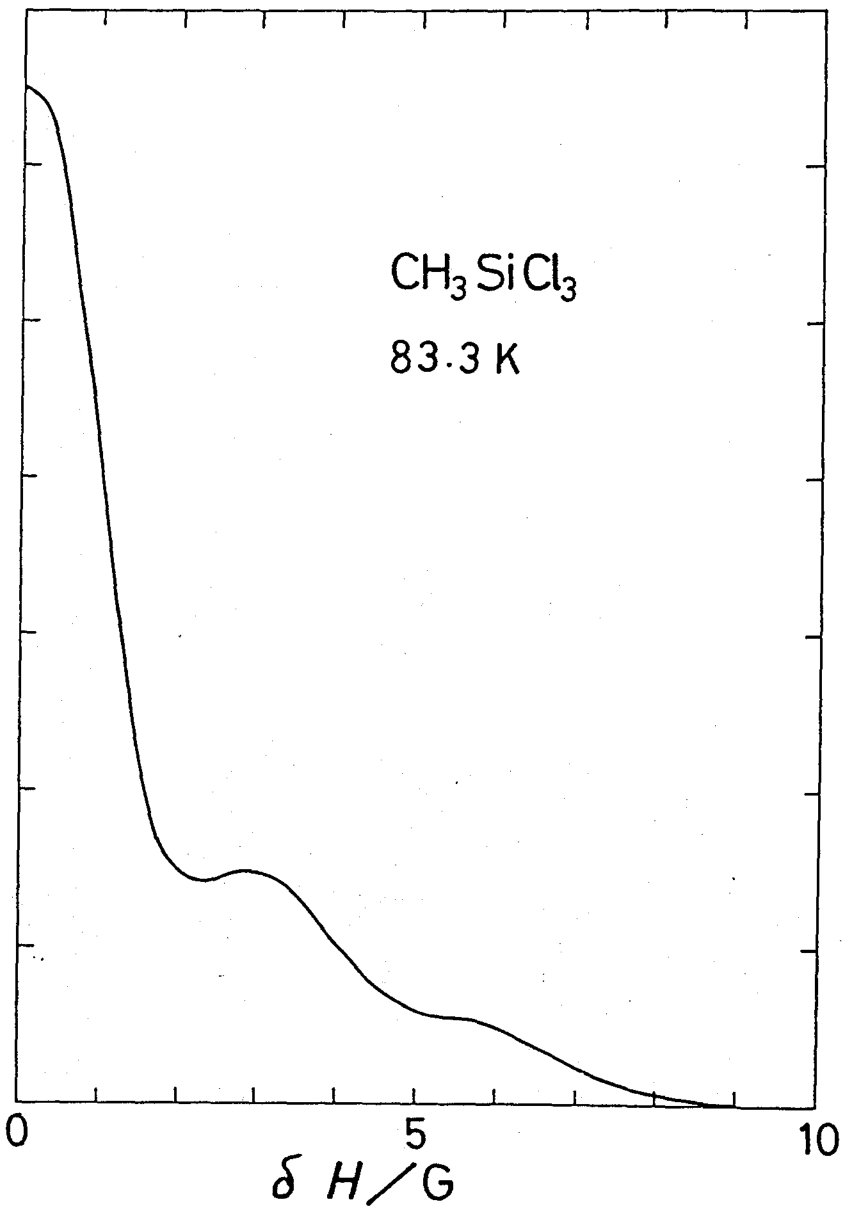

Fig. 11 A half of absorption line of trichloromethylsilane, CH_3SiCl_3. The shape was obtained by integrating the observed differential absorption line (Fig. 10).

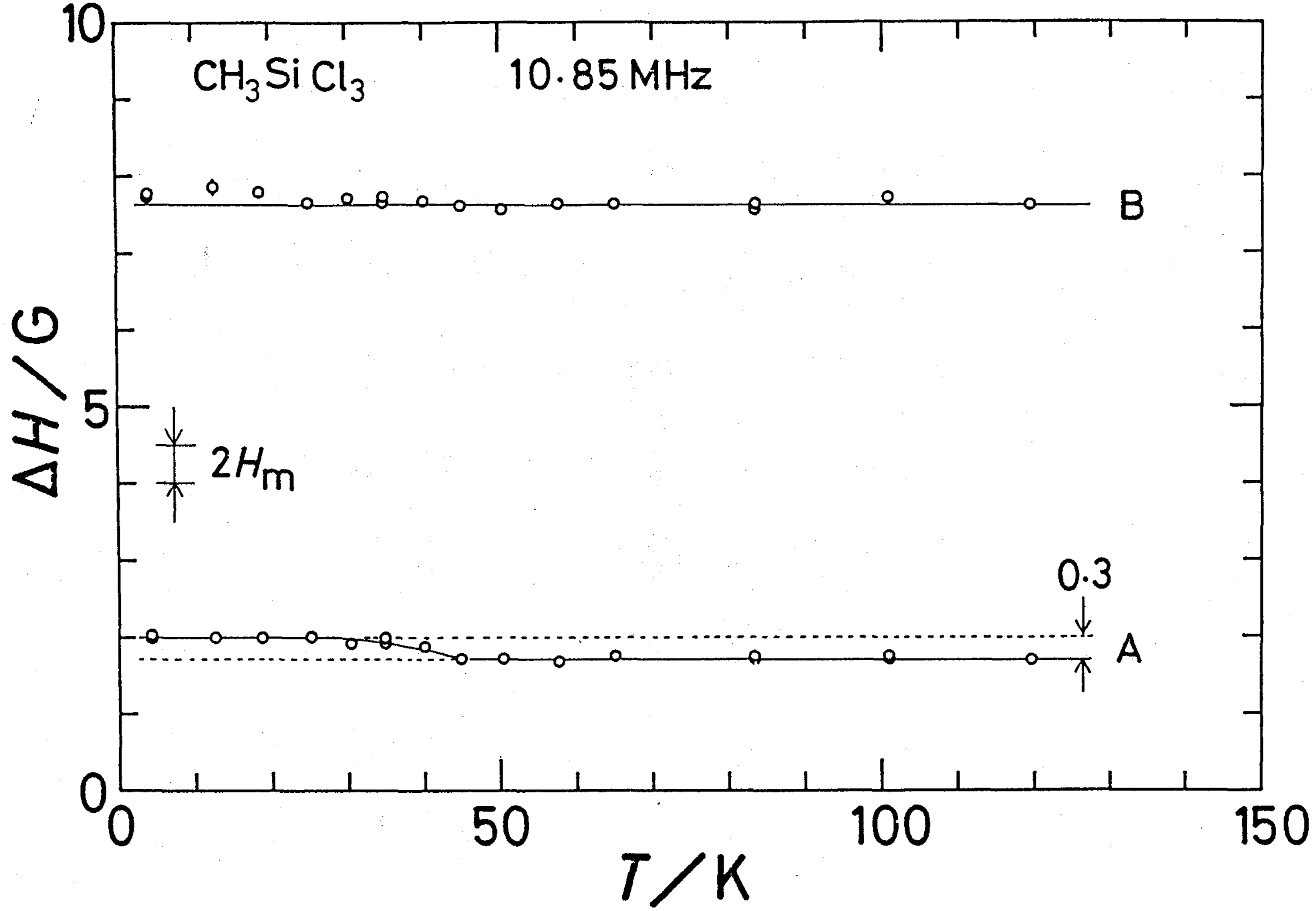

Fig. 12 Temperature dependence of the maximum slope width of the differential absorption line of CH_3SiCl_3. A and B indicate the peaks shown in Fig. 10.

relaxation measurement. The small reduction of line shape at about 30 ~ 45 K in Fig.12 will be discussed in Subsection VI. 7. The expected second moment M_2(intra.) due to intramethyl dipole interaction for a rapidly reorienting or tunneling methyl group is 5.26 G^2 2-4,17), assuming an interproton distance of 1.80 Å (C-H distance equals 1.10 Å). The observed intermolecular contribution M_2(inter.) of CH_3SiCl_3, which is partially averaged by the methyl rotation, is 1.3 G^2. This value is much smaller than 4 G^2 and 5 G^2 for T.M.P. and T.M.S.1), respectively (see in Subsection VI.7). To estimate the intermethyl contribution to the second moment for rapidly rotating methyl group, we can cram the three spins in a methyl group at the center of a triangle of the methyl group. The amplitude of the second moment is proportional to the inverse of the sixth powers of a distance R.18) When we consider the effective (averaged) distance $\langle R \rangle$ between the centers of the methyl groups and we use M_2 (inter.) $\propto \langle R \rangle^{-6}$. The value of $\langle R \rangle$ for CH_3SiCl_3 is larger than that for T.M.P. and T.M.S. by about 20%. The mechanical coupling between the methyl groups is considered to be induced by the repulsive force between the protons in different methyl groups. The amplitude of this force is proportional to $\langle R \rangle^{-12}$ if one assume the Lennard-Jones type potential. The strength of the repulsive force between the methyl groups in CH_3SiCl_3 crystal is wearker than that for T.M.P. and T.M.S. by the factor of about one order. This estimate suggests that the effect of mechanical coupling betweeen the methyl groups for CH_3SiCl_3 does not play an impotant role in the torsional dynamics unlike as the cases of durene, T.M.P., T.M.S., and H.M.B. (see in

Subsection VI.3,4, and 5).

Each of the observed peaks of magnetization is one of the pair which is expected to appear at the conditions that $\omega_t = \omega_0$ and $\omega_t/2 = \omega_0$ as described in Subsection IV.2. We can estimate which peak of the pair we observed by the field cycling experiment (Fig.8). It is useful method for extimating the magnitude of tunneling frequency ω_t to measure the frequency dependence of relaxation time at low temperature limit, i.e. the condition that $(\omega_t + n\omega_0)^2 \tau_c{}^2 \gg 1$ becomes satisfied. In this limit the spin-lattice relaxation time is proportional to

$$\sum_{n=-2}^{+2} a_n (\omega_t + n\omega_0)^2 \tau_c \qquad (6)$$

where τ_c is the correlation time of the rotation of a methyl group. It is expected from Eq.(6) that we obtain the $\omega_0{}^2$ -dependence of the spin-lattice relaxation time T_1 at high frequency limit ($\omega_t \ll \omega_0$) and on the other hand T_1 is independent on the Larmor frequency at low frequency limit ($\omega_t \gg \omega_0$). Figure 13 shows the result of ω_0 -dependence of the slowly-relaxing component T_{1s} measured by the field cycling technique, which indicates the neary $\omega_0{}^2$-dependence at 1.1 T (46.8 MHz). Therefore it is not probable to consider that each of the observed peaks in Fig.8 corresponds to $\omega_t/2$. The peaks corresponding to $\omega_t/2$ probably exist at 17.3 MHz (0.41 T) and 20.2 MHz (0.47 T). These peaks are concealed by the "cross relaxation" effect (Fig.8).

Assuming the sinusoidal potential barrier hindering the

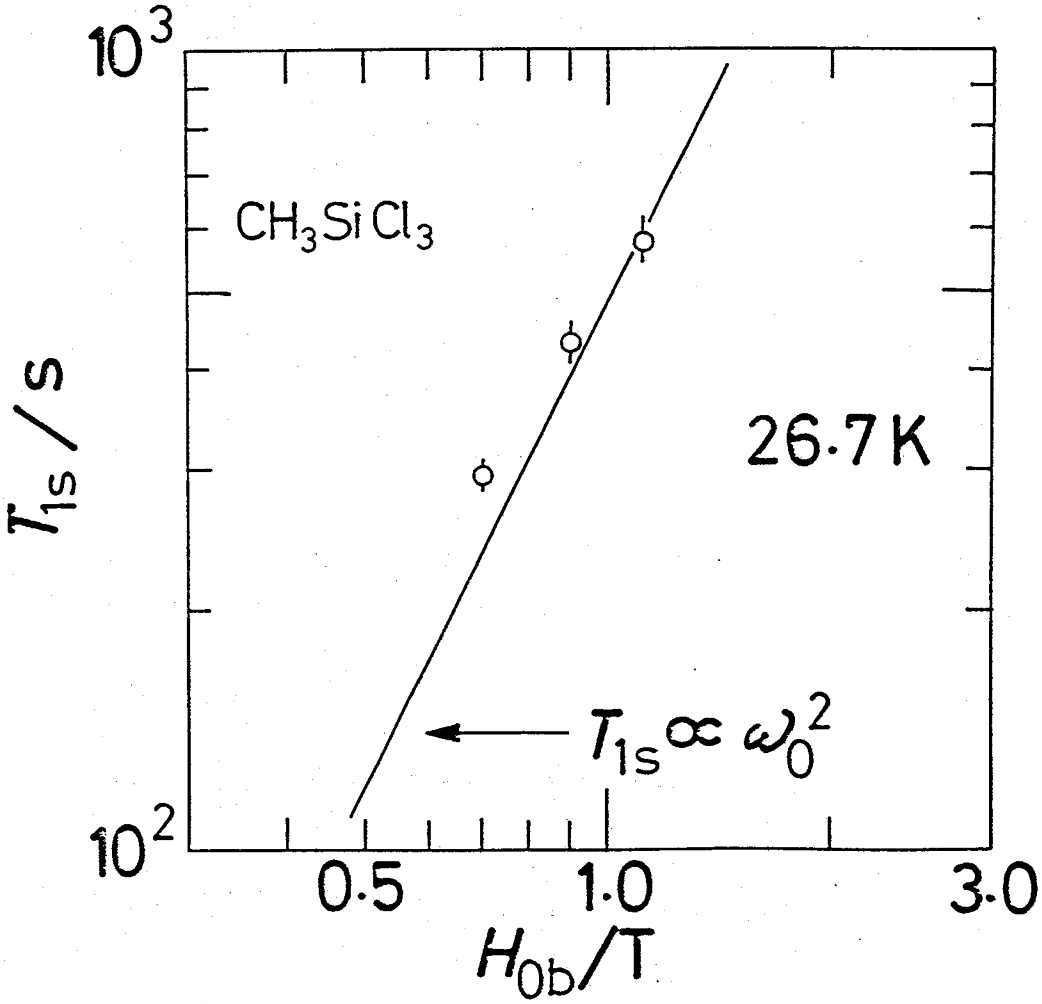

Fig. 13 Frequency dependence of the slowly-relaxing component of spin-lattice relaxation time (T_{1s}) of CH_3SiCl_3.

rotation of a methyl group as follows,

$$V(\theta) = (V_3/2)(1 - \cos 3\theta). \qquad (7)$$

We can estimate the torsional energy and tunneling splitings by using the table of characteristic values of Mathecis equation[19)] and the activation energy E_a=5.8 kJ mol^{-1}obtained from the T_1 measurement. The result of T_1 measurement will be discussed later. The estimated tunneling splitting Δ_0 of the torsional ground state (E_0) is 48.4 MHz with the hindering varrier V_3= $E_a + E_0$ =6.74 kJ mol^{-1}and the separation (E_1-E_0) between the torsional first excited and ground state is estimated to be 113 cm^{-1}. The observed torsional energy is 160 cm^{-1} which was obtained by inelastic neutron scattering experiment[21)]. The observed peak was not broad unlikely as that of $Si(CH_3)_4$. The discrepancy between the observed and estimated values probably comes from the higher terms of the potential function which were neglected in Eq.(7). The difference of 0.2~0.3 kJ mol^{-1} of V_3 value in Eq.(7) induces the variation of 2~17 MHz in Δ_0 and the variation of 2~3 cm^{-1} in the torsional energy (E_1-E_0). This small difference (0.2~0.3 kJ mol^{-1}) of the hindering barrier is to be produced by the different surroundings of the methyl groups in solid.

It was revealed that the tunneling frequencies in torsional ground state of a methyl group in CH_3SiCl_3 solid were 34.6 and 40.4 MHz which correspond with the different circumstances of the methyl groups in the crystal. The temperature dependence of the tunneling frequencies was not observed directly. However, the indirect evidence of decreasing tunneling frequency as temperature increased was obtained from the behavior of the temperature dependence of the magnetization recovery, which will be discussed in the next.

VI. 2.2 The spin-lattice relaxation time.

The "cross relaxation" effect between the proton and chlorine nucleus is effective to shorten the T_1 value of the proton below about 0.6 T (corresponds to the Larmor frequency 25.5 MHz of proton) as demonstrated in Fig. 8. It must be noted that the spin-lattice relaxation time should be measured with the Larmor frequency larger than 25.5 MHz to eliminate the effect of cross relaxation and to obtain the reliable values of T_1 due to methyl rotation.

The temperature dependence of T_1 measured at 29.9 MHz is shown in Fig.14. The characteristic behavior of the magnetization recovery has been already described in Subsection.

VI. 1 The weight of the fast-recovering component T_{1f} of this material is very small in the low temperature branch and T_{1f} component was confirmed by this experiment at least below 36.9 K. However the presence of this component was confirmed by this experiment at least below 36.9 K. The weight of the T_{1f} component became small and further became unobsevable when the temperature increased. This result is to be compared with the prediction by Punkkinen, et al[22). that the weight of the T_{1f} component becomes small when the value of ω_t/ω_0 becomes small.

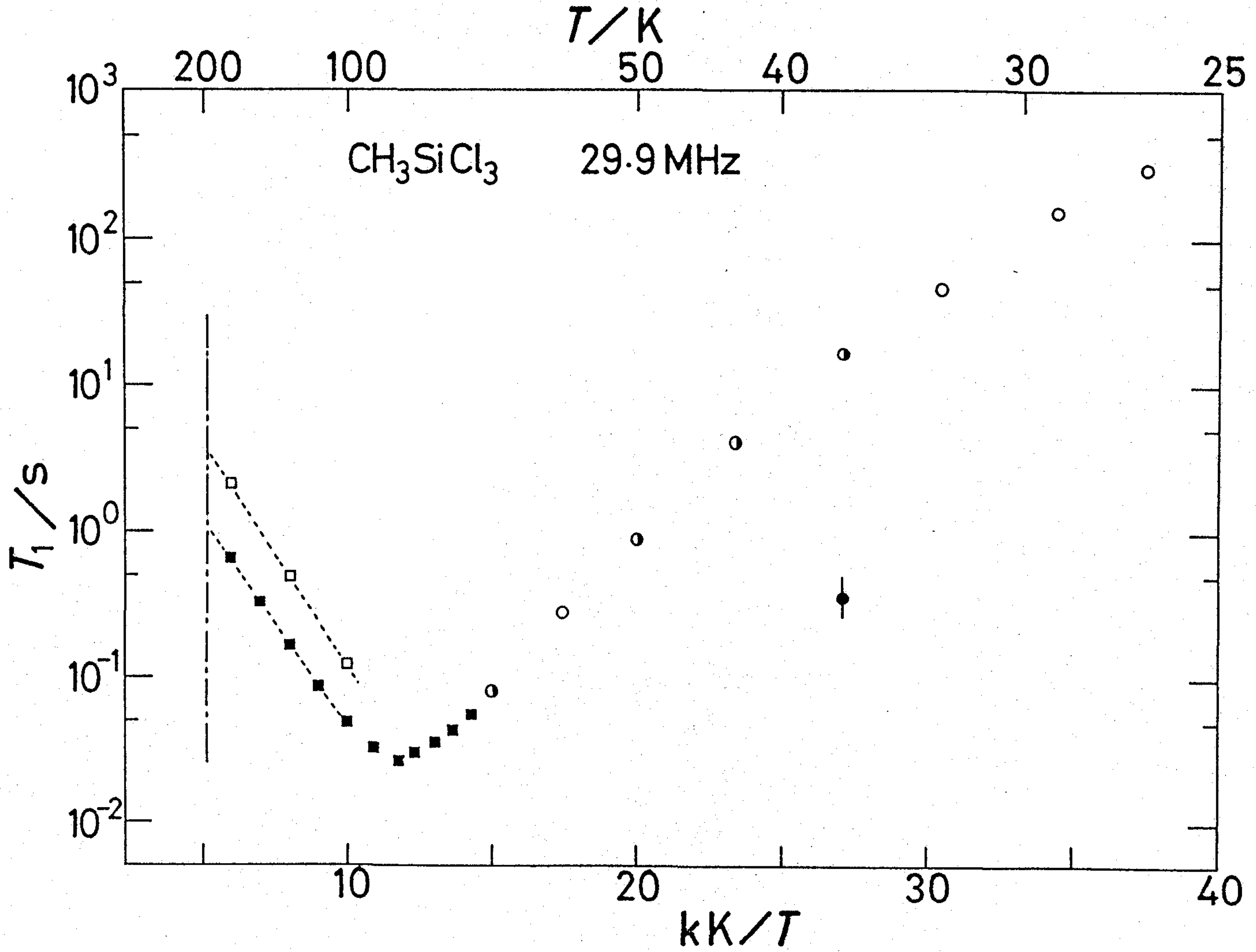

Fig. 14 The temperature dependence of spin-lattice relaxation time at 29.9 MHz of CH_3SiCl_3. □ (■) s determined from $(\ln 2)^{-1}\tau_{1/2}$ where $\tau_{1/2}$ is the half recovery time of magnetization. □ (○) was obtained by method A while ■ (●) was obtained by method B. ◑ indicate that the slow component (T_{1s}) by B (●) falls on ○. ● also shows the fast component (T_{1f}) of relaxation.

This comparison leads us to the conclusion that the effective tunneling frequency ω_t of a methyl group of CH_3SiCl_3 decreases when the temperature increases. The detailed dependence on the temperature was not obtained.

The condition that $\omega_0=\omega_t$ ($\omega_0/2\pi$ = 29.9 MHz) will be satisfied between 20.5 and 67 K. 20.5 K is the temperature at which the tunneling frequencies were observed by field cycling technique and 67 K is the temperature at which the character of the coupling between the Zeeman system and the tunneling system disappeared and the character of the coupling between the Zeeman and rotational polarization systems became strong. Because the weight of T_{1f} of CH_3SiCl_3 is small, the tunneling assisted minimum of the spin-lattice relaxation time, which should appear only in the T_{1f} component as described in Subsection IV.2 and as will be demonstrated for $Si(CH_3)_4$ in Subsection VI.4, was not detectable. However the tunneling assisted minimum exists. Indeed the peaks of the magnetization in the field cycling spectrum were observed which is caused by the tunneling assisted minimum of the spin-lattice relaxation time through the equation (1) in Section IV. Wei and Johnson[23)] reported the non-exponential relaxation in the vicinity of the T_1 (min.) and on the high temperature side of the T_1 (min.). This is in good agreement with our results and is understood in the framework of S.R.S.D. theory as described in this Section. It should be noted that the nonexponentiality also exists in the low temperature side of T_1 (min.) and the tunneling assisted relaxation exisists although the weight of T_{1f} is small and it is difficult to obtain that by the measurement of the spin-lattice relaxation time v s. temperature.

In the low temperature branch ($T \lesssim 60$ K) the relaxation time determined by the method A was in good agreement with the slow component (T_{1s}) by the mehtod B. The magnetization recovery was also non-exponential and depended on the method employed near and above the T_1 (min.) temperature (Fig.14). But the detailed characters of the magnetization recovery below and above the T_1 (min.) temperature were different from one another, which correspond with the different nature of the coupled relaxation between the Zeeman system and other systems. In the low temperature region the Zeeman system is coupled with the other three systems, especially to the tunnel system. On the other hand the Zeeman system is coupled only to the rotational polarization system near and above the T_1 (min.) temperature. In the latter case it was confirmed that the fast-relaxing component T_{1f} was in good agreement with the autorelaxation time of the Zeeman system[52] (Subsection II. 1.3). The autorelaxation rate of the Zeeman system is described by.

$$T_1^{-1} = \frac{9}{20} \frac{\gamma^4 \hbar^2}{r^6} \left(\frac{\tau_c}{1 + \omega_0^2 \tau_c^2} + \frac{4\tau_c}{1 + 4\omega_0^2 \tau_c^2} \right) \qquad (8)$$

for classical jump-reorientation of a methyl group, i.e. $\omega_t=0$ (see Eq.(30) in Subsection II.1.3).

The T_{1f} and T_{1s} components were decomposed from the magnetization recoveries measured by the pulse sequence B and are shown in Fig.15. The low temperature branch of the T_{1s} curve includes

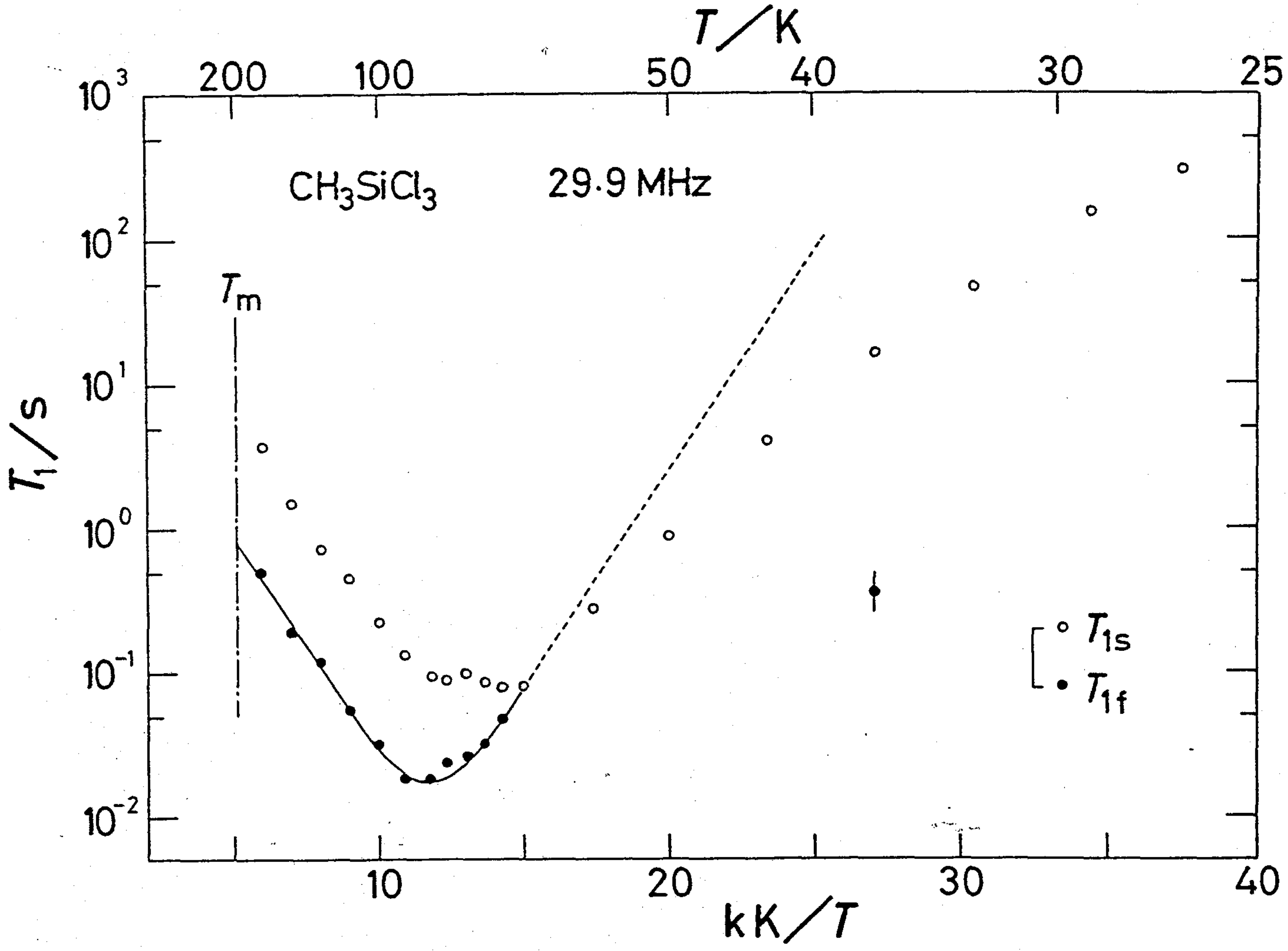

Fig. 15 The temperature dependence of the spin-lattice relaxation time at 29.9 MHz of CH_3SiCl_3. The fast-relaxing component T_{1f} (●) and slowly-relaxing component T_{1s} (○) were separately shown in the whole temperature region.

the T_1 values determined by the pulse sequence A which are in good agreement with the T_{1s} component determined by method B. The solid curve is the calculated value using Eq.(8), which is applicable only for T_{1f} at and above the minimum temperature as shown in Fig.15. We can derive the rate ω_3 with which a methyl group jumps between the potential wells, where the relation between ω_3 and τ_c for the classical reorientation is $3\omega_3 = \tau_c$ as described in Subsection III.4. The derived ω_3 is described as

$$\omega_3 = 3.62 \times 10^{11} \exp (-5.8 \ \mathrm{kJ\,mol^{-1}} / RT) \qquad (9)$$

Here we considered only the second term of the correlation time in Eq.(35) in Subsection II.1.4. This term is most effective at and above the T_1 (min.) temperature of the observed T_{1f} curve. In this temperature region the nature of the rotation of a methyl group can be understood as a jump-reorientation over the potential barrier. The first term of Eq.(35) in Subsection II.1.4 plays an impotant role at low temperatures. For the complete fitting of T_{1f} and T_{1s} over the full temperature region one must solve the coupled differential equation (Eq. (29) in Subsection II.1.3) numerically. If we do so the averaged value of the first term of correlation time in Eq.(35) in Subsection II.1.4 is obtained. We do not treat this problem in this thesis.

VI. 3 1,2,4,5-tetramethylbenzene (durene) and tetramethylpyrazine (T.M.P.)

VI. 3.1 Tunneling spectrum of the methyl groups. An evidence of "coupled rotational tunneling state".

The tunnel spectra of methyl groups in durene observed by field cycling technique between 15.2 and 27.5 K are shown in Fig. 16. The six peaks of magnetization, i.e. A(9.2±0.4 MHz), B(12.2±0.3 MHz), C(15.6±0.5 MHz), D(17.8±0.5 MHz), E(25.3±0.6 MHz), and F(29.3±0.7 MHz), were identified in this temperature region. The positions of these peaks did not change up to 27.5 K. For a single methyl group it is expected that the two peaks of magnetization, which correspond to $\omega_0=\omega_t$ and $\omega_0=\omega_t/2$, should appear in the field cycling spectrum. When we consider this pairwise relation of magnetization peaks due to one kind of tunneling spliting ω_t, we find the three pairs of magnetization peaks in Fig.16. The different three sets are A-D, B-E, and C-F. Therefore the three kinds of tunneling splittings $\hbar\omega_t{}^i$ (i=1,2,3) were clearly observed for the methyl groups of durene. This relation is tablated for three kinds of splittings $\hbar\omega_t{}^i$ in Table 1.

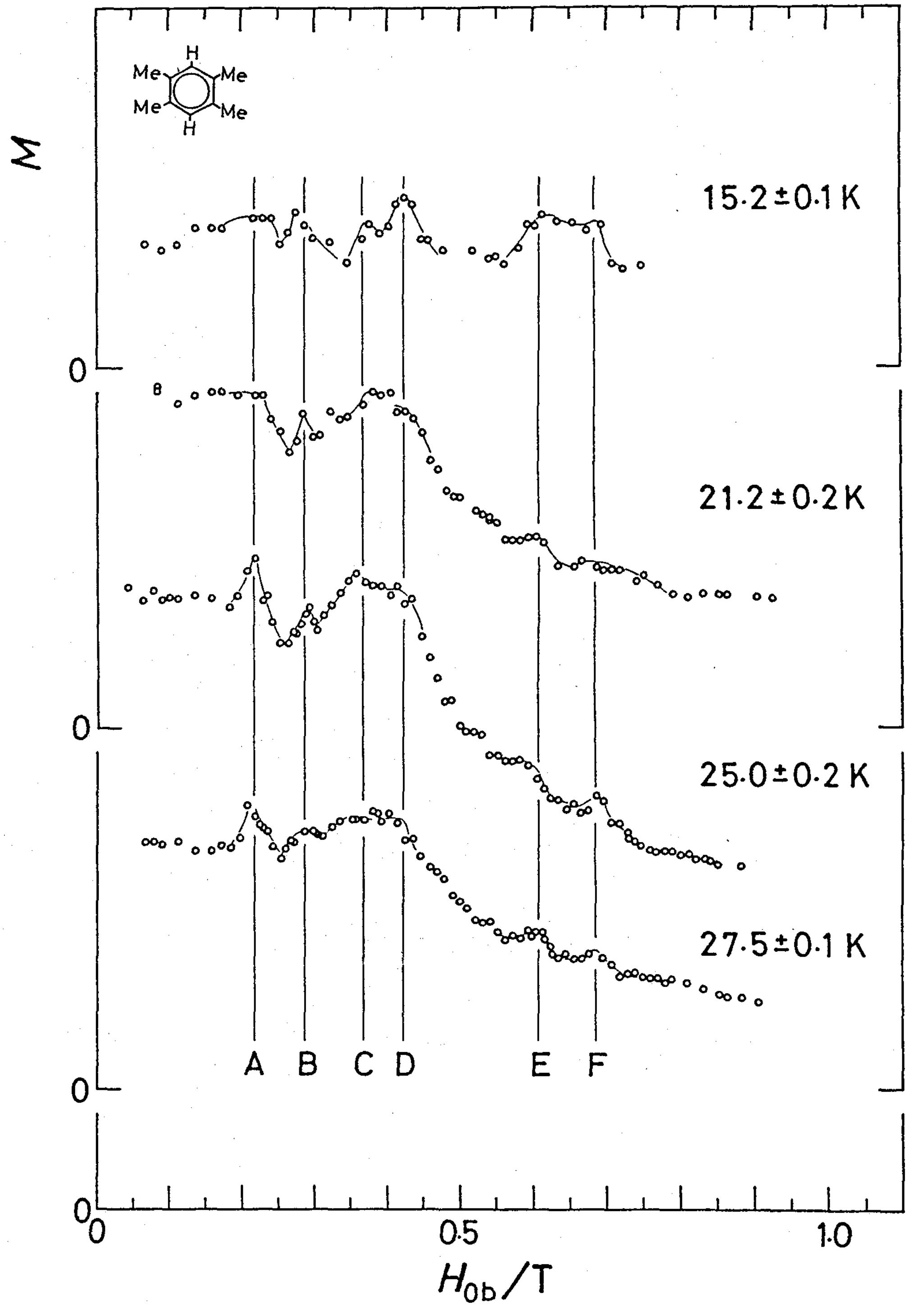

Fig. 16 Results of field cycling runs for durene. The magnetization M is plotted in arbitrary scale against the external magnetic field H_{0b}. The reference field is 0.47 T (20.5 MHz). The time τ was chosen as 608 ± 6 s (15.2 K), 153 ± 2 s (21.2 K), 61.5 ± 0.1 s (25.0 K), and 27.4 ± 0.1 s (27.5 K).

Table 1.

	$\nu_t^{SS'}$ /MHz	$(\nu_t^{SS'}/2)$/MHz
ν_t^1	29.3 ± 0.7	15.6 ± 0.5
ν_t^2	25.3 ± 0.6	12.2 ± 0.3
ν_t^3	17.8 ± 0.5	9.2 ± 0.4

The tunnel spectra of the methyl groups in T.M.P. observed between 4.2 and 30.3 K are shown in Fig.17. The arrengement of methyl groups in a T.M.P. molecule is similar to that of durene. The identified peaks of magnetization are five kinds, i.e. A (6.4 ± 0.7 MHz), B (9.5 ± 0.8 MHz), C (14.3 ± 0.6 MHz), D (20.2 ± 0.8 MHz), and E (26.8 ± 0.8 MHz). The positions of the peaks did not change up to 30.3 K. When we consider the pairwise relation of peaks as we did for durene, we find the two sets of pairs. These are B-D and C-E. If the counterpart of the magnetization peak A is concealed in the peak C or exists at 0.075 T (3.2 MHz) in the field cycling spectrum (Fig.17), the different sets of pairs of peaks are three kinds. Therefore the three different tunneling splittings were obtained for T.M.P. like as in the case of durene. This relation between the observed peaks is tablated in Table.2.

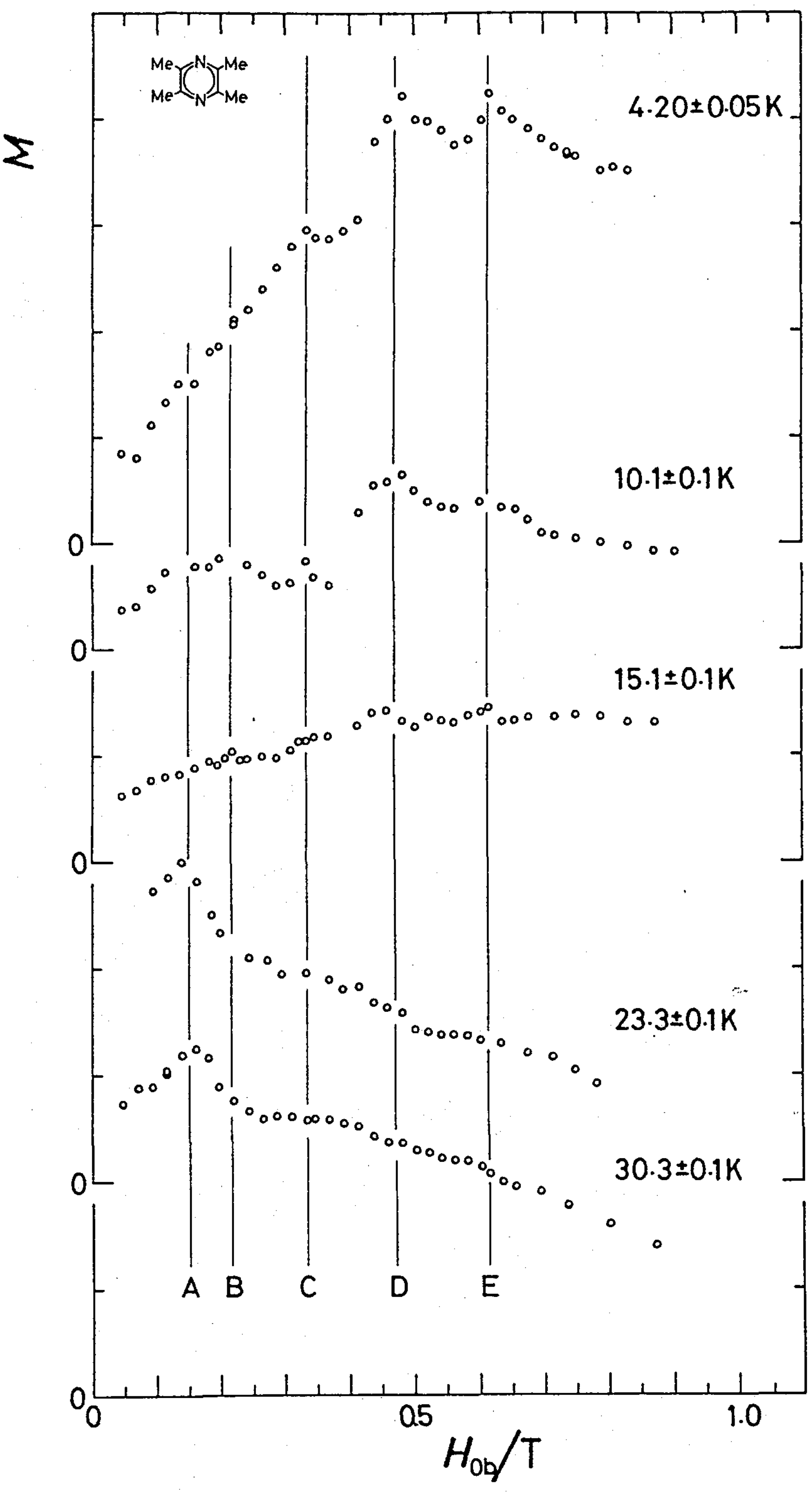

Fig. 17 Results of field cycling runs for tetramethylpyrazine. The magnetization M is plotted in arbitrary scale against the external magnetic field H_{0b}. The reference field H_{0a} is 0.47 T. The time τ was chosen as 911 ± 1 s (4.20 K), 911 ± 1 s (10.1 K), 833 ± 3 s (15.1 K), 548 ± 3 s (23.3 K), and 111 ± 1 s (30.3 K).

Table 2

	$\nu_t^{SS'}$ /MHz	$(\nu_t^{SS'}/2)$/MHz
ν_t^1	26.8 ± 0.8	14.3 ± 0.6
ν_t^2	20.2 ± 0.8	9.5 ± 0.8
ν_t^3	6.4 ± 0.7 or 14.3 ± 0.6	--------- 6.4 ± 0.7

A tetramethylpyrazine molecule includes two ^{14}N nuclea which are crystalographically identical.[24,25] The spin I of ^{14}N nucleus is 1 and therefore it has a finite quadrupolemoment. The pure quadrupole resonance lines were observed by Guibe and Lucken[26] at 77 K. They reported that the value of e^2qQ was 4.672 MHz and the asymmetry parameter η was 0.450 at 77 K. The energy scheme of the spin state of ^{14}N nucleus is shown in Fig.19. The energy splittings are described by[27]

$$E_{\pm} = \frac{e^2qQ}{4} \pm \left\{(\hbar\,\Omega)^2 \cos^2\theta + \left(\frac{e^2qQ}{4}\right)^2 \eta^2\right\}^{1/2}$$

$$E_0 = -\frac{e^2qQ}{2} \qquad (10)$$

We cannot a priori neglect the possibility that the effect of "cross relaxation" between the proton and ^{14}N nucleus appears in the field cycling spectrum as in the case of CH_3SiCl_3 (Subsection VI.2). The possible maxaimum separation between the spin state of ^{14}N nucleus can be estimated in the frame-

TMP

1,2,4,5,TMB

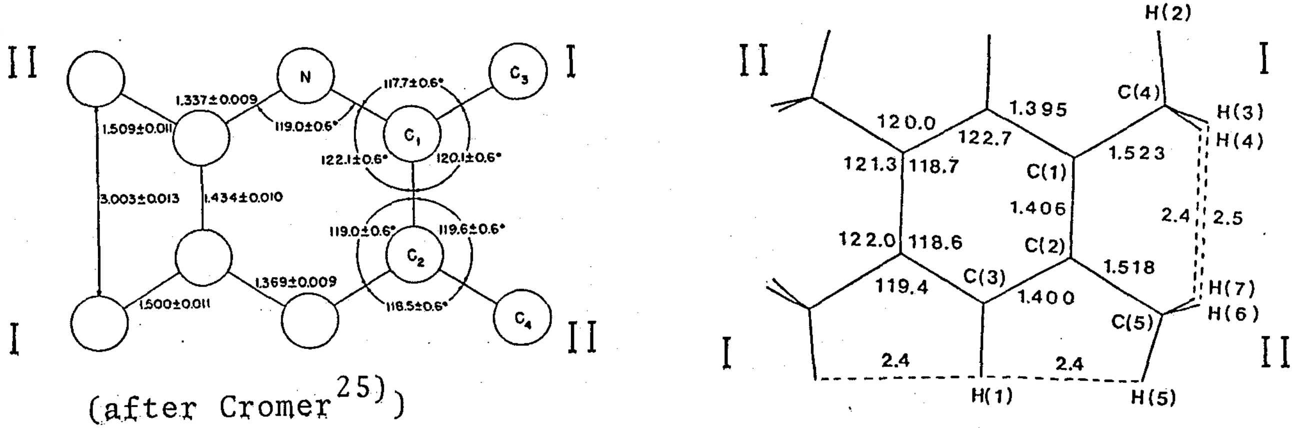

(after Cromer$^{25)}$)

(after Stam$^{28)}$)

ORTHORHOMBIC

Pbca

$a = 8{\cdot}35$ Å

$b = 9{\cdot}27$ Å

$c = 10{\cdot}62$ Å

$Z = 4$

MONOCLINIC

$P2_1/a$

$a = 11{\cdot}59$ Å

$b = 5{\cdot}74$ Å

$c = 7{\cdot}04$ Å

$\beta = 112{\cdot}8°$

$Z = 2$

Fig. 18 Crystal structures and molecular structures of durene and tetramethylpyrazine.

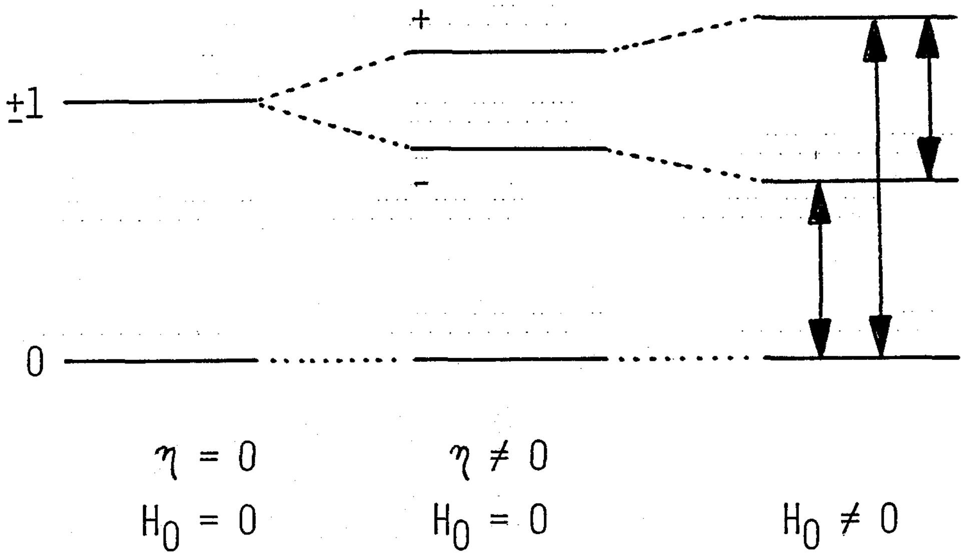

Fig. 19 Spin-states of ^{14}N nucleus. η is the asymmetry parameter and H_0 is the external magnetic field.

work of Eq.(10) using the deta obtained by Guibe, et al. The maximum value is 4.2 MHz at 0.15 T (correspond to 6.4 MHz of proton) with the condition that $\cos\theta=1$. The observed magnetization peaks in the field cycling spectrum appeared at and above 6.4 MHz (0.15 T). Therefore the identified peaks listed in the Table 2 are not due to the effect of cross relaxation between the proton and ^{14}N nucleus.

Because the crystal structure of durene [28)] and T.M.P. [24,25)] are known, we can examine the origin which the three kinds of tunneling splittings $\hbar\omega_t^i$ (i=1,2,3) come from. The crystal and molecular structure determined by X-ray diffraction at room temperature for durene and T.M.P. are shown in Fig.18. The important characters of the crystal structures are two fold. One is that all molecules in an unit cell are crystalographically idintical for both durene and T.M.P.. The other is that the center of inversion symmetry exists at the center of each molecules in the crystals of durene and T.M.P.. Therefore two kinds of crystalographically inequivalent methyl groups I and II exist in a molecule as shown in Fig.18. When we consider that these inequivalent two methyl groups I and II rotate in a completely independent manner, the expected tunneling spectrum which is to be observed by field cycling technique is the simple superposition of the spectra for a single methyl group shown in Fig.3 in Section IV. The observable maximum number of the magnetization peaks in a field cycling spectrum is only four. However, the six peaks were clearly identified for durene and also T.M.P.. This experimental result cannot be deduced from the energy scheme of a single methyl group but indicates the complicated energy scheme. This is due to the coupling or collective motion between the two adjacent methyl groups in a molecule. An evidence was obtained that the rotational tunneling of the two adjacent methyl groups is described by the new feature, which we would like to call as "coupled rotational tunnel state".

The collective motion of two methyl groups in a molecule also gives rise to separation of torsional levels of different nature (torsional normal mode). Indeed, a separation of torsional first excited state of durene was reported to be 35 cm^{-1} by inelastic neutron scattering.29) The similar result was reported for o-xyline29). The energy scheme of the torsional states of coupled two methyl groups of durene has been shown in Fig.1 in Section III.1.

For the detailed analysis of the tunneling spectrum, in addition to rotor level scheme of the coupled two methyl groups we should furthermore consider the spin states completely, because what we observe is the effect of tunneling splittings on the "spin-lattice relaxation" of the proton. The main problem, which must be solved before the complete explanation of the tunneling spectrum (Fig.16, Fig.17), is whether the spin system should be treated with six spin system (I=3) or with the simple superposition of 3/2-spin systems. A little considerations are able to be performed.

In the case of a single methyl group, three protons are located on the vertexes of a triangle and the conformation of these spins are considered to be rigid at any time for considering the N.M.R. problem, i.e. the internuclear distance within a methyl group is rigidly fixed even when the rotation of a methyl group takes place. On the other hand, in general case of two methyl groups as in durene and T.M.P. molecule the internuclear distances between two methyl groups change when the rotation of two methyl groups take place unlike as the internuclear distance within a methyl group. The rigidity of the six spin system is not holded for the rotating methyl groups. Therefore the spin system of coupled two methyl groups is probably described by I=3/2 and the rotor system should be described as coupled methyl groups.

In the case of lithium acetate dihydrate ($CH_3COOLi \cdot 2H_2O$) the problem is special one30). The methyl groups are essentially arranged in coaxial pairs with a methyl plane separation of 2.5 Å31) and the direction of C_3 symmetry axes of whole methyl groups are in accordance with the b-axis of the crystal. Allen30) has reported that the N.M.R. absorption line of the single crystal of partially deuterated material ($CH_3COOLi \cdot 2D_2O$) for $\beta=0$, where β is an angle between the C_3 symmetry axis and the direction of external magnetic field, showed a different character of the dipole shift due to the "intermethyl dipole interaction" from the intra-interaction. The spin system is to be considered as a rigid six-spin system even for the rotating methyl groups. The inelastic neutron scattering study32) and the N.M.R. relaxation study 33) revealed that the hindering potential of a methyl group in this crystal is very small, the activation energy is 130 ± 30 J mol^{-1} in the low temperature branch and 250 ± 40 J mol^{-1} on the high temperature side of T_1 (min.)33). It can be speculated that interaction between the two metyl groups is rather strong comparing with the rest interactions. In addition to this situation, the "coaxial structure" of two methyl groups probably retains the rigidity of the six spins of two methyl groups which rotate like as the rotation of "cyclohexane ring" about its S_6 symmetry axis. This example is a special case but the spin states of coupled two methyl rotors is probably described by 3/2-spin system.

Although the details of the coupling of the spin states to the rotor states of mechanically coupled two methyl groups is not known, the tunneling spectrum obtained by field cycling technique clearly indicate that the adjacent two methyl groups are not independent.

The observed line shape of N.M.R. absorption mode of T.M.P. was nearly Gaussian type (see Subsection VI.7). The derived second moment from the observed absorption line was 9 G^2 at 100 K and the portion of the intermethyl interaction was about 4 G^2 which was as large as that of intrainteraction (about 5 G^2). This is consistent with the small separation between the methyl groups.

3.2 The spin-lattice relaxation time of T.M.P.

The temperature dependence of the spin-lattice relaxation time, which was observed at 20.5 MHz with different two pulse sequences (A and B; see Section V.1) is shown in Fig. 20. The characteristic behavior of magnetization recovery was discussed in Subsection VI.1. In the low temperature branch of T_1(min.) (kK/T $\gtrsim$16), the two components, which were obtained by pulse

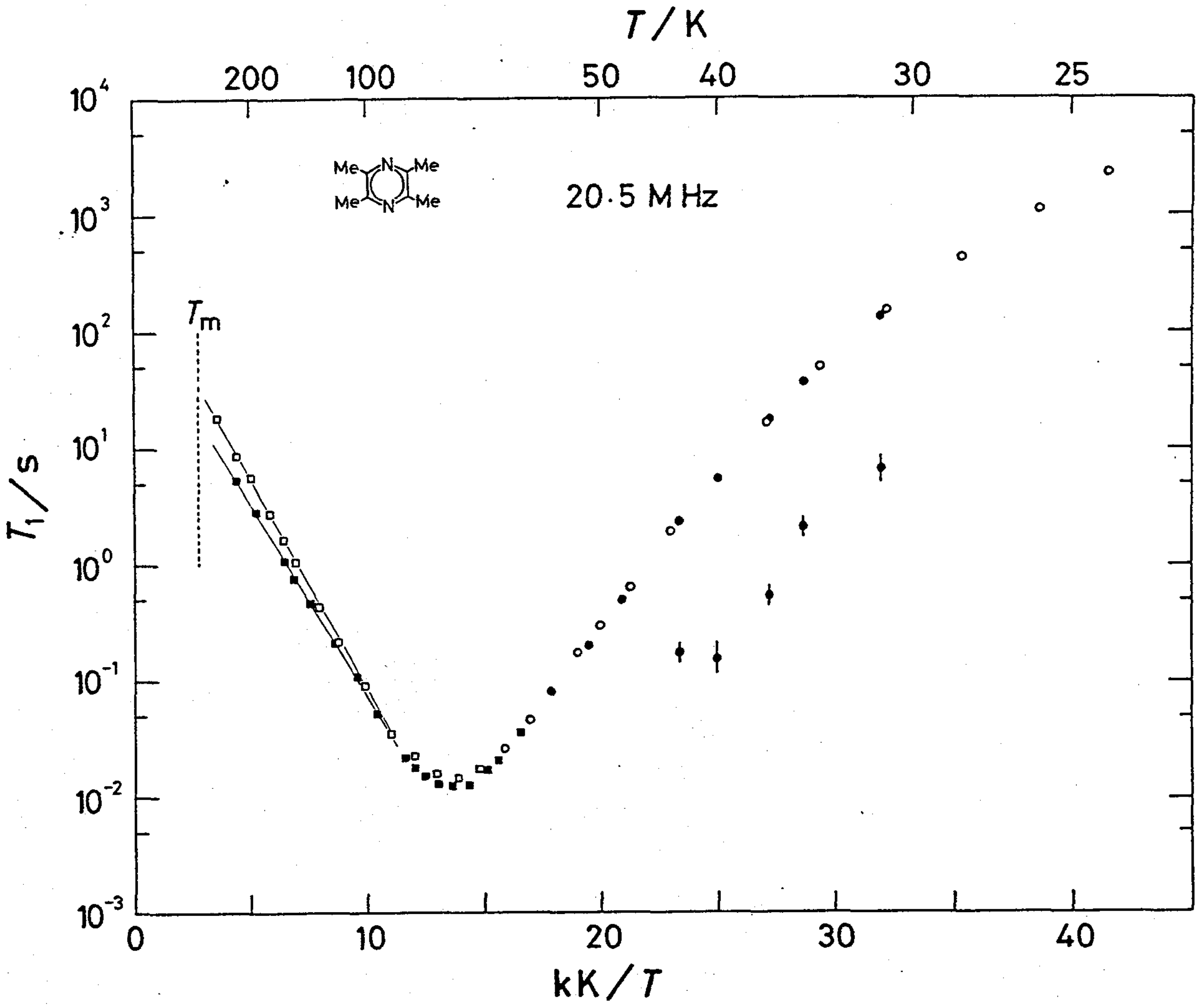

Fig. 20 Temperature dependence of the spin-lattice relaxation time of tetramethylpyrazine at 20.5 MHz □ (■) was determined from (ln2)$^{-1}\tau_{1/2}$ where $\tau_{1/2}$ is the half recovery time of magnetization. □ (○) was obtained by method A while ■ (●) was obtained by method B (short train). ● shows the fast and slow components (T_{1f} and T_{1s}) of the spin-lattice relaxation time.

sequence B, are separately shown. The slowly-recovering component T_{1s} by method B is in good agreement with the time constnat obtained by method A. The weight of the fast-recovering component decreased when the temperature increased (Fig. 44) like as in the case of CH_3SiCl_3 (Subsection VI.2) and $Si(CH_3)_4$ (Subsection VI.4). The detailed behavior of the weight of T_{1f} component of T.M.P. can not be directly compared with the prediction by Punkkinen, et al.[22) that the weight of T_{1f} component decreases with decreasing ω_t/ω_0 for a powder sample, because they treated a single methyl group with a simple tunneling spectrum unlike as the case of T.M.P.. But the qualitative character of decrease of this weight is probably the same as that for a single methyl group. This is the indirect evidence of the decreasing tunneling frequencies $\omega_t^{SS'}$ as temperature increases. The details of the temperature dependence of $\omega_t^{SS'}$, of which the frequencies in the low temperature limit were obtained by the field cycling experiment (Subsection VI.3.1), were not observed.

In the vicinity and above the temperature of T_1(min.) the nonexponential recovery was observed by both methods, A and B (This result is the character of the coupling between the Zeeman system and rotational polarization system as discussed for CH_3SiCl_3 in Subsection VI.2.2). The value of $(\ln 2) \times \tau_{1/2}$ was plotted in Fig.20, where $\tau_{1/2}$ is the half-recovery time of the magnetization. It should be noted that the activation energies obtained by two kinds of pulse sequences (A and B) were different from each other and that the T_1(min.) value obtained by method A was longer than that by B as shown in Fig.20.

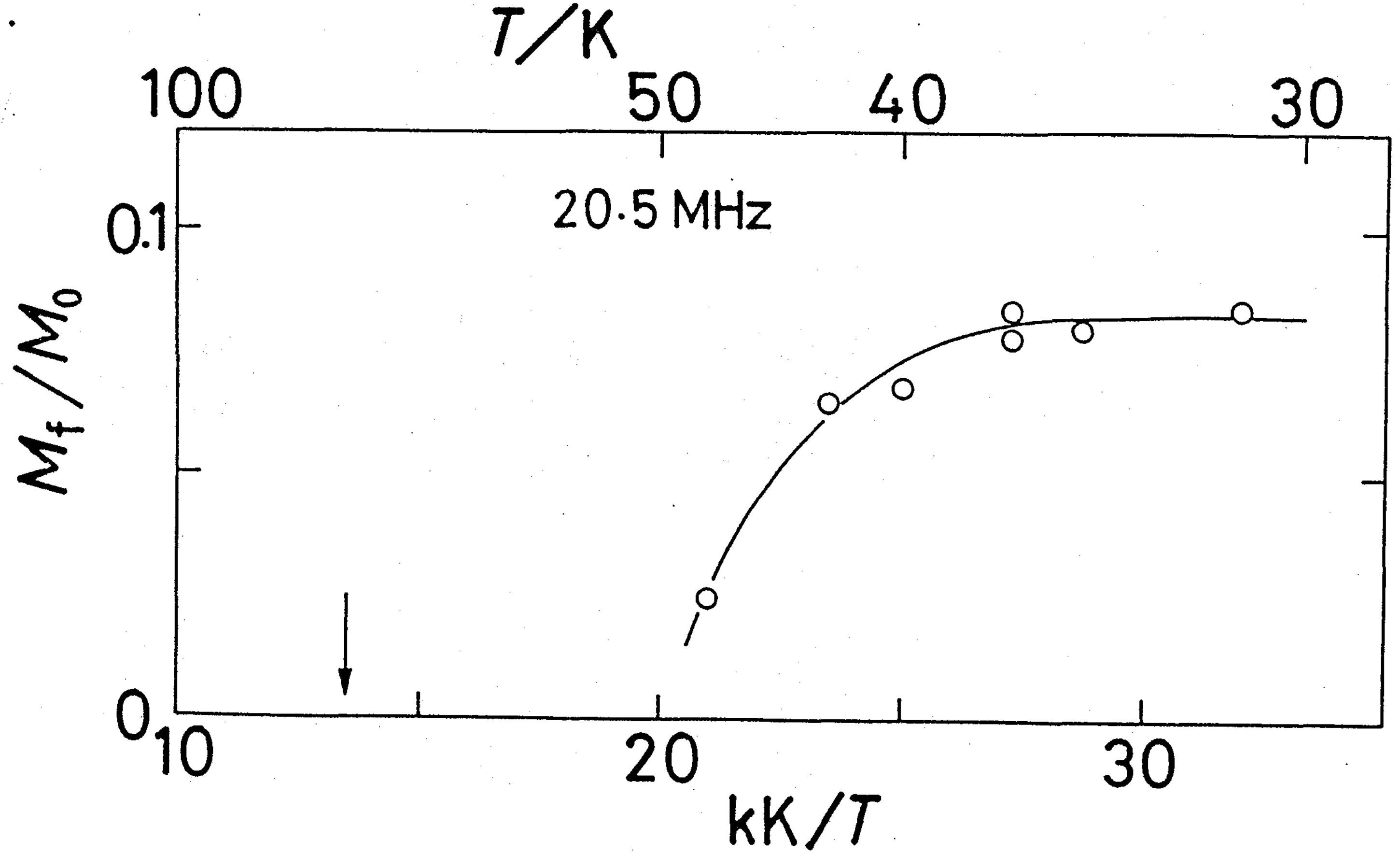

Fig. 45 Temperature dependence of the relative weight (M_f/M_0) of the fast-recovering component of magnetization of tetramethylpyrazine. The arrow indicates the T_1 minimum temperature.

We can safly apply Eq.(8) to only the fast-recovering component by method B as we do so for CH_3SiCl_3 (Subsection VI.2.2). T_{1f} and T_{1s} were decomposed with the least square refinement $^{6)}$ from the magnetization recovery by method B and these are shown in Fig.21. Where in the low temperature branch the time constant observed by method A is also included, because it is in good agreement with the T_{1s} component by method B in this temperature region. The solid curve is the calculated value using Eq.(8) which is applicable to the observed T_{1f} curve only near and above the T_1(min.), where the averaged tunneling frequencies $\omega_t^{SS'}$ are zero. Here we considered only the second term in Eq.(35) in Subsection II.1.4. We obtained the jumping rate ω_3 $(=\tau_c^{-1}/3)$ with which the methyl groups jump between the potential wells. It is

$$\omega_3 = 1.51 \times 10^{12} \exp\ (-6.3\ \mathrm{kJ\,mol^{-1}}\ /RT\ ) \qquad (11)$$

This term is most effective on the spin-lattice relaxation in the high temperature region of the observed T_{1f} curve. And in this temperature region the nature of the rotation of the methyl groups can be understood as a classical one. In the classical limit we have already discussed the effect of correlated motion of two methyl groups on the autorelaxation rate of Zeeman system in Subsection III.5. But it is not so effective on the spin lattice relaxation time that we can determine by the measurement of T_1 value whether the two adjacent methyl groups in T.M.P. molecule reorient correctively or independently. Therefore we used the Eq.(8), which is based on a single methyl group, and

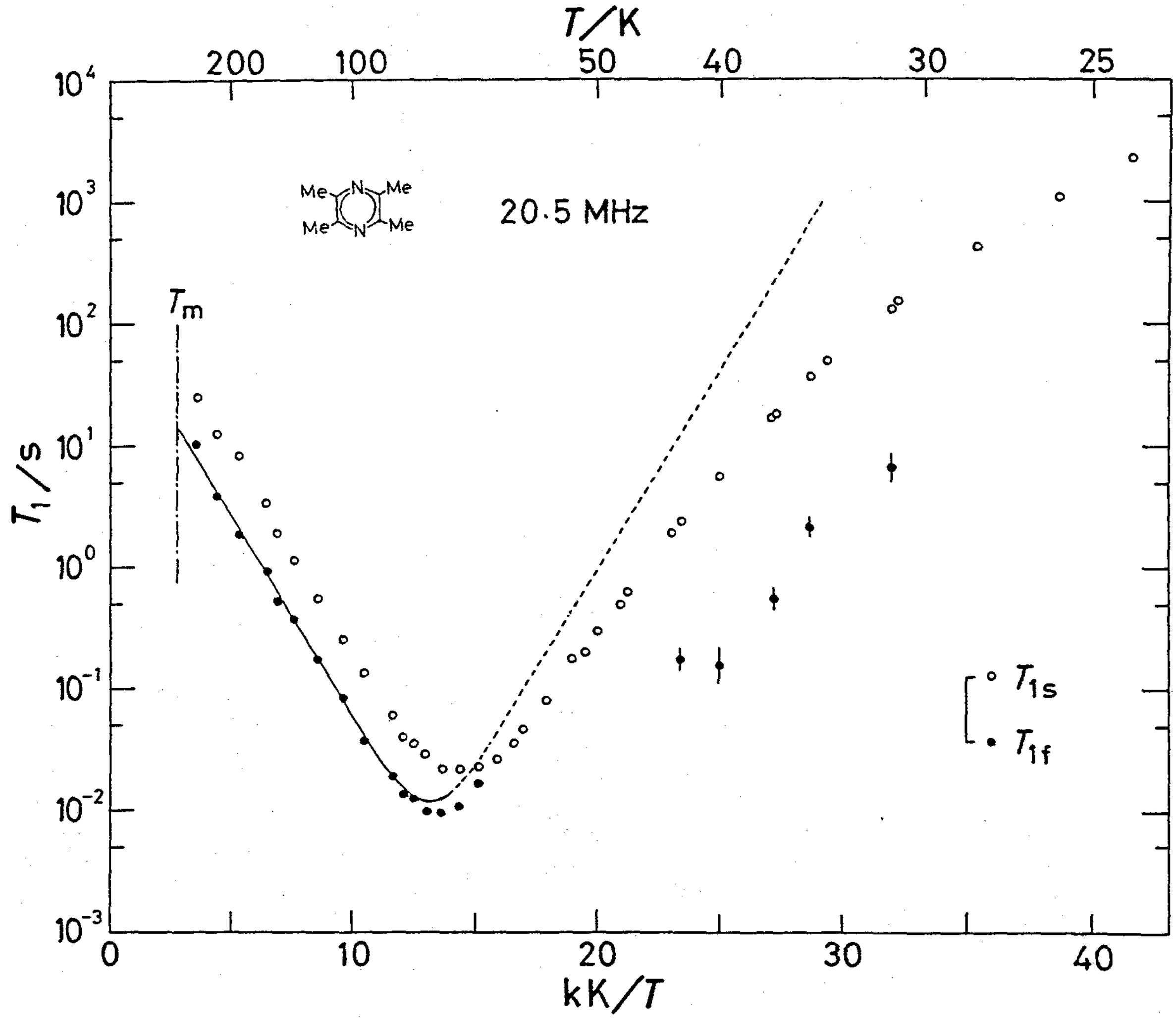

Fig. 21 Temperature dependence of spin-lattice relaxation time of tetramethylpyrazine at 20.5 MHz . The fast-relaxing (●) and slowly-relaxing (○) components are separately shown in the whole temperature range.

we considered only the intramethyl dipole interaction to obtain the jumping rate ω_3 (Eq.(11)). The intermethyl dipole interaction within a molecule is not effective on the T_1 value as discussed in Subsection III.5.

For a complete explanation of the observed T_{1s} and T_{1f} curve, we should solve the problem of the detailed energy scheme of the two-methyl system (spin and rotor system) and we should solve the coupled differential equation, which is similar to but different from the equation (29) in Subsection II.1.3. This is the problem to be solved in the next step and we will not treat it in this thesis.

VI. 3.3 The Larmor frequency dependence of the spin-lattice relaxation time T_{1s} of T.M.P. and durene at low temperature limit.

As discussed in Subsection VI.2.1 the spin-lattice relaxation time is descibed by Eq.(3) in the low temperature limit, where the condition that $(\omega_t + n\omega_0)^2 \tau_c^2 \gg 1$ is satisfied. The ω_0-dependences of the slowly-relaxing component T_{1s} of T.M.P. and durene observed by field cycling technique are shown in Fig.22 and Fig.23, respectively. The ω_0^2-dependence was observed at high frequency and the deviation from ω_0^2-dependence was clear at low frequency region. These results are in consistent with that the tunneling frequencis of these materials are the order of a few decade MHz.

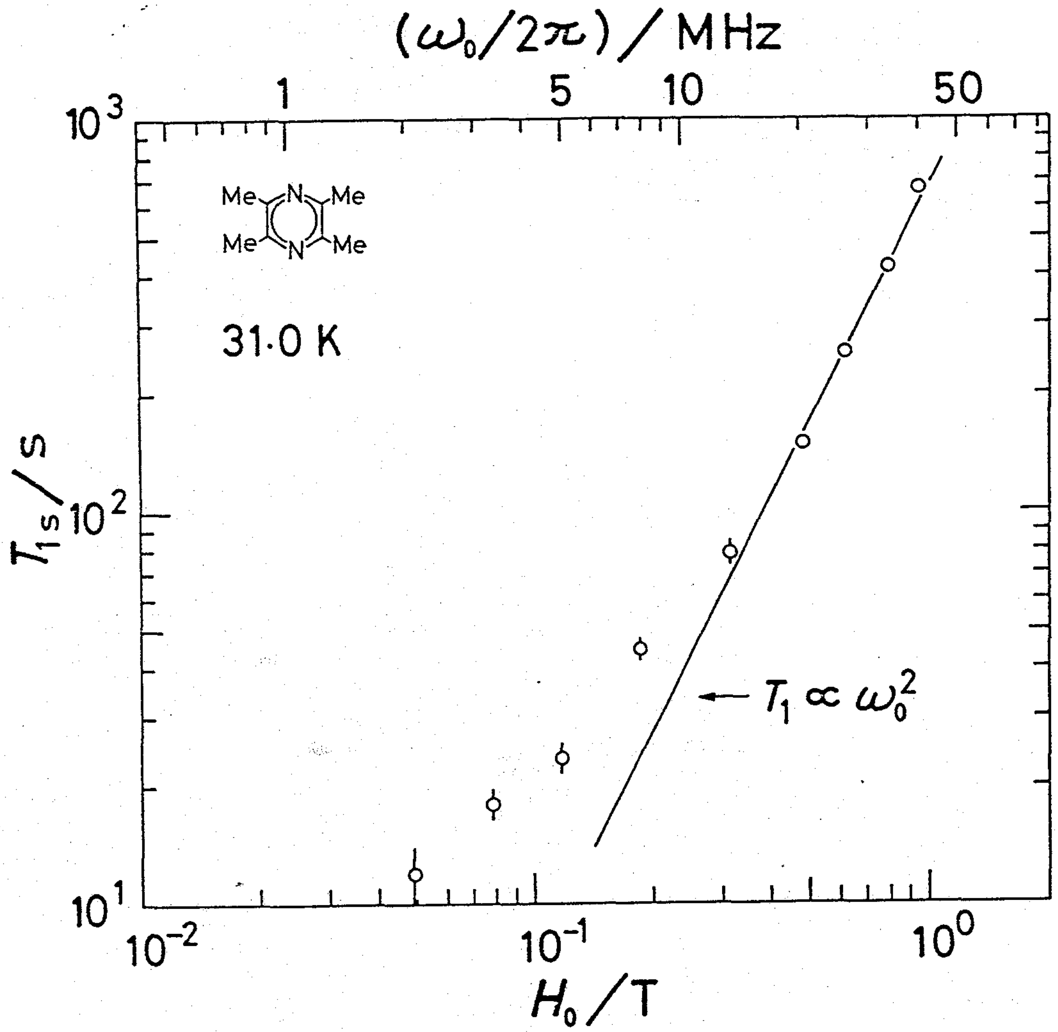

Fig. 22 The frequency dependence of the slowly-relaxing component, T_{1s}, of tetramethylpyrazine. The solid line indicates the ω_0^2-dependence of T_{1s}.

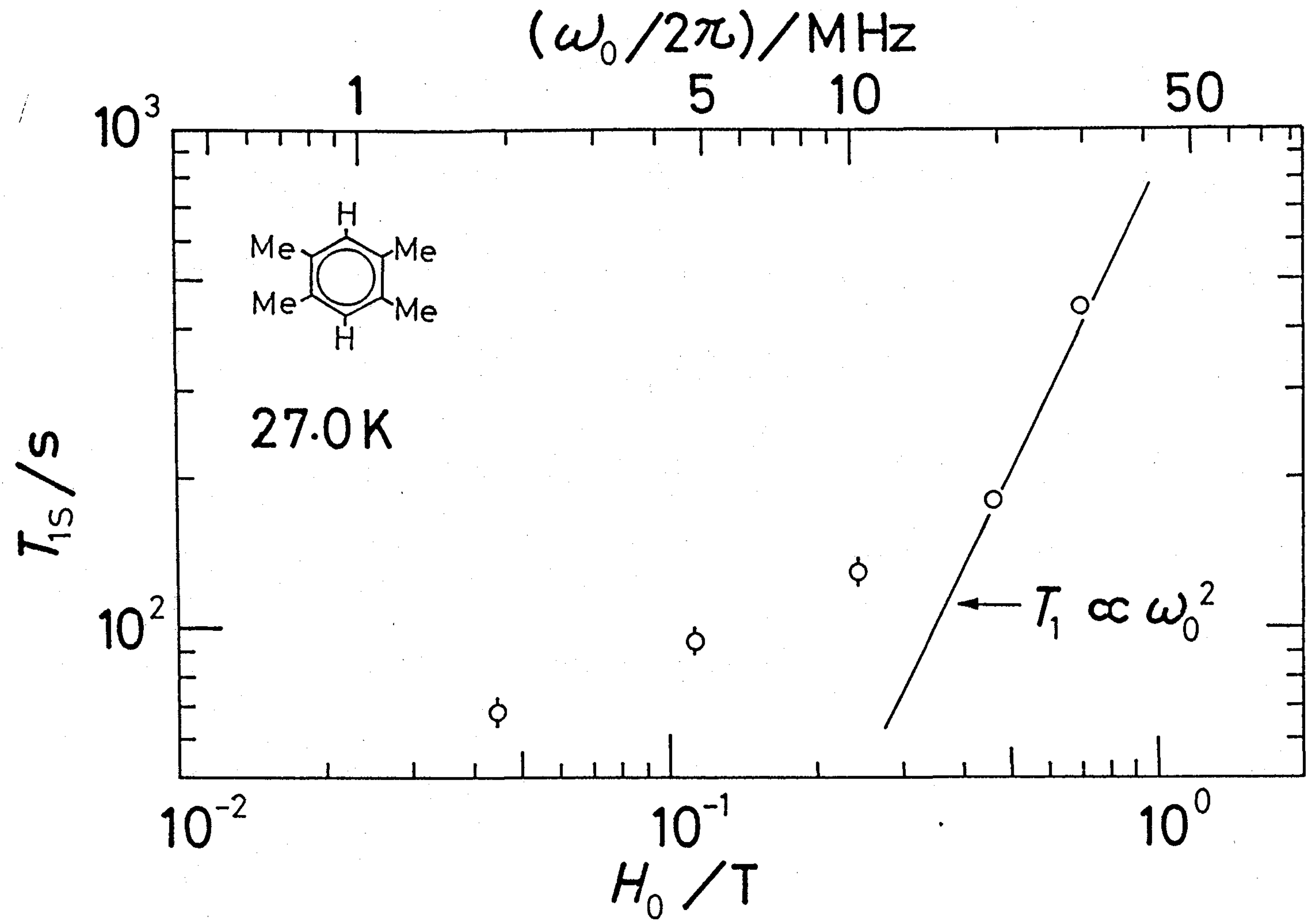

Fig. 23 The frequency dependence of the slowly-relaxing component, T_{1s}, of durene. The solid line shows ω_0^2-dependence of the spin-lattice relaxation time.

VI. 4. Tetramethylsilane, $Si(CH_3)_4$[*].

VI. 4.1 The temperature dependence of the spin-lattice relaxation time in the β and γ phases. The tunneling assisted minima.

The temperature dependence of the spin-lattice relaxation time of the β and γ phases measured at 10.0 MHz is shown in Fig.24. The characteristic behavior of the magnetization recovery has already been discussed in Subsection VI.1. In the low temperature branch ($kK/T \gtrsim 13.5$ or $T \lesssim 74$ K for the β and γ phases) the relaxation time measured by pulse sequence A was in good agreement with the slow somponent (T_{1s}) by pulse sequence B. In this temperature region minima of the fast component T_{1f} were clearly observed both for the β and γ phases. These are so-called "tunneling-assisted minima", which appear only in the T_{1f} at the condition that $\omega_t + n\omega_0 = 0$ but not in the T_{1s}. This feature of Zeeman relaxation is what is expected if the tunneling frequency is temperature dependent as demonstrated by Ligthelm, et al.[34)] who solved the coupled relaxation equation (Eq.(29) in Subsection II.1.3) numerically under the condition of S.R.S.D. The weight of the fast-recovering component decreased both for the β and γ

---

[*] Proton N.M.R. and Coupled Rotational Tunneling of Methyl Groups in β and γ Phases of Tetramethylsilane.
Sadamu Takeda and Hideaki Chihara,
J. Phys. Soc. Japan 51 (1982) in press.

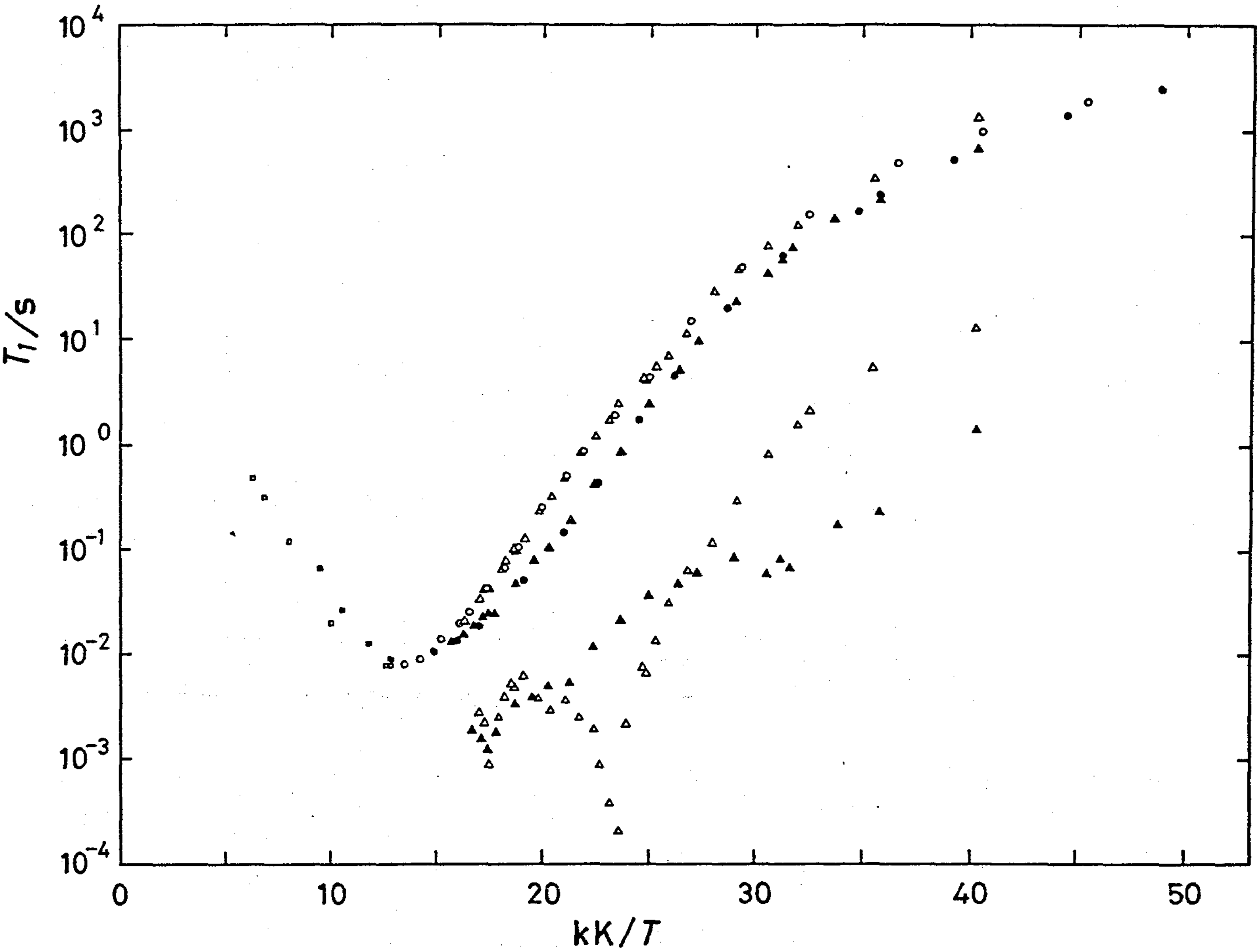

Fig. 24 The temperature dependence of spin-lattice relaxation time at 10.0 MHz, △, ○, and □ is for the γ phase and ▲, ●, and ■ for the β phase. □ (■) was determined from (ln 2)$^{-1}\tau_{1/2}$ where $\tau_{1/2}$ is the half recovery time of magnetization. □ (■) was obtained by method A (long train). ○ (●) was obtained by method A while △ (▲) was obtained by method B. △ (▲) slao show the fast component (T_{1f}) of the relaxation.

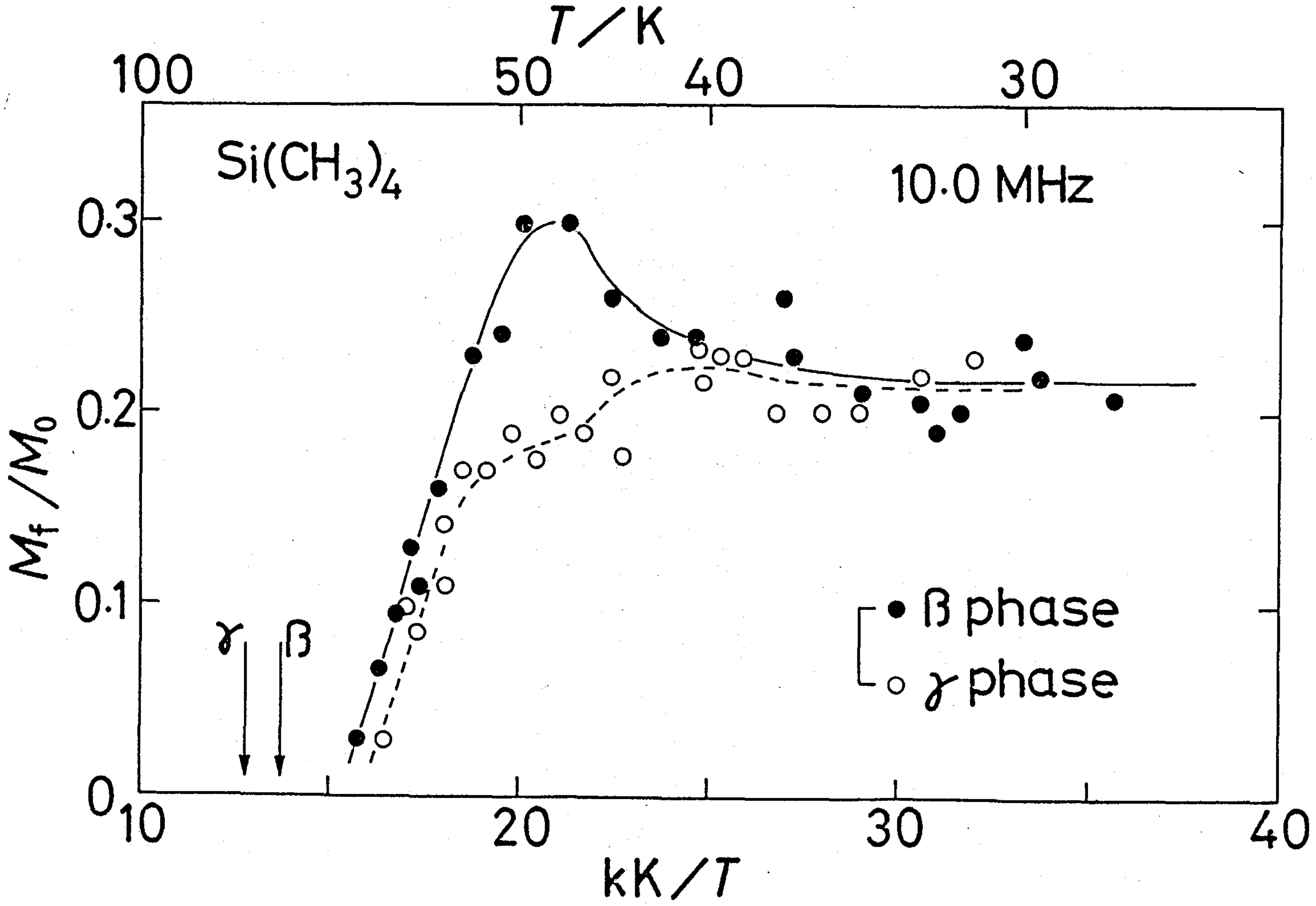

Fig. 25 The temperature dependence of the relative weight of T_{1f} component in the low temperature branch of T_1 curve (Fig. 24).. The arrows β and γ , respectively, indicate the T_1 mimimum temperatures in the β phase and in the γ phase.

phases when the temperature increased (Fig.25). This results is to be compared with the prediction by Punkkinen, et al[22)] and is consistent with the observed temperature dependence of the tunneling frequencies which will be discussed in Subsection IV.4.2. In the vicinity and above the T_1(min.) temperature ($T \gtrsim 74$ K) the magnetization recovery was always non-exponential by the pulse sequence A or B. This behaviour is to be compared with the experimental result that the tunneling frequencies decreased as temperature incleased and became zero in the vicinity of the T_{1s}(min.) temperature by accident as will be demonstrated in Subsection VI.4.2. This change of the Zeeman relaxation behaviour in the vicinity of the T_{1s}(min.) temperature corresponds with the fact that below this temperature the relaxation of Zeeman system is mainly coupled with the tunnel system because of $\omega_t^{SS'} \approx \omega_0$ (the same order) while above this temperature it is coupled only to the rotational polarization system because of $\omega_t^{SS'} = 0$. The materials cited in this thesis show the similar results with regard to the proton spin-lattice relaxation due to tunneling rotation and/or jump reorientation of the methyl groups.

VI. 4.2 Tunneling spectrum in the γ phase.

Figure 26 shows some examples of the results of field cycling experiment of the γ phase from 10.1 K to 26.7 K. The results at several temperatures show the four peaks; A (7.4 ± 0.8 MHz), B(12.0 ± 1.3 MHz), C (15.8 ± 0.9 MHz), and D (24.0 ± 1.4 MHz), the positions of which did not change up to 29.0 K.

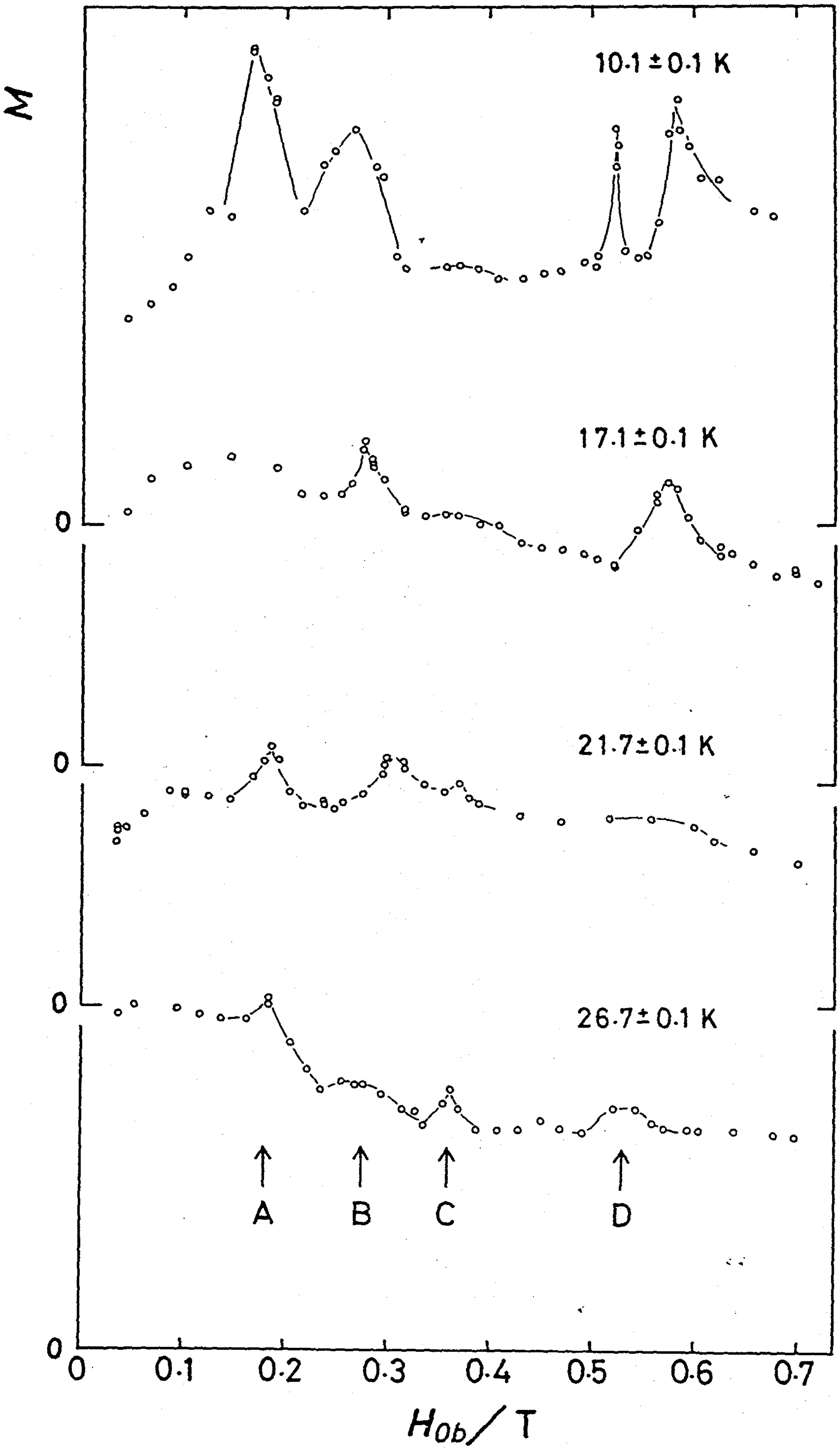
M
10·1 ± 0·1 K
17·1 ± 0·1 K
21·7 ± 0·1 K
26·7 ± 0·1 K
0
0
0
0
0
0·1
0·2
0·3
0·4
0·5
0·6
0·7
A
B
C
D
H_Ob / T

Fig. 26

Fig. 26 (caption)

Results of field cycling runs for the γ phase. The magnetization M is plotted in arbitrary scale against the external magnetic field H_{0b}. The reference field H_{0a} is 0.23 T. The time τ was chosen as 876 ± 3 s (10.1 K), 416 ± 2 s (17.1 K), 307 ± 3 s (21.7 K), and 76 ± 1 s (26.7 K).

The peak D which appears as a single peak above 17.1 K splits into two peaks at 10.1 K. The temperature dependence of the tunneling frequencies above 29.0 K was obtained by measuring the temperature - and ω_0-dependence of the spin-lattice relaxation rates (T_{1s}^{-1} and T_{1f}^{-1}) because the relaxation times become so short that our field cycling technique was not adequate, i.e. we cannot make the fiel-sweep time t_1 in Fig.2 in Section IV shorter than several seconds in our present apparatus. The tunneling assisted minima in T_{1f} at the condition that $\omega_t^{SS'} + n\omega_0 = 0$ were obtained at several Larmor frequencies. We can determine the temperature dependence of the tunneling frequencies from the temperatures at which the tunneling assisted minima appear and Larmor frequencies at which the relaxation times were measured. Figure 27 shows examples of the dependence of T_{1f}/T_{1s} on frequency and temperature in the γ phase. The minima a, b, c, d, and e of T_{1f}/T_{1s} in Fig. 27 were identified, corresponding to the peaks in the field cycling spectrum (Fig.26). These correspond, respectively, to the peaks D, C, D, B, and D at corresponding temperatures.

$$\xrightarrow{\text{Temperature}}$$

$B \longrightarrow d$

$C \longrightarrow b$

$D \longrightarrow a \longrightarrow c \longrightarrow e$

The maxima A and C form a pair because these frequencies are in the ratio of 1:2 and so do the maxima B and D (Fig.26). The same ratio also holds for the d/a pair at a common temperature.

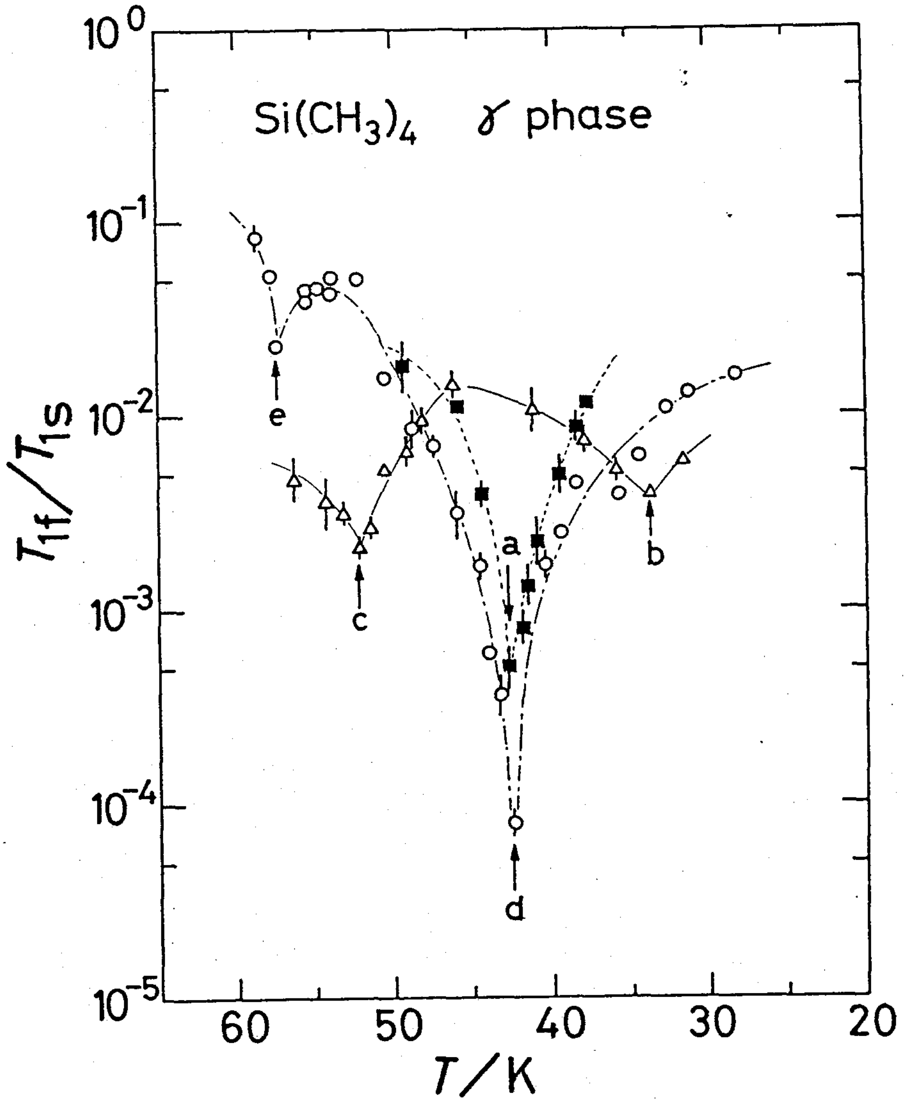

Fig. 27 Temperature and frequency dependences of the ratio T_{1f}/T_{1s} in the γ phase, ○ at 10.0 MHz, △ at 13.6 MHz, and ■ at 20.1 MHz.

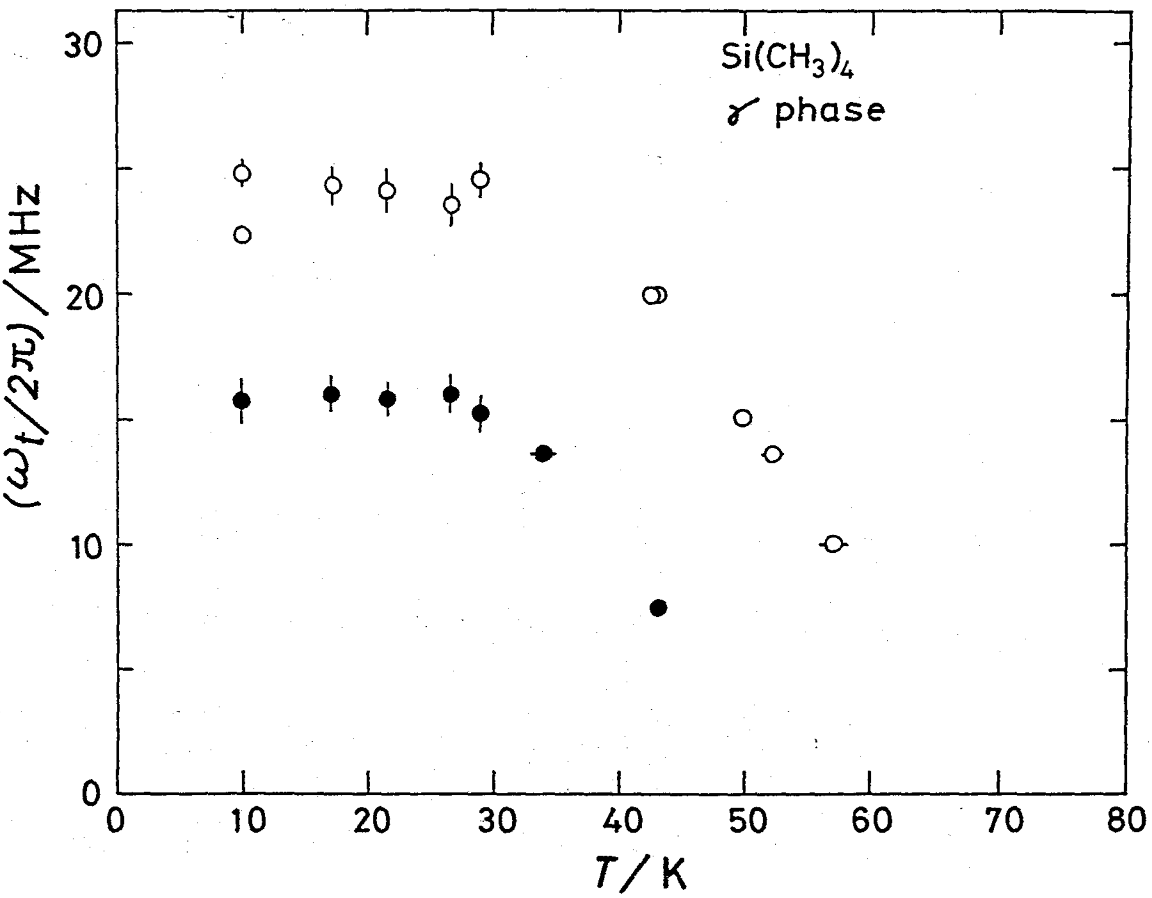

Fig. 28 Temperature dependences of tunneling frequencies of methyl groups in the γ phase of $Si(CH_3)_4$.

We see that the frequencies of the peaks of a pair change, as the temperature changes, in the fixed ratio of 1:2 if these pairs of peaks arise from the condition, $\omega_t^{SS'} + n\,_0 = 0$. Therefore we obtain two different tunneling splittings. In the low temperature limit, these are as follows.

Table 3

	$\nu_t^{SS'}$ /MHz	$(\nu_t^{SS'}/2)$/MHz
ν_t^1	15.8 ± 0.9 (C)	7.4 ± 0.8 (A)
ν_t^2	24.0 ± 1.4 (D)	12.0 ± 1.3 (B)

The derived temperature dependence of these two observable tunneling frequencies $\omega_t^{SS'}$, which correspond to peaks C and D in Fig.26 is shown in Fig.28.

The fact that two tunneling frequencies rather than one were recognized as in Fig.28 can be interpreted in the same way as in durene and T.M.P. (Subsection VI.3), i.e. the mechanical coupling betweeen the methyl groups operates in such a way that the torsional ground state of methyl groups splits into a number of tunnel sublevels and the separations between the sublevels happen to fall into two separate groups. For instance, the peak D in Fig.26 above 17.1 K further splits into two when cooled down to 10.1 K and this fact probably indicates that the level structure is not so simple as to give only two kinds of tunneling splittings. The mechanical coupling between the four methyl groups in a $Si(CH_3)_4$ molecule also induces the energy separation between the torsional normal modes as described in Section III.2. Indeed, the separation between A_2 and

F_1 modes in the first excited torsional state was observed to be 14 cm^{-1} by far infrared spectroscopy[35)] between 83 and 128 K, which was also suported by inclastic neutron scattering experiment at 77 K[21)]. The "collective rotation" due to the mechanical coupling between the methyl groups is the important feature in the torsional dinamics and undoubtedly "in the rotational tunneling" of four methyl groups in $Si(CH_3)_4$.

The detailed explanation of the observed tunneling spectra needs the details of the tunneling energy scheme and needs the coupling of the spin states to the rotor states of four methyl groups. But these are not known. The spin state of four methyl groups is probably described by the simple superposition of 3/2 spin state as discussed in Subsection VI.3.

VI. 4.3 The temperature dependence of the tunneling frequencies in the γ phase.

The temperature dependence of the resolved two tunneling frequencies was shown in Fig.28. We cannot explicitly apply the formura described by Eq.(42) in Subsection II.2 to the temperature dependence of these tunneling frequencies, because the energy scheme of the methyl groups in $Si(CH_3)_4$ molecule is not so simple that this formula can be applied. However, the basic mechanism of the decrease of observable tunneling frequencies as the temperature increase is probably the same, i.e. the rapid transition due to the non-magnetic interaction (H_{RP}; Section II.1.1) takes place and the quasi-equilibrium state is established among the same spin symmetry states. But if one apply Eq.(42) in Subsection II.2 to the two splittings in Fig. 28 by considering only two lowest torsional states, i.e.

$$\omega_t = \frac{\Delta_0 - \Delta_1 \exp(- E_1/kT)}{1 + \exp(- E_1/kT)} \tag{12}$$

the value corresponding with E_1 in the framwork of Eq.(12) is 150 ± 18 cm^{-1} for both splittings in the low temperature limit, i.e. $\exp(-E_1/kT) \ll 1$. The temperature dependence of observed tunneling frequencies can be described by exponential function (Fig.44). The torsional frequencies of A_2 and F_1 modes reported by Durig, et al 35) are, respectively, 163.5 and 177.5 cm^{-1} at 83 K.

VI. 4.4 Tunneling spectrum in the β phase.

The tunneling spectra in the β phase determined by field cycling technique are given in Fig.29. the unresolved spectra extending up to about 1.5 T (64 MHz) were observed above 21.1 K. The peaks below about 0.6 T (26 MHz) become sharper with decreasing temperature. These spectra are apparently more complicated than in the γ phase (Fig.26). Corresponding to such character of the tunneling spectra by field cycling, the ratio T_{1f}/T_{1s} does not show sharp minima (Fig.30) as observed in the γ phase (Fig.27). While the temperature dependence of T_{1f}/T_{1s} suggests the decreasing tendency of tunneling splittings with increasing temperature in this region, i.e. the tunneling assisted minima of T_{1f} component were clearly observed (Fig.24 and Fig.30), it was not possible to determine which peak in

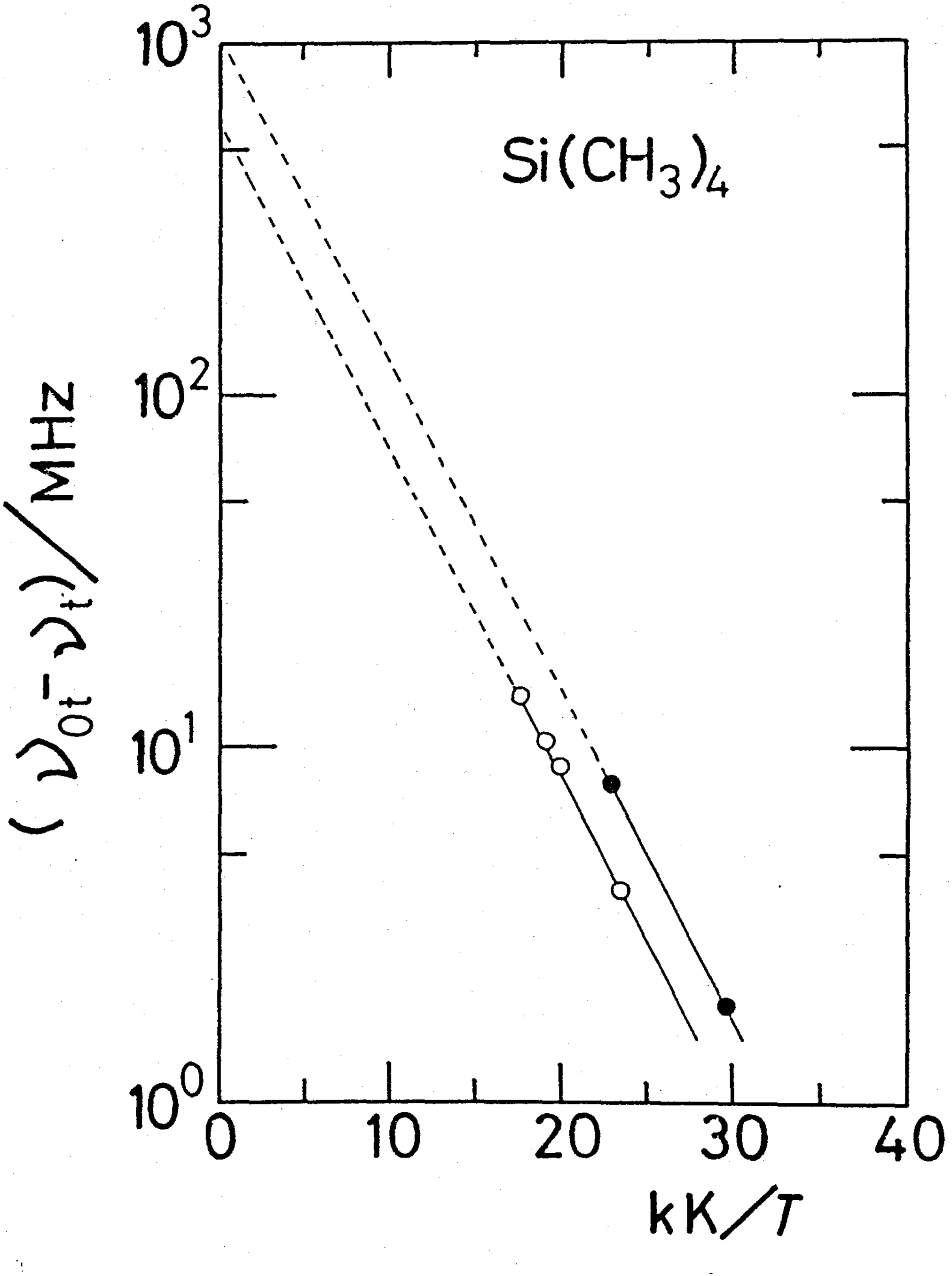

Fig. 44 The decrease in the tunneling frequencies as a function of inverse temperature in the γ phase of $Si(CH_3)_4$. The low temperature limiting values are taken to be 15.8 MHz (●) and 24.0 MHz (○).

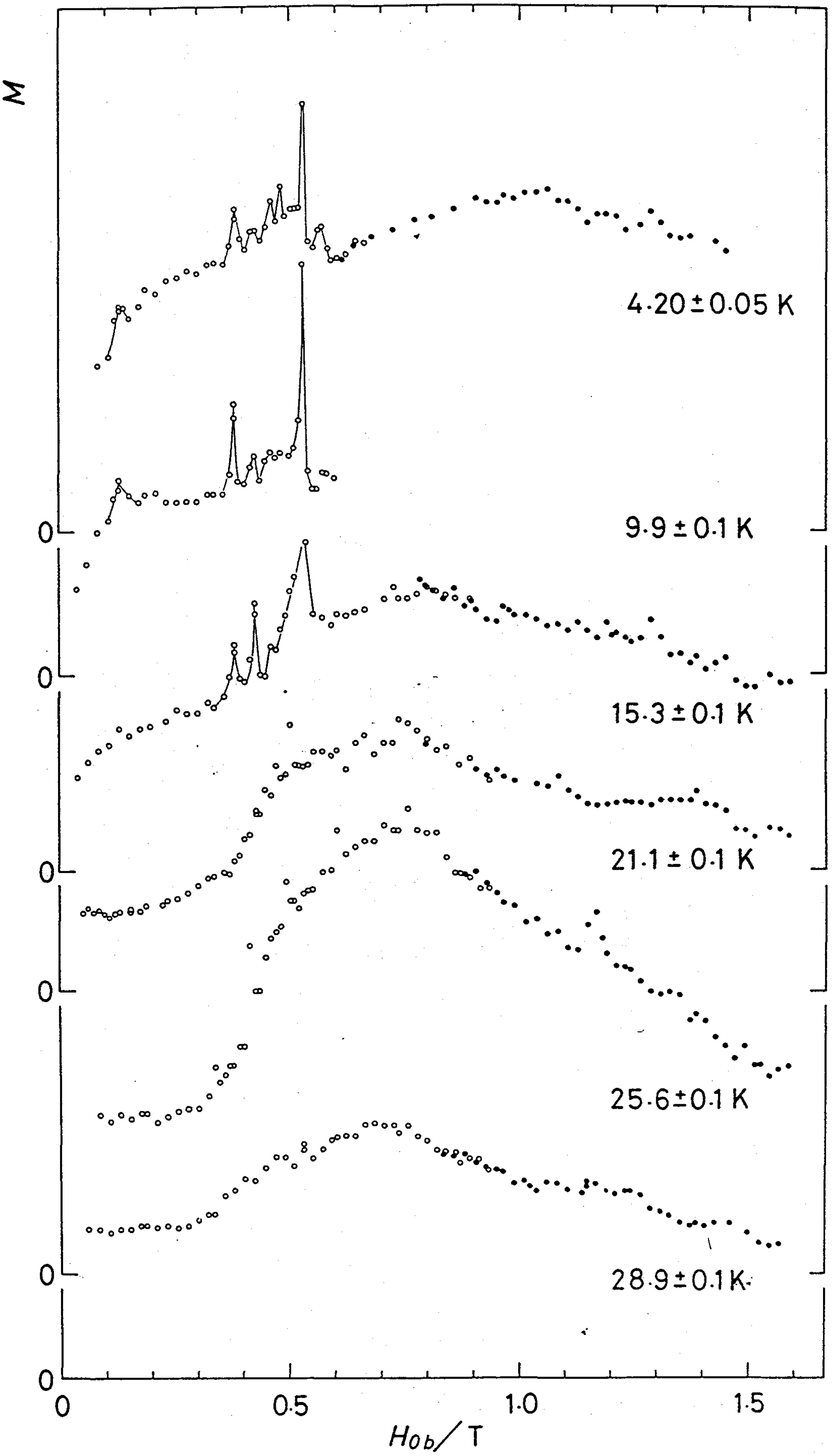
M
4·20±0·05 K
9·9±0·1 K
15·3±0·1 K
21·1±0·1 K
25·6±0·1 K
28·9±0·1 K
0
0
0
0
0
0
0
0·5
1·0
1·5
H_{0b}/T

Fig. 29

Fig. 29 (caption)

Results of field cycle runs for the β phase. The magnetization M is plotted in arbitrary scale against the external magnetic field H_{0b}. The reference field H_{0a} is 0.47 T (for ○) and 1.11 T (for ●). The time τ was chosen as 662 ± 2 s (4.2 K), 662 ± 2 s (9.9 K), 463 ± 3 s (15.3 K), 311 ± 3 s (21.1 K), 123 ± 2 s (25.6 K), and 34.5 ± 1 s (28.9 K).

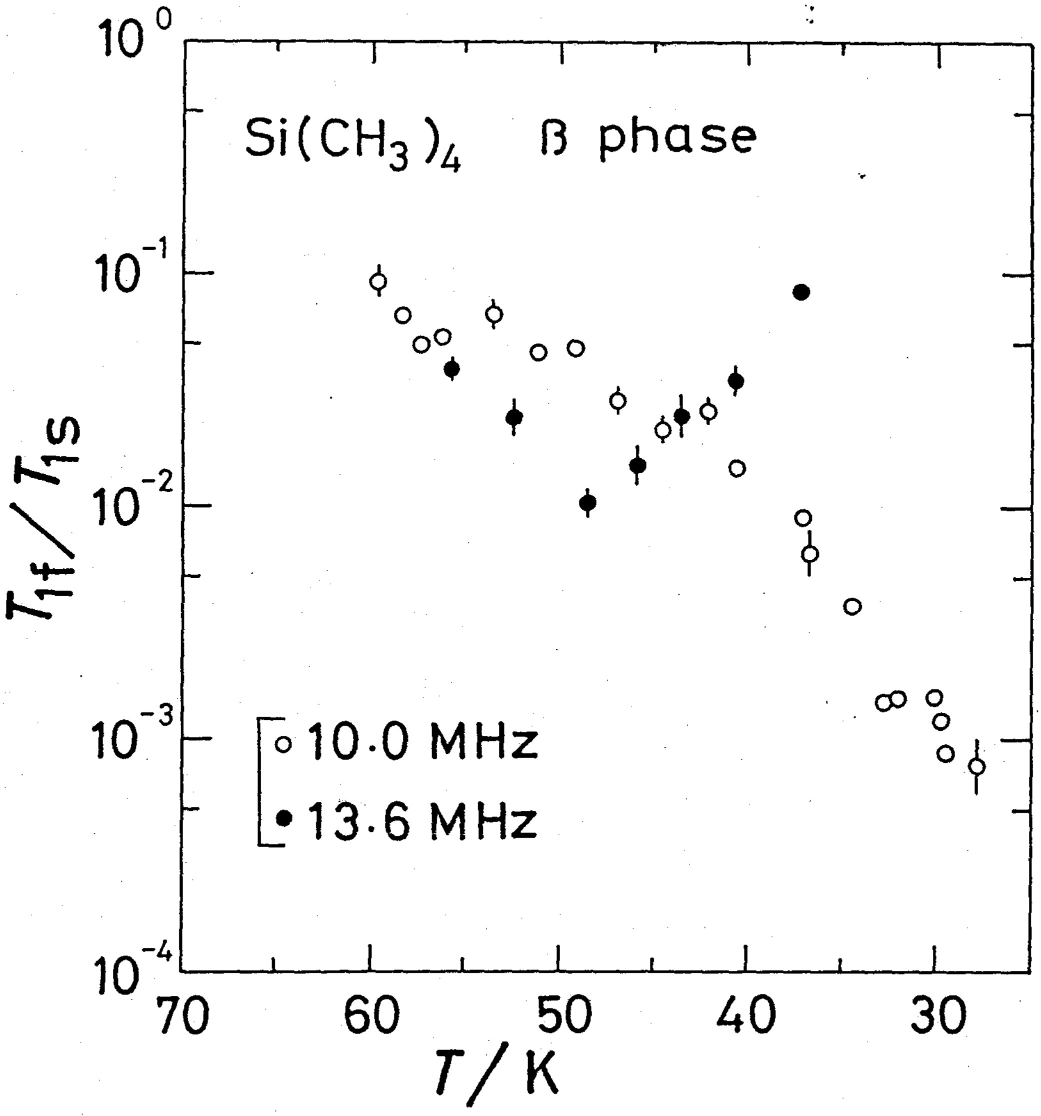

Fig. 30 Temperature and frequency dependences of the ratio T_{1f}/T_{1s} in the β phase.

Fig. 29 corresponds to $\omega_t^{SS'}/2$ and which one to $\omega_t^{SS'}$. The decreasing tendency of tunneling splittings was also confirmed by the decrease of the weight of fast-recovering component T_{1f} as described in Subsection VI. 4.1. The difference in behavior of tunneling spectrum between the β and γ phases must come from intermolecular origin. In the absence of knowledge of crystal structure of the two phases, it is difficult to make a meaningful explanation of this behavior But if the intermolecular portion of the hindering barrier operates in such a way that the orientations of four methyl groups do not hold a good symmetry, T_d symmetry, the tunneling energy scheme becomes probably more complicated one. The lattice vibrational modes of the β and γ phases determined by Raman scattering experimant are similar to one another. The small difference was observed(36). For the intramolecular vibrational modes, the resolution of the bands is clearer in the γ phase than in the β phase. Although the thermodynamical properties, e.g. melting point, heat of fusion, and entropy change of fusion, are similar to one another,(37) these properties indicate that the degree of disorder is slightly larger in the β phase than in the γ phase. Indeed it was revealed by N.M.R. measurements(38) that the molecular tumbling was excited at lower temperature and its activation energy was smaller in the β phase than in the γ phase.

The frequency dependence of the slowly relaxing, component T_{1s} in the β and γ phases are shown in Fig.31. This result shows that the tunneling frequencies of methyl groups in the β phase are larger than those in the γ phase as one understands in the framwork of Eq.(6) in Subsection VI.2. This result is in

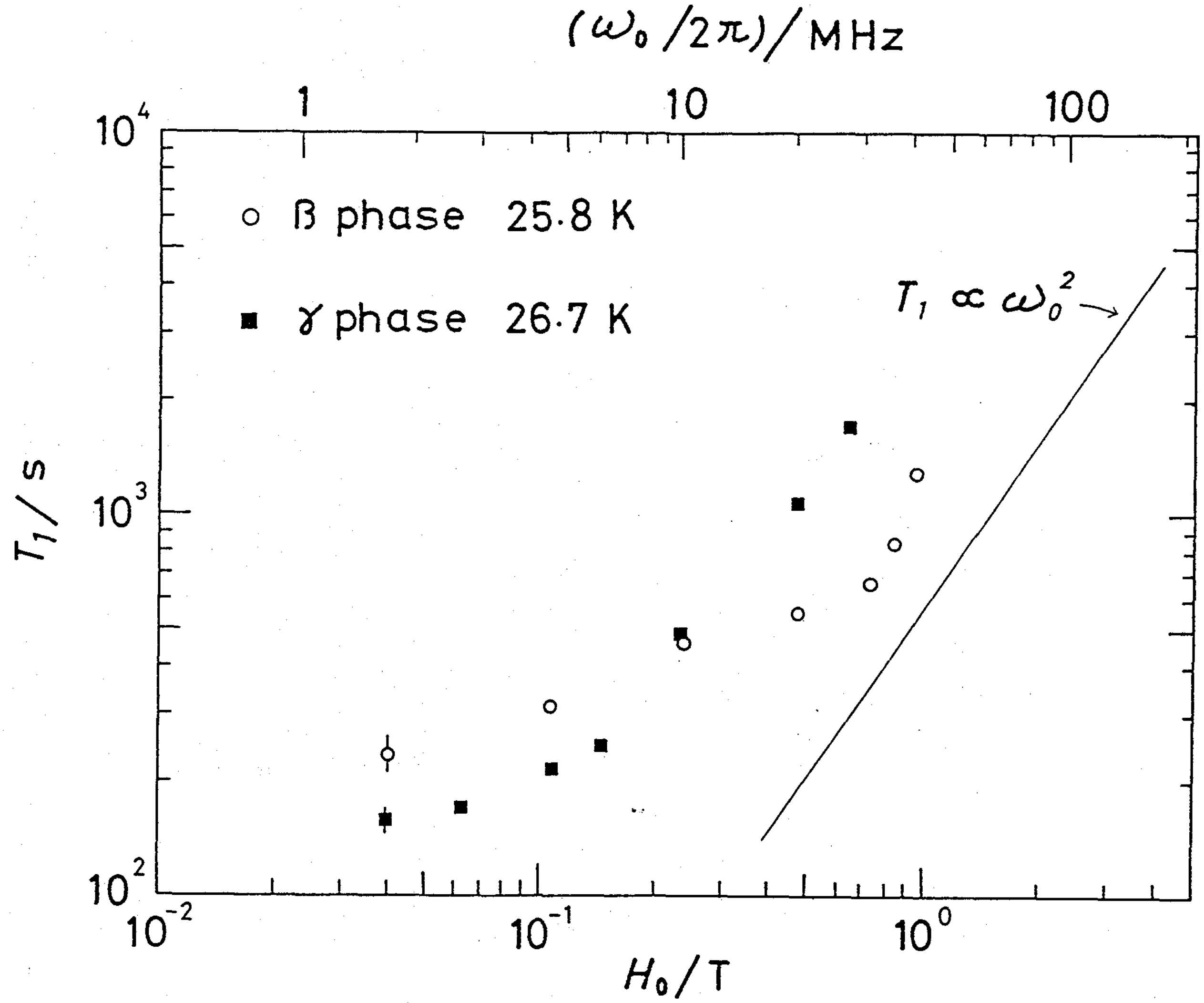

Fig. 31 The frequency dependence of the slowly-relaxing component of T_1 in the β phase (○) and in the γ phase (■). The solid line shows the $\omega_0^{\,2}$-dependence of the spin-lattice relaxation time.

consistent with the field cycling experiments (Fig.26 and Fig.29).

VI. 4.5 The effect of molecular tumbling motion on the behavior of the magnetization recovery.

The behavior of the non-exponential magnetization recovery and its dependence on the experimental methods (A and B, described in Subsection V.1) were discussed in Subsection VI.4.1. Above the T_{1s}(min.) temperature the relaxation of Zeeman system is coupled with that of rotational polarization system and the magnetization recovery was always non-exponential by method A or B. Albert, et al.[39] observed that this non-exponential character disappeared near 140 K in the γ phase by $90^\circ - \tau - 90^\circ$ method (method B in this thesis). This behavior was also the same by the pulse sequence A in our mesurement (Fig.32). This is considered to be due to progressive excitation of molecular tumbling motion. This motion was also examined by previous N.M.R. studies.[38,39] The molecular tumbling motion reorients the C_3 symmetry axis of a methyl group randomly against the direction of external magnetic field H_0. Therefore this tumbling motion produces the same effect as does the sample rotation about the axis perpendicular to H_0[40,41] on dicoupling the Zeeman system from the rotational polarization system. After this decoupling the relaxation of Zeeman system is described by a single exponential function and its time constant is the autorelaxation rate S_{ZZ} of Zeeman system (see in Section II.1.3). For the β phase, the situation is the same. Because the molecular tumbling motion is excited at lower temperature than in the γ phase, this change occurs at lower temperature.

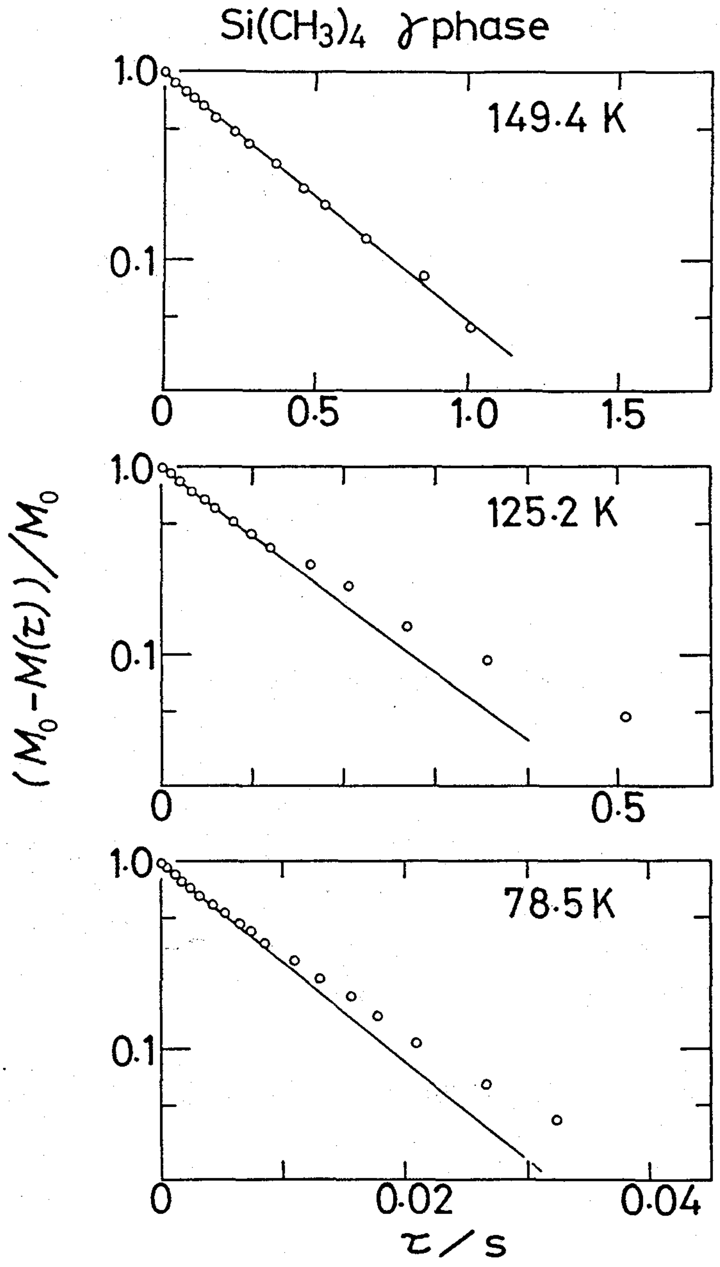

Fig. 32 The effect of molecular tumbling on the behavior of the magnetization recovery in the γ phase of $Si(CH_3)_4$. The magnetization recovery was obtained by the method A (long train). The motional narrowing due to molecular tumbling as a whole was observed at about 145 K (see in Fig. 38). The β phase showed a similar results.

VI. 5 Hexamethylbenzene, H.M.B.*

VI. 5.1 Tunnel spectrum of six-methyl system.

The results of the field cycling runs are shown in Fig. 33. The maxima A and A' form a pair whose frequencies are in the ratio of 2:1 and so do the maxima B and B'. This ratio for the maxima B and B' holds even when the frequencies of these maxima decrease with increasing temperature as will be described later. The Larmor frequencies at which the maxima A and B appear are then equal to the tunneling frequencies $\omega_t^{SS'}$ of the methyl groups in hexamethylbenzene molecule in its Phase III. The values were 9.6 ± 0.4 MHz (A) and 7.9 ± 0.4 MHz (B) at 4.2 K.

Jones and Bloom[42)] attempted to determine the tunneling frequency of methyl groups in hexamethylbenzene by the level crossing method (see in Section IV.1) and obtained an approximate value of 11.0 ± 2.5 MHz at 4.2 and 24 K which agrees with the present result for a peak A within the combined experimental error. They failed to observe the other tunneling frequency (B) because the method employed by them is not appropriate to resolve the

---

* Evidence of Coupled Retational Tunnel States of Methyl Groups of Hexamethylbenzene by Nuclear Magnetic Resonance. Sadamu Takeda, Gen Soda and Hideaki Chihara ; Solid State Commun, 36 (1980) 445.

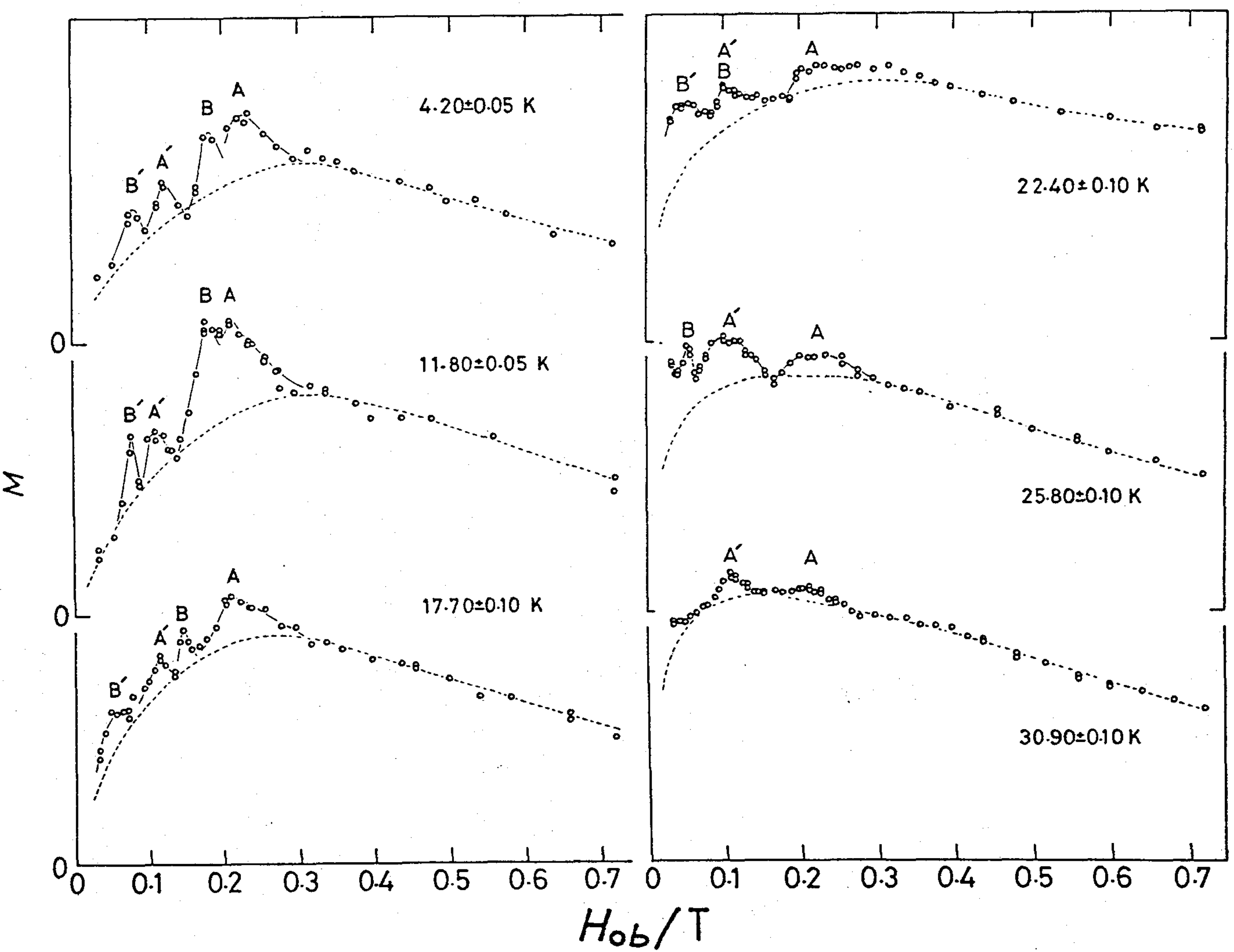

Fig. 33 Result of field cycle runs for hexamethylbenzene. The magnetization M is plotted in arbitraly unit vs. the external magnetic field H_{0b}. The reference field H_{0a} is 0.23 T (10.0 MHz). The time τ was chosen as 651 ± 5 s (4.2 K), 643 ± 5 s (11.8 K), 390 ± 4 s (17.7 K), 198 ± 1 s (22. 4 K), 69 ± 1 s (25.8 K), and 30 ± 1 s (30.9 K).

complicated tunneling spectrum.

As the temperature rises the maxima move toward lower frequencies; B and B' move much faster than A and A' (Fig.33) holding the ratio 2:1 for their frequencies. The temperature dependences of these tunneling frequencies, ν_t^A ($= \omega_t^A/2\pi$) and ν_t^B ($=\omega_t^B/2\pi$), are plotted in Fig.34. If we apply Eq.(12) to the frequency B in Fig.34 in the low temperature limit, i.e. $\exp(-E_1/kT) \ll 1$, as we do so for $Si(CH_3)_4$ in Subsection VI.4, we obtain the linear plot of Fig.35with $E_1/\hbar = 50 \pm 5$ cm^{-1} in the framework of Eq.(12). The derived frequency 50 cm^{-1} is very small for the energy separation between the torsional ground and first excited state of a methyl group. The frequency A did not decrease up to 30 K by this experiment. The tunneling frequency of methyl groups in H.M.B. at 60 K was estimated to be about 2 MHz$^{47)}$ within the framework of the energy scheme of a single methyl group by the temperature dependence of $T_{1\rho}$ (spin-lattice relaxation rate in the rotating frame). Although this estimation by $T_{1\rho}$ measurement is based on the inappropriate energy scheme, this result probably indicates that the tunneling frequency A decreases above 30 K and becomes about 2 MHz at 60 K. The temperature dependences of peak A and B are very differnt from one another, although the tunneling splittings 9.6 MHz(A) and 7.9 MHz (B) are not so different. These experimental results can not be reasonably understood by considering the isolated single methyl group but are probably comprehended when we consider the effect of mechanical coupling between the six methyl groups and its complicated energy scheme. The tortional first excited state splits into sublevels of four different symmetries A_{2g}, E_u, E_g and A_{1u}

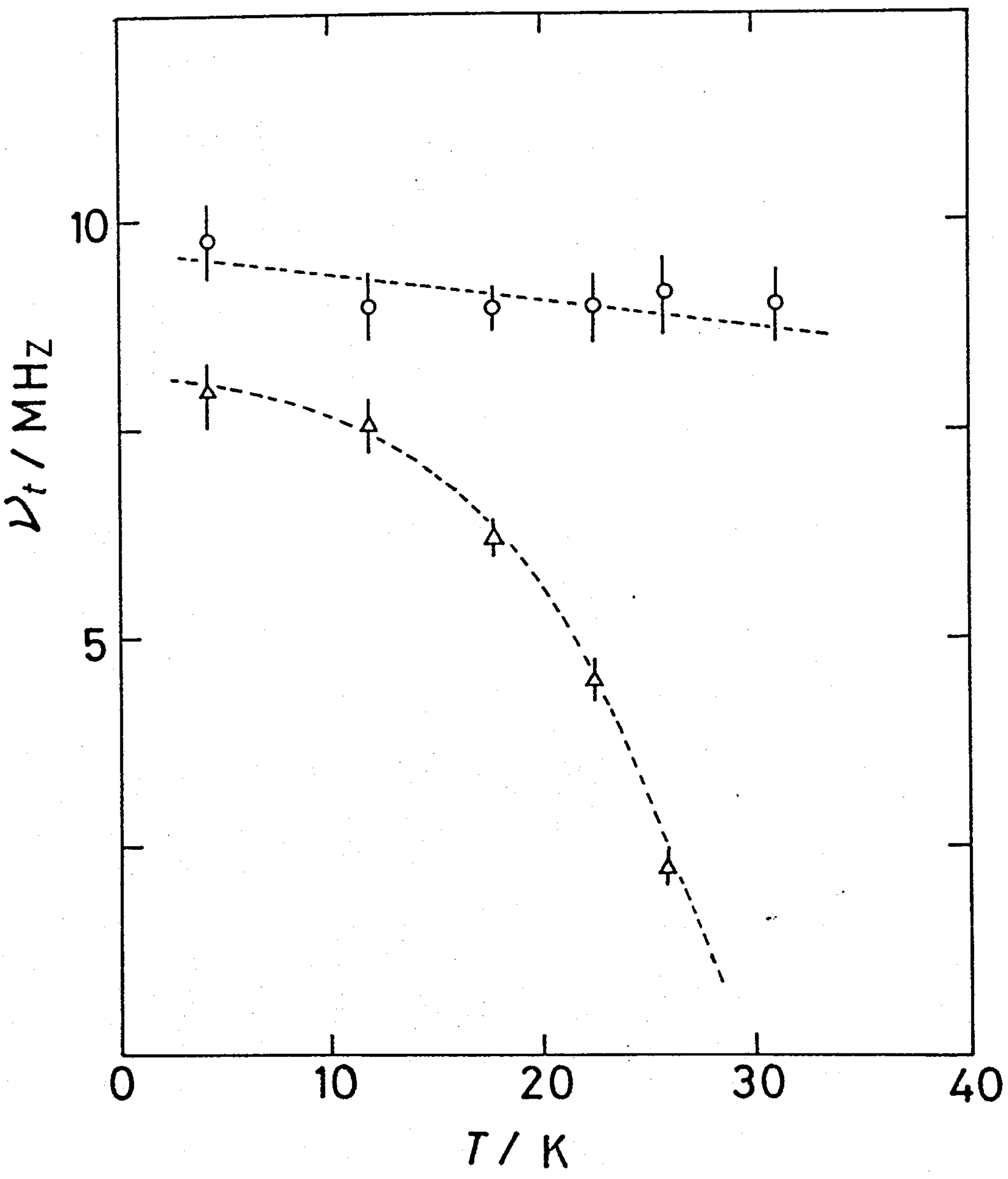

Fig. 34 Temperature dependence of tunneling frequencies of hexamethylbenzene. ○ tunneling frequency A, △ tunneling frequency B in Fig. 33.

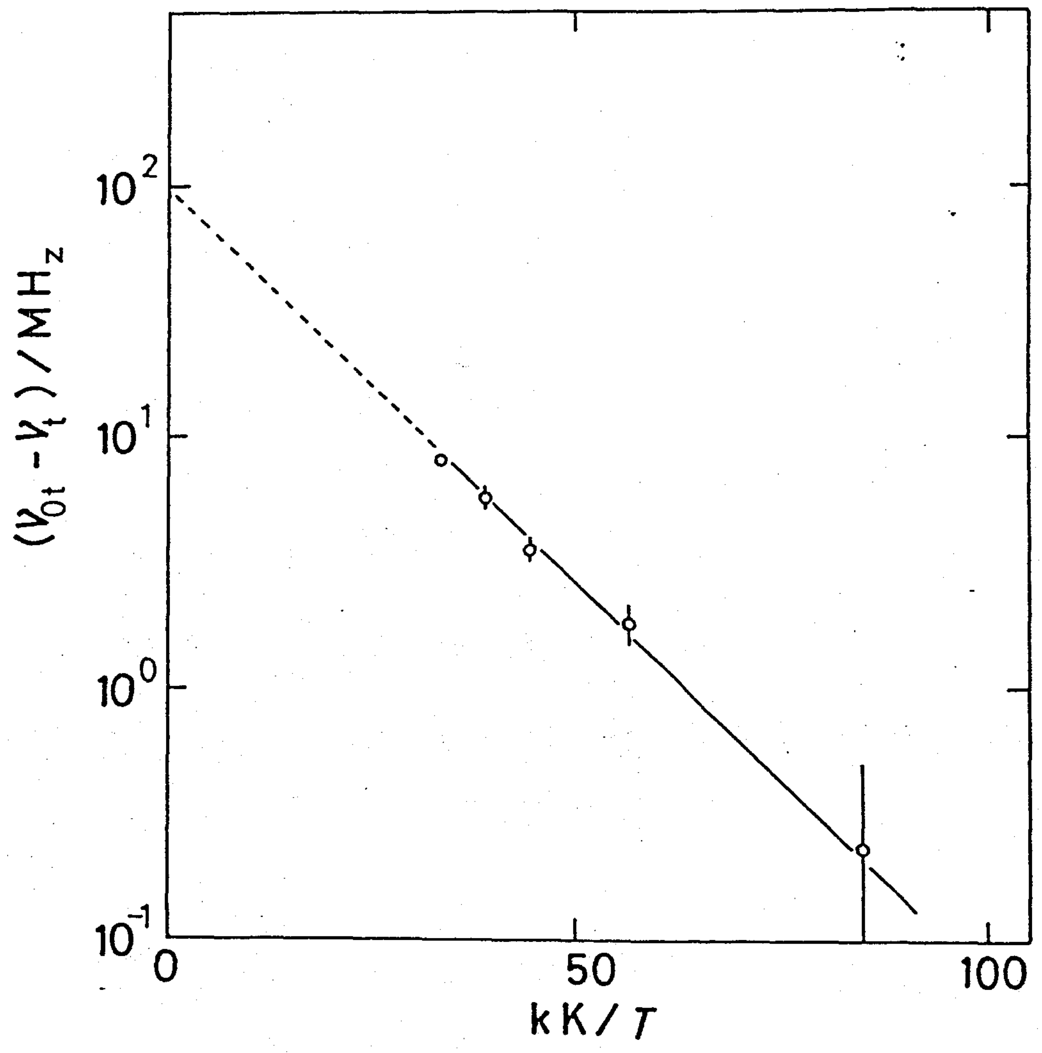

Fig 35. The decrease in the tunneling frequency B in Fig. 33 as a function of inverse temperature. The low temperature limiting value was taken to be 7.9 MHz.

if one assumes D_{3d} symmetry for a molecule[43)] (see in Fig.6 in Subsection III.3). The Raman scattering experimant gave 170 cm^{-1} for the E_g transition at 20 K[44)] but other transitions were not known. The inelastic neutron scattering experiment on H.M.B.[45)] was not conclusive for the separation of the "torsional normal modes" owing to poor resolution but the broad peak was observed in the frequency range of torsional vibrations. The fact that we observed two pairs of maxima as shown in Fig.33 does not necessarily mean that there are only two well-defined tunnel splittings of the torsional ground state in hexamethylbenzene. Instead they probably correspond to collections of splittings, indicating that such collections will fall into two more or less separate groups.

VI. 6 Discussions of mechanical coupling of the adjacent methyl groups. The new feature of "coupled rotational tunnel state" in solid.

The problem of the tunneling rotation of methyl groups in solid has been always treated as a problem of a single methyl group, i.e. the energy scheme of a single methyl group was considered. It is demonstrated in this thesis for the first time that the mechanical coupling between the adjacent methyl groups plays an important role in the rotational tunneling of these methyl groups even in the solid state. For durene and tetramethylpyrazine, it is clear that the observed tunneling spectrum of the methyl groups can not be explained by considering the energy scheme of a single methyl group. The derived tunneling spectra of these materials are due to the mechanical coupling between the two adjacent methyl groups in a molecule. Tetramethylsilane (Subsection VI.4) and hexamethylbenzene (Subsection VI.5) show the evidences of the coupling of the methyl groups similar to the case of durene and tetramethylpyrazine. The new feature of "coupled rotational tunnel state" in solid was demonstrated experimentally.

The mechanical coupling is caused by the hindering barrier to rotation of the methyl groups. Some discussions of the origin of the potential barrier are available. Ab initio calculations of hindering potential were performed for some molecules 53). The computation involves calculating the electronic energy of the molecule for different nuclear configurations, i.e. for different values of internal rotation angle. The energy may be expressed as the sum of four terms,[53)]

$$H = T_e + V_{ee} + V_{nn} + V_{en} \qquad (13)$$

where T_e is the kinetic energy of the electrons,

V_{ee} represents electron-electron repulsion,

V_{nn} represents internuclear repulsion,

and

V_{en} represents electron-nuclear attraction.

In this expression the first three terms (T_e, V_{ee}, and V_{nn}) make positive term, while the fourth term is negative and is referred to the attractive term.

For an ethane molecule, which consists of two methyl groups and the barrier to internal rotation is determined by the interaction of two methyl groups, the accurate computations were carried out.[53)] In order to make the origin of barrier to relative rotation of methyl groups clear, the contributions of Eq.(13) was divided into an attractive term ($V_a = V_{en}$) and a repulsive term ($V_r = V_{ee} + V_{nn} + V_e$). The variation of both the attractive (ΔV_a) and repulsive (ΔV_r) components with internal rotation angle is considerably larger than the barrier but they have the oposite sign to each other, where ΔV_a and ΔV_r represent the differences of V_a and V_r with respect to change of the internal rotation angle. A potential barrier to relative rotation of two methyl groups results from the sum of these two terms and it has a repulsive character, since $|\Delta V_r|$ is larger than $|\Delta V_a|$. There is a similarity between the relative rotation of methyl groups in ethane molecule and the situation of the interaction of two helium atoms. This is believed to show that the C-H bonds at either end of ethane molecule interact in a similar manner to the familiar repulsions that occur when two helium atoms are brought close to each other.

Therefore the interaction between the two methyl groups, which is considered to cause the mechanical coupling of these methyl groups, has a repulsive nature. The magnitude of this repulsion depends on the distances between the intermethyl hydrogen atoms (or C-H bonds).

The H---H distances between the adjacent methyl groups in durene, tetramethylsilane, and hexamethylbenzene molecule are listed in Table 4. The positions of the hydrogen atoms in hexamethylbenzene molecule were determined by neutron diffraction experiment in its phase II (130 K)54). The coordinate of hydrogen atoms of durene was obtained from difference map (X-ray diffraction experiment). For tetramethylsilane molecule the molecular structure in the gas phase determined by electron diffraction method55) was used, because its molecular structure in its crystalline phase is not available. The tetrahedral angle was assumed for all bond angles. This table indicates that the mechanical coupling effect is strongest in the case of hexamethylbenzene molecule, because the H---H distance of 2.0 Å is so short that it is comparable in value to the distance 1.8 Å within a methyl group. For hexamethylbenzene molecule the potential barrier to rotation of the methyl groups was estimated by Hamilton, et al.54) Assuming a Buckingham potential for atom-atom interactions. The shape and height of the hindering potential of

Table 4 H···H distances between the different methyl groups in Å unit

	1,2,4,5-tetra-methylbenzene	tetramethyl-silane (gas phase)	hexamethyl-benzene (phase II)
intra-molecule	2.4	3.06	2.040
	2.5	3.56	2.292
		4.34	2.328
		4.88	2.373
			2.420
			2.747
			2.756
			2.815
inter-molecule	2.7	-----	2.397
			2.476
			2.544
			2.583
			2.597
			2.609
			2.658
			2.687
			2.721

four kinds of "normal modes" of methyl rotation were very different from each otehr. This result also indicates that the repulsion between intermethyl hydrogen atoms plays an important role for the hindering barrier. The shortest intermethyl H---H distance of $Si(CH_3)_4$ molecule is 3.06 Å, which is rather longer than that of hexamethylbenxene (2.04 Å) and durene (2.40 Å). This fact means that the mechanical coupling between the methyl groups of $Si(CH_3)_4$ molecule is weaker than other molecules and it seems to correspond to the fact that the tunneling energy scheme of four methyl groups is likely to be affected by the change of the surroundings corresponding to the phase change (β phase and γ phase, see in Subsection VI.4). It is very probable that the change of intermolecular interaction, corresponding to the phase change, causes the change of relative orientation of four methyl groups in a molecule.

The intermolecular H---H distances of hexamethylbenzene and durene are also listed in Table 4. The crystal structure of phase III of hexamethylbenzene is not known. The tunneling spectrum of hexamethylbenzene was observed in its phase III. It was reported that the crystal symmetry of phase III is higher (hexagonal or trigonal) 56) than that of phase II (triclinic) 57). Although the intermolecular H---H distances change corresponding to the phase transition, H---H distances in phase II are listed for the measure of intermolecular contribution to the potential barrier to rotation of methyl groups. When we compare the repulsive potential due to intramolecular term with that due to intermolecular term by considering only the nearest hydrogen atoms and by assuming a Lennard-Jones potential, we only consider the distances 2.040 Å (intra) and 2.397 Å (inter), the repulsive potential of "intra" part is greater than that of "inter" part by a factor of 6.9. For durene, when we consider the same problem as we did for hexamethylbenzene, the "intra" part is greater than that of "inter" part by a factor of 4.1. These facts indicate that the mechanical coupling or collective motion of methyl groups in these molecules is mainly determined by intramolecular interactions.

When the intermolecular interactions strongly contributes to the mechanical coupling of the methyl groups of different molecules, it seems necessary that interacting methyl groups should satisfy an appropriate configaration with each other. In many cases, intermolecular interactions are probably included in the non-coupling terms (or independent terms) of the potential function.

When we say that the adjacent methyl groups are coupled to each other or they are independent, we should take into account a relevant criterion. In this thesis, it was emphasized that the mechanical coupling between the adjacent methyl groups is important in the rotational tunneling, because the coupling effect induces the dramatic variation of the tunneling energy scheme. Therefore the degree of the change of energy scheme of the methyl groups from that of a single one is one of the relevant criteria for the dynamical properties of the methyl groups. We should start to consider the dynamical properties of these systems from the appropreate energy scheme.

VI. 7 A different behavior of the intermethyl dipolar broadning from the intramethyl dipole shift.

The small reduction of line width and second moment at low temperature (10∼50 K) have been observed for some materials containing methyl groups, e.g. durene[46], hexamethylbenzene[47], tetramethylsilane[1], and methyl iodide[48]. For these materials, the rigid lattice value of the second moment M_2 was not observed but the reduced value was obtained even at and below about 20 K, which indicates that the tunneling splittings of the tortional ground state of a methyl group in these materials are much greater than the dipole energy ($\sim 10^2$ kHz)[49]. Indeed the details of the tunneling splittings of the methyl groups in these materials except for CH_3I were directly determined to be the order of Zeeman energy ($10^1 \sim 10^2$ MHz; see in the previous Subsections VI.3, VI.4, VI.5). However the origin of the small reduction is not clear. To make the origin of this phenomena appearent, the careful experiment was done for T.M.P., $Si(CH_3)_4$, and CH_3SiCl_3 of which the details of tunneling spectrum were determined in this thesis.

Because the spin-lattice relaxation times of these materials are very long at the liquid belium temperature (Figs.15,21, and 24), e.g. several hours at 4.2 K, the special attention was payed to eliminate the saturation effect on the absorption line. As possible as low power of Rf-field was used for measuring the absorption line. It was examined by comparing the differential absorption lines, one of which was observed with the increasing field sweep and the other was observed with decreasing field sweep, whether the saturation effect appeared or not. The time of sweep through the signal was taken as 35 or 70 minuts for all the runs. The effect of the sweep time on the observed line shape was examined for T.M.P. at 25 and 29 K. The values of T_{1s} at 25 and 29 K are, respectively, 1500 and 200 s at 20.5 MHz and this examination was done at 12.95 MHz with Robinson type spectrometer. The result obtained by the condition of 35 minuts-sweep and that by 70 minuts-sweep were in good agreement with each other.

Because the spin-lattice relaxation at 4.2 K is several hours, it takes very long time that the spin-system becomes complete thermal equilibrium at that temperature. After the sample is cooled down to 4.2 K from about 80 K, the signal grows into its thermal equilibrium state. On the other hand small Rf-power diminishs this signal. Then we observe the line shape at the steady state, i.e. the state of the balance of these two effects. The time interval affects the populations in the spin-states when the spin system is not in complete thermal equilibrium. Therefore the effect of the time interval between after the sample was cooled down to 4.2 K and before the measurement was began on the line shape was also examined. Any difference was not observed in the shape and the maximum slope width of absorption line between about 8 hours and 1 hour of the time interval except for the magnitude of the signal. The result described above is consistent with the magnitude of the tunneling splittings which are the order of several decade MHz (Subsection VI.3) and are much smaller than the thermal energy at 4.2 K (8.4×10^{10} Hz). The population difference between the symmetry species (tunnel levels) changes by only 0.1% at thermal equilibrium states when the specimen is cooled down from 80 K to 4.2 K. This very small change of population is not detectable.

The maximum slope width ΔH and second moment M_2 of T.M.P. measured at 12.95 MHz and 59.82 MHz are shown in Fig.36. The small reduction of line width and second moment are clearly obtained at 30 ~ 50 K. The reduction of maximum slope width was slightly depends on the radio-frequency at which the measurement was performed. This dependence on the Rf-frequency was not conclusive for the second moment values. The change of the line shape at this temperature region is illustrated in Fig.37. The spectra measured at 59.82 MHz showed the similar result like as Fig.37. These small reductions of the maximum slope width and second moment are not due to the experimental conditions, e.g. the saturation effect etc.. The value of T_{1s} at 35 K (the line width is the broad one at this temperature) is nearly the same as that at 195 K (the line width is the narrowed one at this temperature) and the experimental conditions, i.e. Rf-power and the sweep time, were the same for both temperatures.

The similar results were observed for the β and γ phases of $Si(CH_3)_4$ (Fig.38). The narrowing above 130 K is due to the molecular tumbling as a whole1). The change of the line shape between 30 and 50 K was very similar to that of T.M.P. as shown in Fig.39. The shaded area in Fig.38 indicates the experimental result measured at 11.0 MHz by Hasebe,et al.1) for the β and γ phases. The differnce between the results at 11.0 KHz and that at 59.82 MHz in the region of small reduction is indicated, which is similar to the result of T.M.P. (Fig.36).

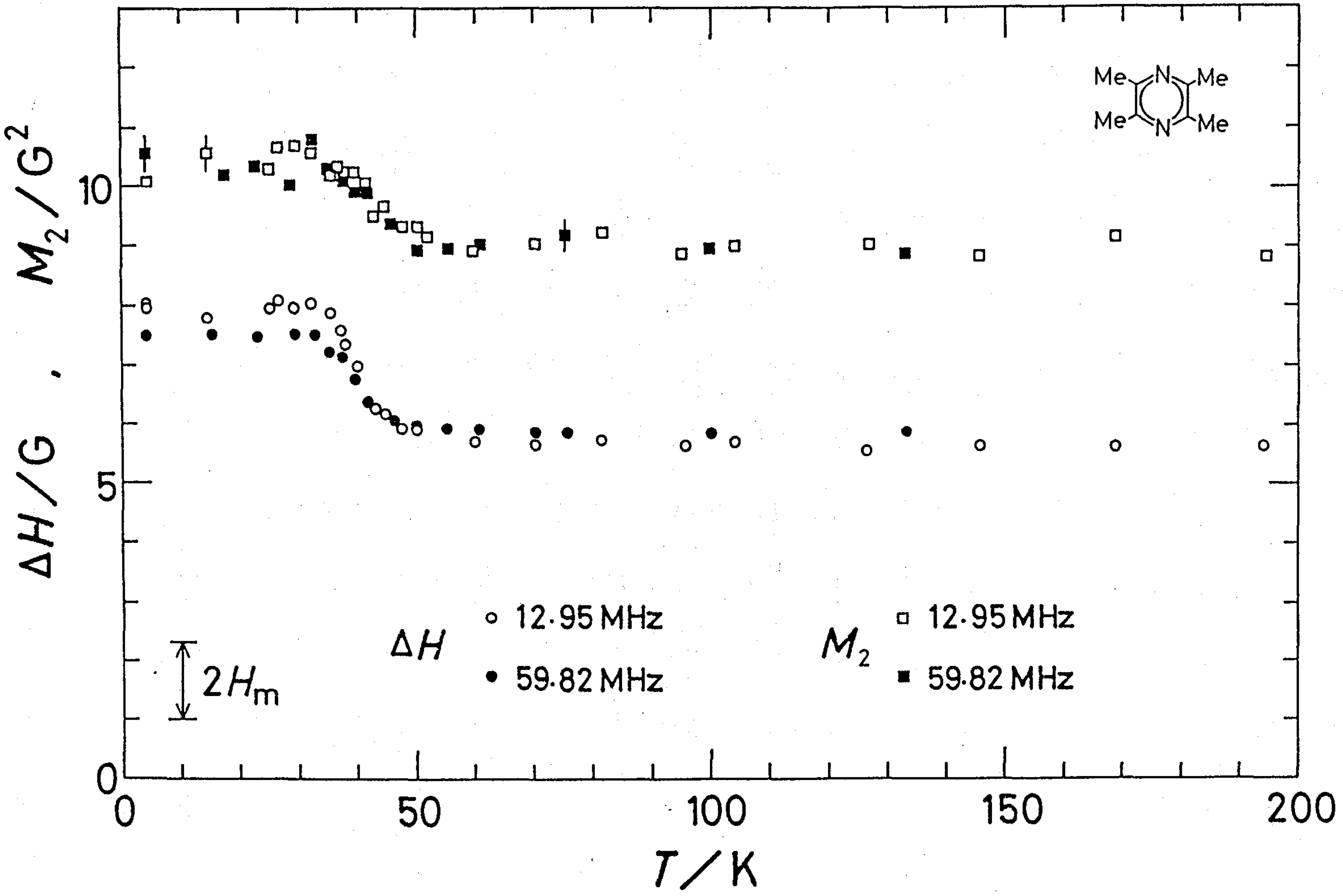

Fig. 36 Temperature dependence of maximum slope width ΔH (○, ●) and second moment M_2 (□, ■) of tetramethylpyrazine. ○ (□) was obtained at 12.95 MHz while ● (■) at 59.82 MHz.

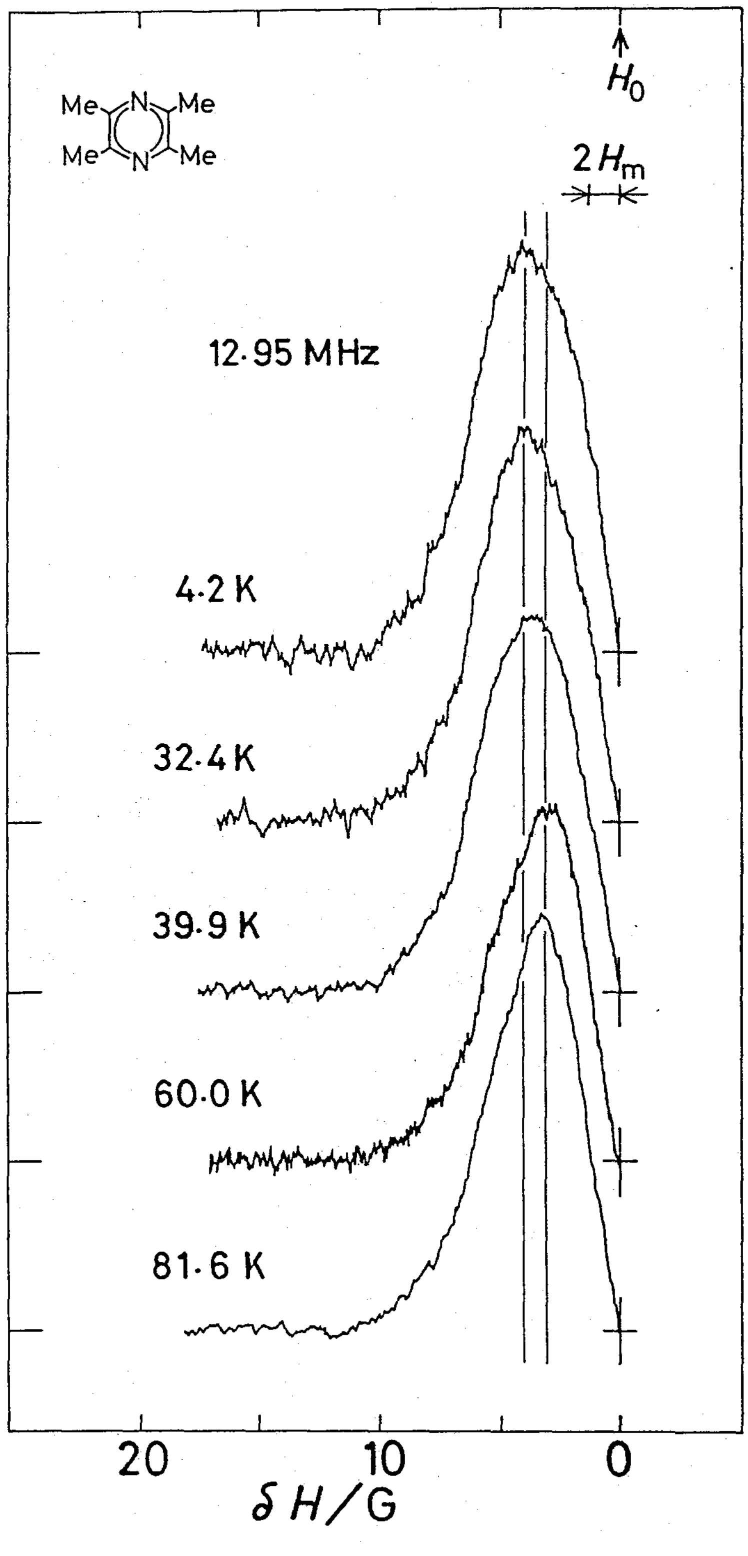

Fig. 37 Temperature variation of the line shape of tetramethylpyrazine. Haves of the differential absorption lines are shown.

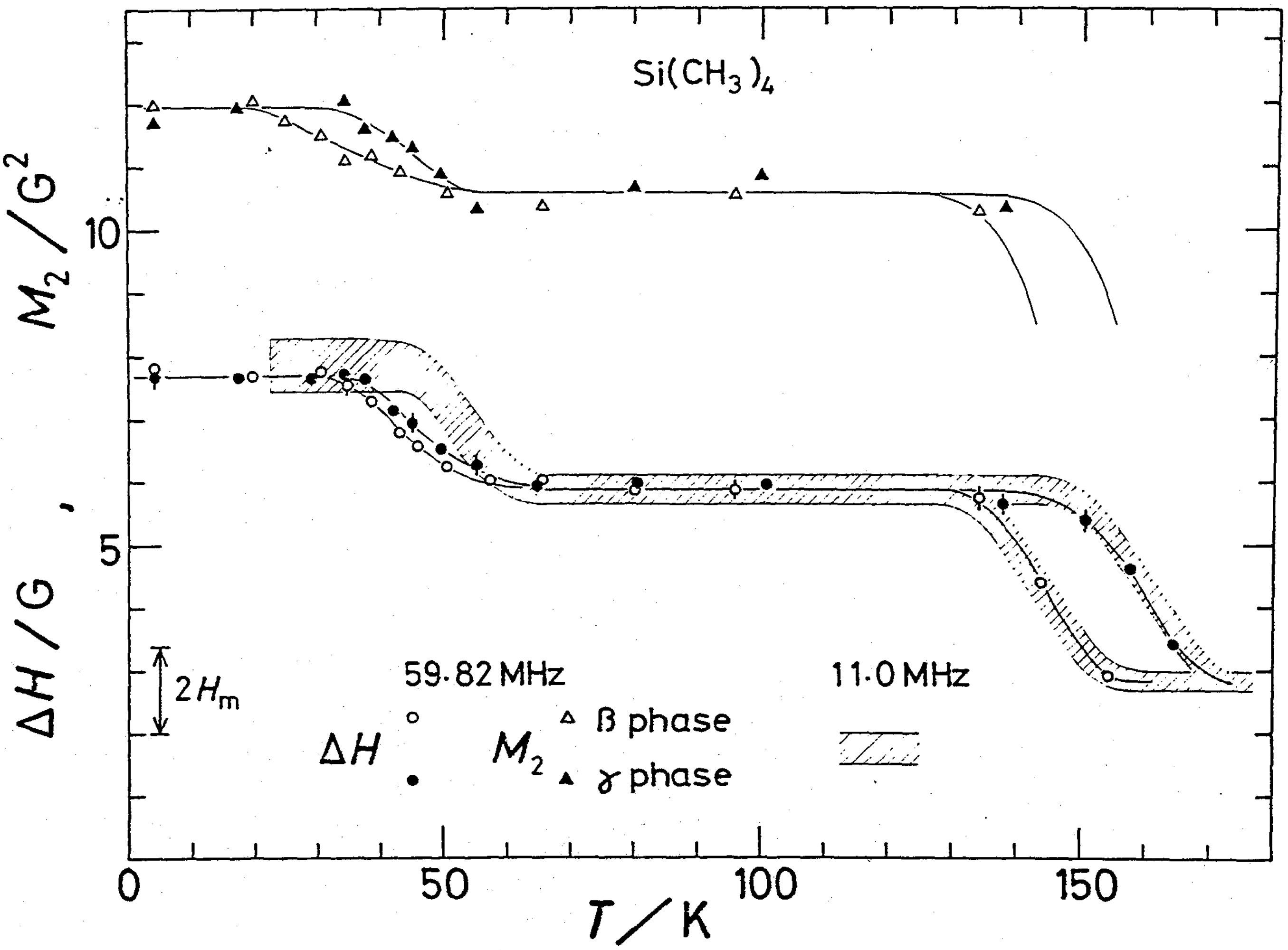

Fig. 38 Temperature dependence of maximum slope width ΔH (○, ●) and second moment M_2 (△, ▲), ○(△) for the β phase, ●(▲) for the γ phase. The shaded area show the experimental results at 11.0 MHz by Hasebe, et al$^{1)}$.

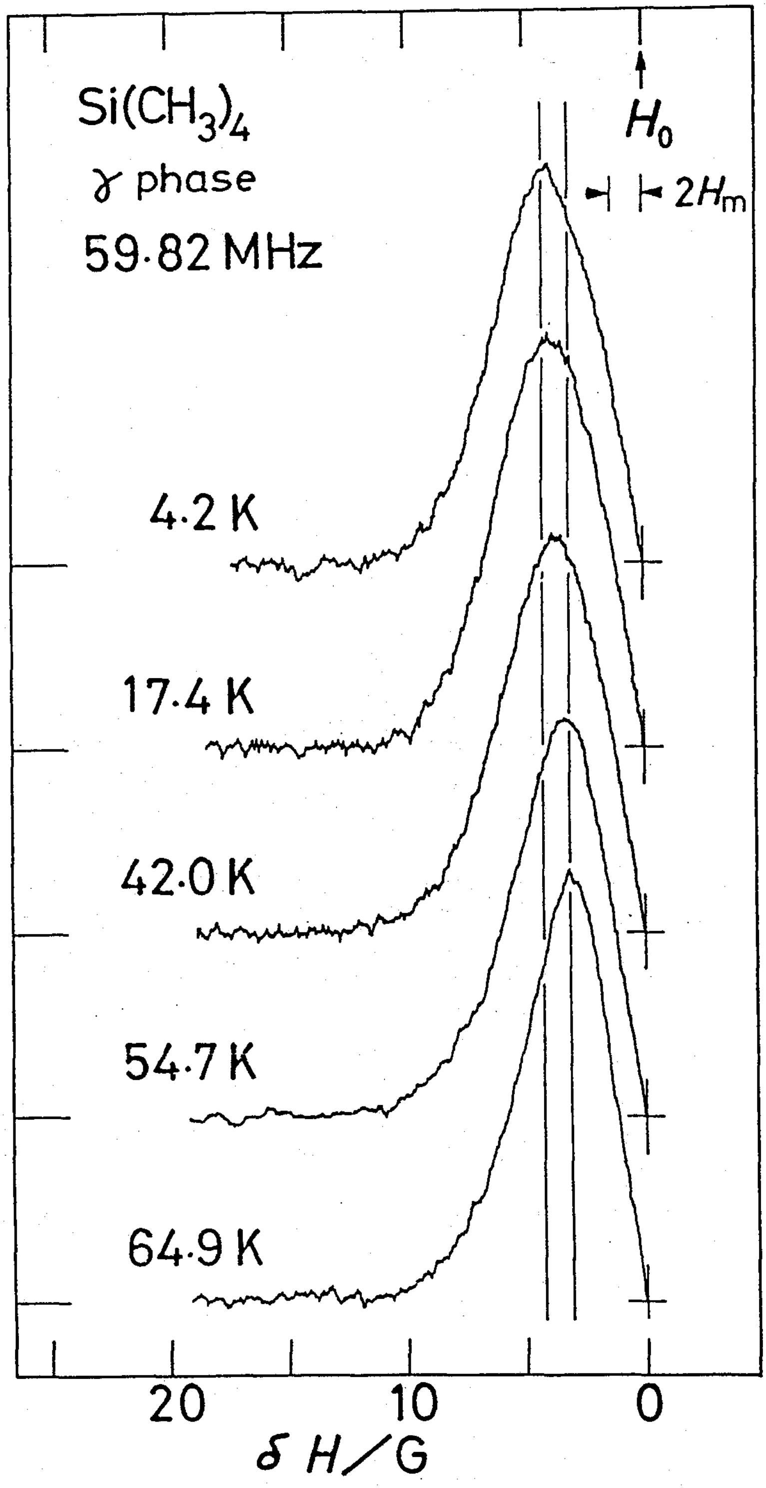

Fig. 39 Temperature variation of the line shape of $Si(CH_3)_4$. in its γ phase. Haves of differential absorptionlines are shown. In the β phase, a similar change of the line shape was observed.

The line width and second moments of the β and γ phases are differnt from each other in the region of small redution, although in the lower and higher temperatures than that region these values are the same except for the effect of molecular tumbling.

Figure 40 shows that the value of the ratio, M_4/M_2^2, (forth moment over the second powers of second moment) of T.M.P. is about 3. This result indicates that the absorption line is a Gaussian type 50). The similar results were observed for the β and γ phases of $Si(CH_3)_4$ (Fig.41).

The intermethyl dipole broading for T.M.P. and $Si(CH_3)_4$ is so large as the structure of the line shape due to intramethyl dipole interaction for a rotating methyl group is concealed. On the other hand the intermethyl dipole interaction is very weak for CH_3SiCl_3 as described in Subsection VI.2. The typical differential line shape and the temperature dependence of the line width are shown in Figs.42 and 43, respectively. Figure 43 show that the reduction also takes place for maximum slop width of peak A about 30 ∿ 45 K but it is very small. For the peak B and C in Fig.42 the details are not clear because the broadness of the peaks. The intramethyl contribution to the second moment is 5.26 G^2 2-4) assuming an interproton distance of 1.80 Å for a rapidly reorienting 2) or tunneling 3) methyl group. The intermethyl contribution to the second moment at about 100 K is 4 and 5 G^2 for T.M.P. and $Si(CH_3)_4$, respectively, while it is 1.3 G^2 for CH_3SiCl_3. For CH_3I it is about 2 G^2 and the reduction of line width is 0.5 G 48).

It is noted that the smaller the intermethyl dipole interaction

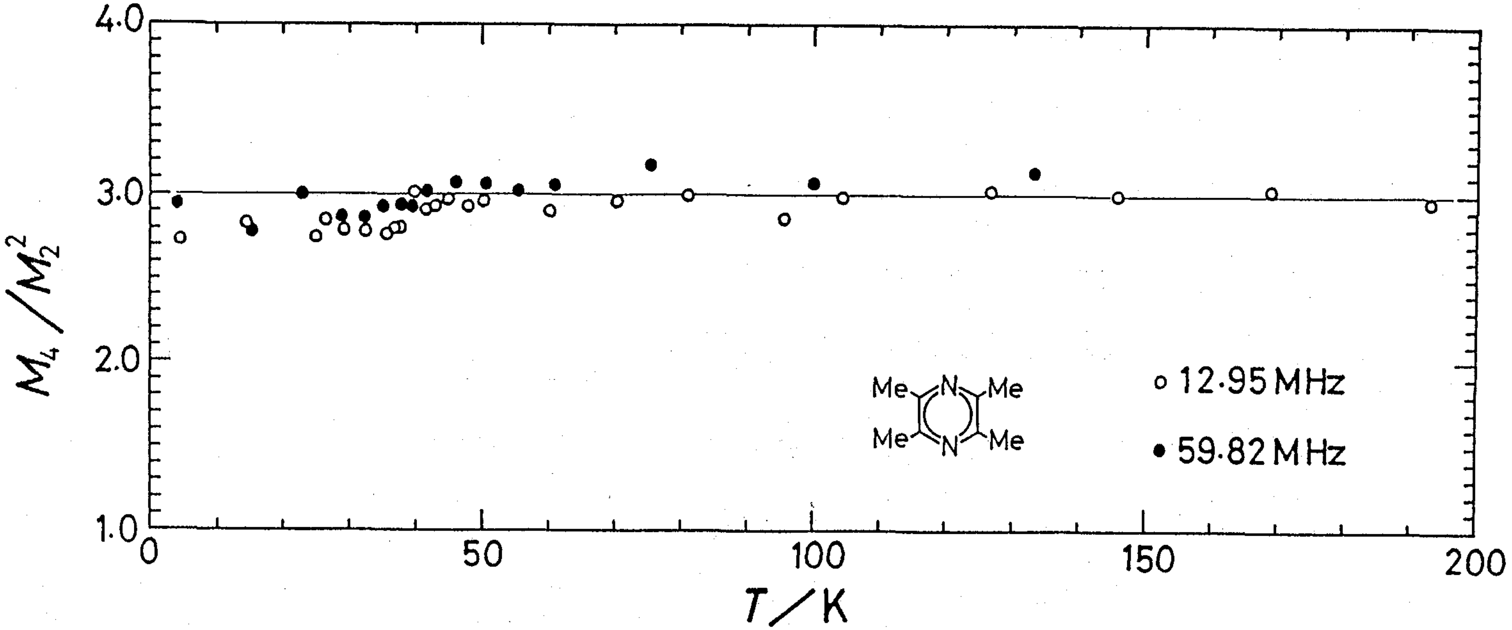

Fig. 40 The ratio M_4/M_2^2 (fourth moment over the second powers of the second moment) of tetramethylpyrazine vs. temperature.

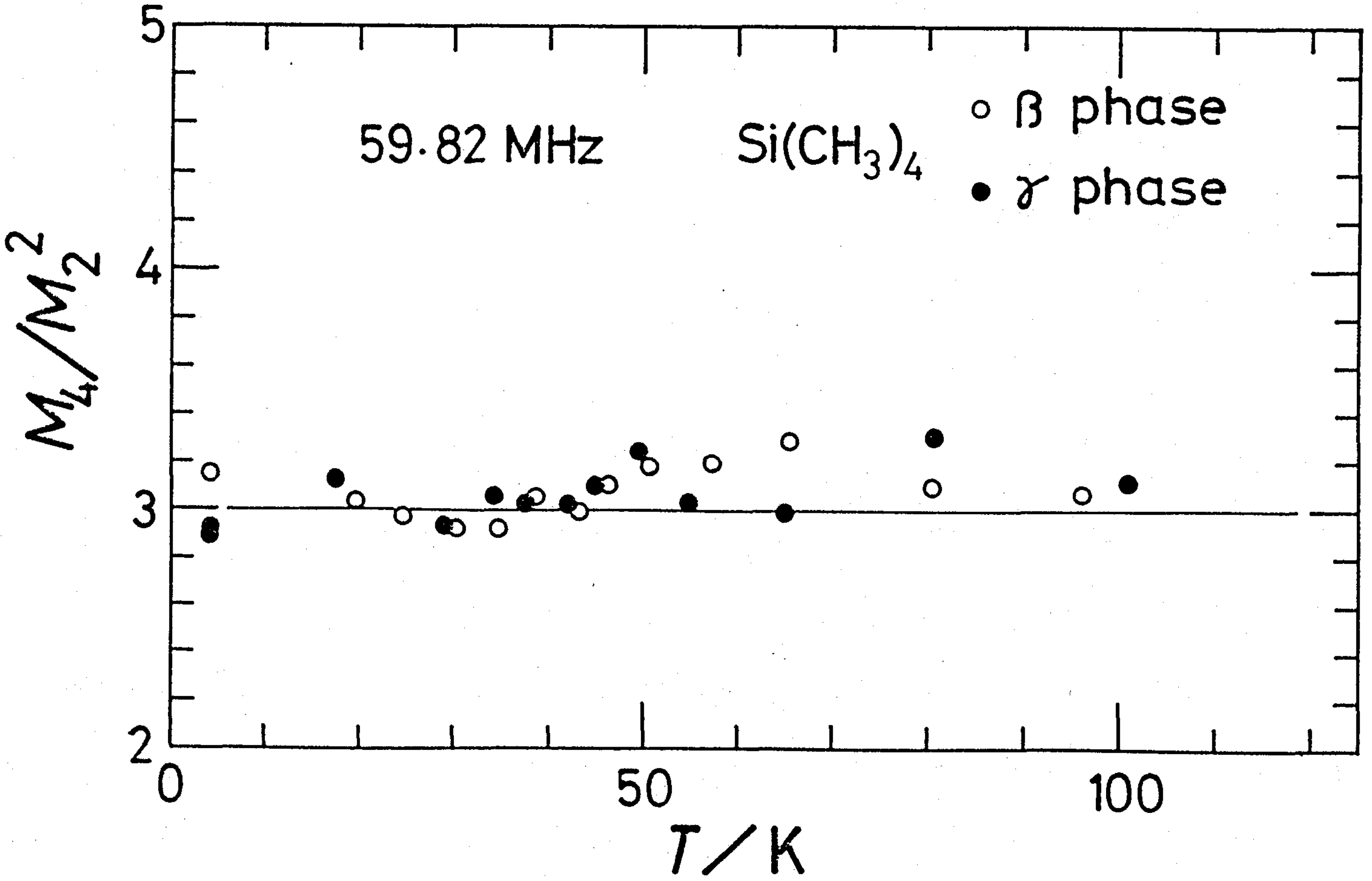

Fig. 41 The ratio M_4/M_2^2 (fourth moment over the second powers of the second moment) of tetramethylsilane vs. temperature.

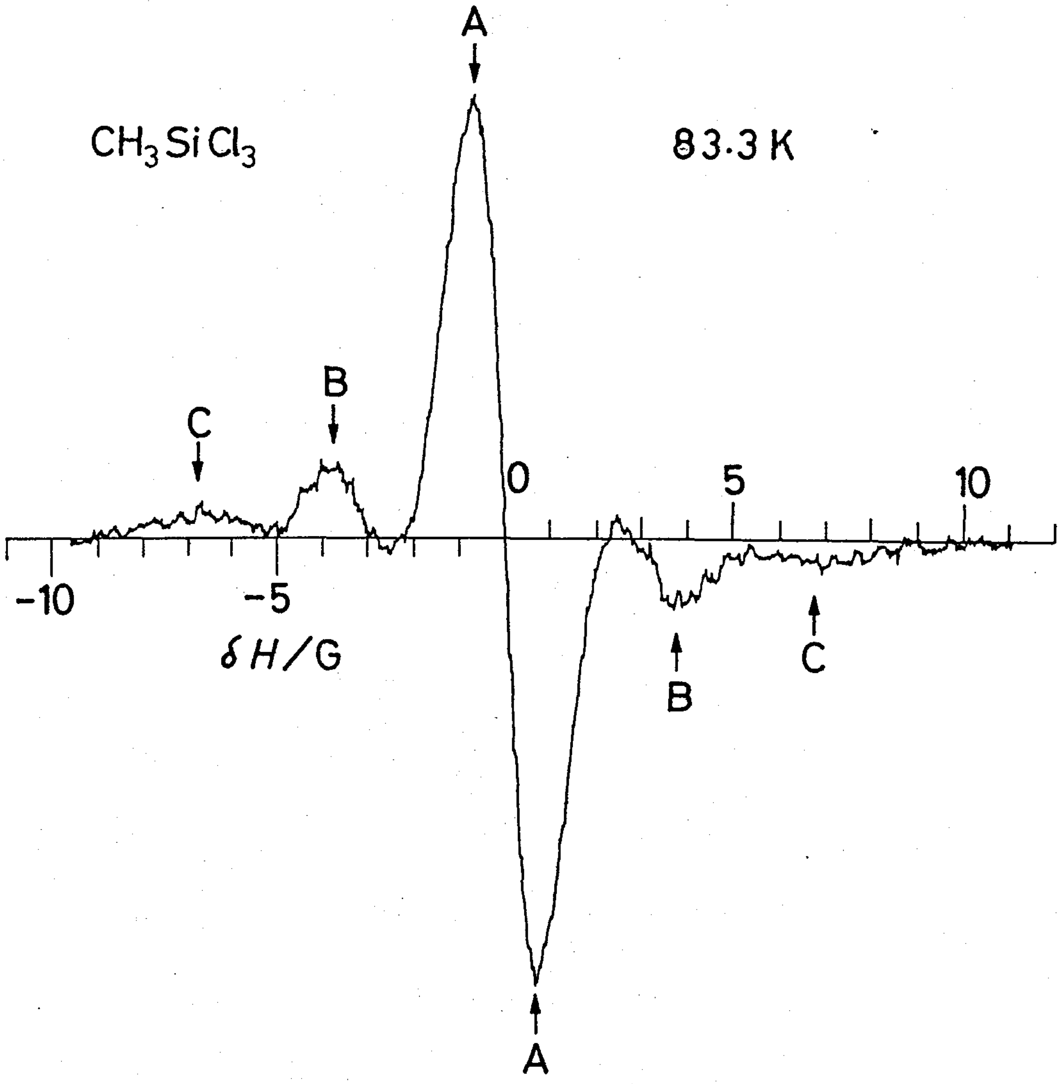

Fig. 42 Typical differetial absorption line of trichloromethylsilane (CH_3SiCl_3).

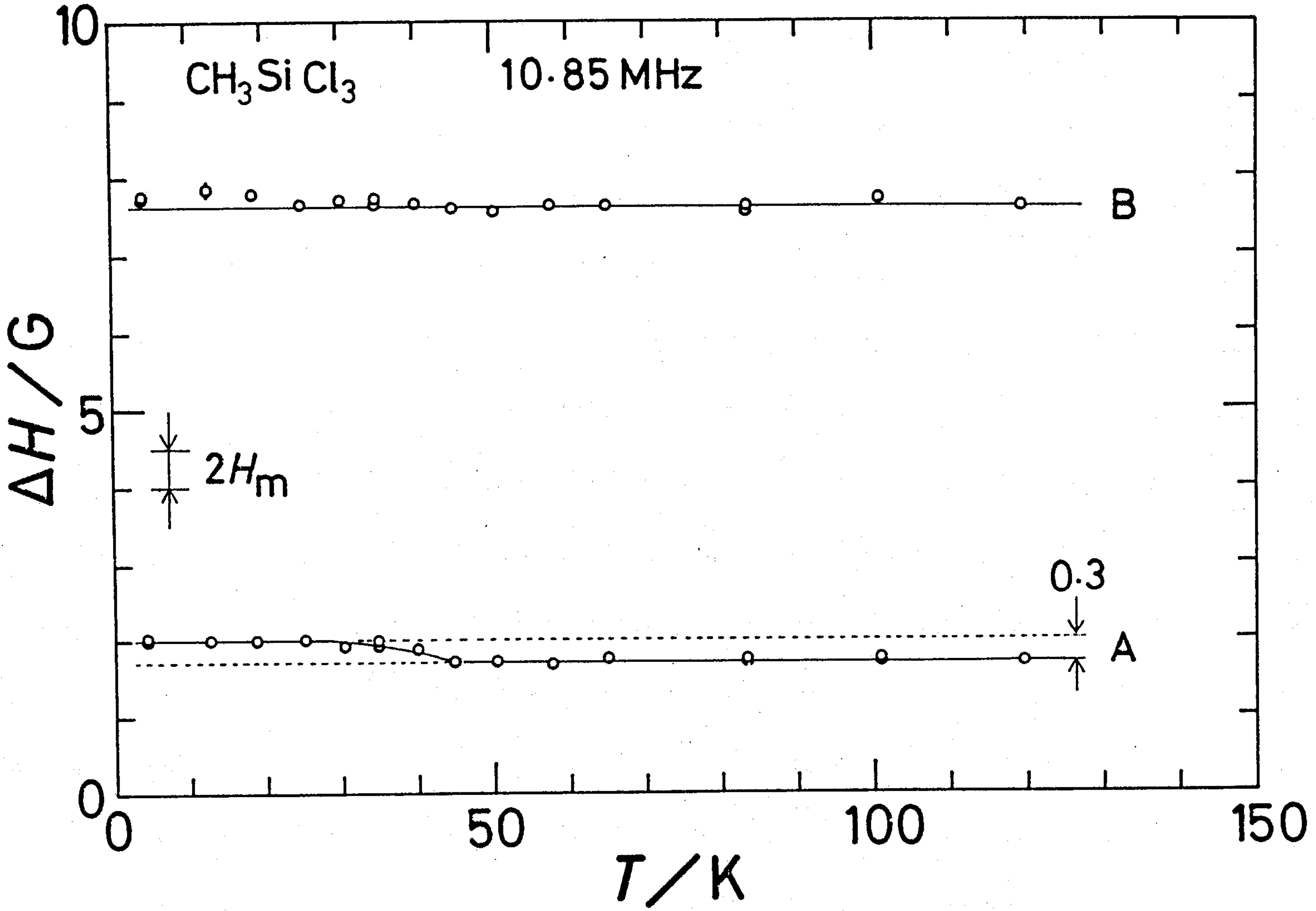

Fig. 43 Temperature dependence of the maximum slope width, ΔH . A and B indicate the peaks shown in Fig. 42. H_m is the modulation width ($H_m \cos \omega t$).

is, the smaller the amplitude of reduction is. From this result it is very probable that the reduction of line width of these materials at low temperature is that of the "intermethyl dipolar broadning". Indeed according to the calculation by Allen,[3)] any reduction of line width and second moment of intra-methyl portion is not expected for a methyl group of which the tunneling splittings are much greater than the dipolar energy.

The activation energies for rotation of methyl groups of $Si(CH_3)_4$, T.M.P., and CH_3SiCl_3 are similar to each other, i.e. about 5.8 ~ 6.8 kJ mol^{-1} and the torsional energy E_1, the separation between the ground and first excited state, is similar magnitude 160 ~ 180 cm^{-1} [21,35)]. For these materials the temperatures, at which the small reduction takes place, are nearly equal to each other, i.e. 30 ~ 50 K. On the other hand that temperature is 10 ~ 20 K for methyl iodide[48)] of which the torsional energy E_1 is 94 cm^{-1} [51)]. This fact is consistent with the idea that the origin of this reduction is the increase of the populations in the higher torsional levels or the increase of the transition rate between the torsional states due to rotation-phonon interaction (H_{RP}) as temperature is raised. For $Si(CH_3)_4$, the small reduction begins at lower temperature in the β phase than in the γ phase (Fig.38). This is probably the same reason as described above, i.e. the difference of the torsional energy scheme between the β and γ phases. The activation energy of the methyl rotation is smaller in the β phase than in the γ phase and the tunneling frequencies of the torsional ground state are larger in the β phase than in the γ phase as described in Subsection VI.4. The reduction was always observed (Fig.38), either when we measured the line shape at higher Larmor frequency than the two tunneling frequencies of γ phase of $Si(CH_3)_4$ or when we did so at lower Larmor frequency. Therefore with respect to the appearance of the reduction, there is no relation between the magnitude of tunneling frequency and that of Larmor frequency at which the line shape measurement is performed.

References

1) T. Hasebe, G. Soda, and H. Chihara, Proc. Japan Acad., 51 (1975) 168.

2) E.R. Andrew and R. Bersohn, J. Chem. Phys., 18 (1950) 159.

3) P.S. Allen, J. Chem. Phys., 48 (1968) 3031.

4) F. Apaydin and S. Clough, J. Phys., C1 (1968) 932.

5) S. Clough, "Nuclear Magnetic Resonance in Solids",(Nato advanced study institutes series), Ed. by L. Van Gerven (1977), Plenum Press.

6) The computer program SALS or Statistical Analysis with Least-Squares Fitting* was used in this calculation.
(*: Program Library Laboratory, Computer Center, The university of Tokyo, Yayoi 2-11-16, Bunkyo-ku, Yokyo 113).

7) S. Emid, R.J. Baarda, J. Smidt, and R.A. Wind, Physica, 93B (1978) 327, and the references cited therein.

8) S. Emid and R.A. Wind, Chem. Phys. Lett., 33 (1975) 269.

9) S. Emid, R.A. Wind, and S. Clough, Phys. Rev. Lett., 33 (1974) 769.

10) D.J. Ligthelm, R.A. Wind, and J. Smidt, Physica, 100B (1980) 175.

11) T.P. Das and E.L. Hahn, "Solid State Phys. (1958), Supplement 1, Nuclear Quadrupole Resonance Spectroscopy".

12) A. Abragam, "The principles of Nuclear Magnetism", (1961) Oxford.

14) H.O. Hooper and P.J. Bray, J. Chem. Phys., 33 (1966) 334.

15) T.B. Cobb and C.S. Johnson, Jr, J. Chem. Phys., 52 (1970) 6224.

16) P.S. Allen and D.G. Taylor, J. Phys., C8 (1975) 3036.

17) E.G. Rochow and H.G. LeClair, J. Inorg. Nucl. Chem., 1 (1955) 92.

18) C.P. Slichter, "Principles of Magnetic Resonance", Second revised and expanded edition, (1978), Springer-Verlag.

19) "Tables Relating to Mathieu Functions", Colunbia Univ. Press, (1951) New York, The application of it for triangle rotor was based on the article by H. Van Kempen, et al.[20)].

20) H.Van Kempen, T. Garofano, A.R. Miedema, and W.J. Huiskamp, Physica, 31 (1965) 1096.

21) C.I. Ratcliffe and T.C. Waddington, J. Chem. Soc. Far. II, 72 (1976) 1840.

22) M. Punkkinen and S.Clough, J. Phys., C7 (1974) 3403.

23) I.Y. Wei and C.S. Johnson, Jr, J. Mag. Reson., 28 (1977) 377.

24) D.T. Cromer, A.J. Ihde, and H.L. Ritter, J. Amer. Chem. Soc., 73 (1951) 5587.

25) D.T. Cromer, J. Chem. Phys., 61 (1957) 254.

26) L. Guibe and E.A.C. Lucken, Mol. Phys., 10 (1966) 273.

27) T.P. Das and E.L. Hahn, " Solid State Phys. (1958), Supplement 1, Nuclear Quadrupole Resonance Spectroscopy".
H. Chihara and N. Nakamura, Kagaku no Ryoiki, 23 (1969) 913.

28) C.H. Stam, Acta Cryst., B28 (1972) 2630.

29) R.C. Livingston, D.M. Grant, R.J. Pugmire, K.A. Strong, and R.M. Brugger, J. Chem. Phys.,58 (1973) 1438.

30) P.S. Allen, Far. Symposia Chem. Soc. No.13 (1978) 133.

31) P.J.L. Galigne and M.M.J. Falgueirettes, Acta Cryst., B26 (1970) 368.

32) S. Clough, A. Heideman, and M. Paley, J. Phys., C13 (1980) 4009.

33) P.S. Allen and P. Branson, J. Phys., C11 (1978) L121.

34) D.J. Ligthelm, R.A. Wind, and J. Smidt, Physica, 100B (1980) 175.

35) J.R. Durig, S.M. Craven, and J. Bragin, J.Chem. Phys.,52 (1970) 2046.

36) T. Shinoda, Bull. Chem. Soc. Japan, 50 (1977) 1382.

37) M. Harada, T. Atake, and H. Chihara, J. Chem. Thermodynamics, 9 (1977) 523.

38) T. Hasebe, G. Soda, and H. Chihara, Proc. Japan Acad., 51 (1975) 168.

39) S. Albert and J.A. Ripmeester, J. Chem. Phys., 57 (1972) 2641.

40) R.A. Wind amd S. Emid, Phys. Rev. Lett., 33 (1974) 1422.

41) D.J. Ligthelm, R.A. Wind, and J. Smidt, Physica, 104B (1981) 397.

42) E.P. Jones and M. Bloom, Phys. Rev. Lett., 28 (1972) 1329.

43) W. Hamilton, J.W. Edmonds, A. Tippe, and J.J. Rush, Diss. Far. Soc., 48 (1969) 192.

44) Von D. Bougeard, P. Bleckmann, and B. Schrader, Ber. Bunsenges. Phys. Chem., 77 (1973) 1059.

45) J.J. Rush, J. Chem. Phys., 47 (1967) 3936.

46) P.S. Allen and A. Cowking, J. Chem. Phys., 49 (1968) 789.

47) K. Morimoto, J. Phys. Soc. Japan, 50 (1981) 2404.

47) P.S. Allen and A. Cowking, J. Chem. Phys., 47 (1967) 4286.

48) T. Yamamoto, Thesis (1980) Osaka University.

49) P.S. Allen, J. Chem. Phys., 48 (1968) 3031.

50) R. M. White, "Quantum Theory of Magnetism", (1975) Chapter 5, Advanced Physics Monograph Series, Ed. by W.A. Nierenberg, McGraw-Hill Book Company.

51) M. Ito, J.Chem. Phys., 41 (1964) 1255.

52) R.A. Wind, W.M.M.J. Bovee, J.C.F. Kupers, and J. Smidt, Z. Naturforsh., 34a (1979) 631.

53) D.G. Lister, J.N. Macdnard, and N.L. Owen, "INternal Rotation and Inversion", Chapter 4 and 5, (1978) Academic Press, and the references cited therein.

54) W. Hamilton, J.W. Edmonds, A. Tippe, and J.J. Rush, Diss. Far. Soc., 48 (1969) 192.

55) "Kagaku Binran", Kiso-hen II, (1975) Maruzen K.K..

56) G. Celotti, Acta Cryst., A31 (1975) 582.

57) L. O. Brockway and J.M. Robertson, J. Chem. Soc., (1939) 1324.

VII. Summary and conclusion

Rotational behavior of methyl groups in some molecular solids was investigated by the nuclear magnetic resonance method. A particular interest exists in the "mechanical coupling" between the methyl groups which are close to each other.

The effect of collective rotation or "geared rotation" of the two methyl groups on the spin-lattice relaxation rate (T_1^{-1}) was discussed in the classical limit (Section III). But because the difference between the observable T_1^{-1} value due to correlated reorientation and that due to independent reorientation is very small, it is not conclusive from the usual experiment that the two adjacent methyl groups under go the collective reorientation or independent reorientation. The experiment for the partially deuterated sample is probably useful to distinguish the collective and independent rotations as discussed in Section III.

The principal work in this thesis is to investigate the coupling effect on the "rotational tunneling" of the adjoining methyl groups in the solid state.

The tunneling spectra ($\omega_t^{SS'}$) of the methyl groups of trichloromethylsilane (Subsection VI. 2), 1,2,4,5 - tetramethylbenzene (durene) and teramethylpyrazine (Subsection VI.3), tetramethylsilane (Subsection VI.4), and hexamethylbenzene (Subsection VI.5) in their solid states were directly observed by the N.M.R. methods. One of the methods is to measure the dependence of the spin-lattice relaxation rate on the Larmor frequency(ω_0) and on the temperature. The other is the "N.M.R. field cycling technique" which is equivalent to the method described above and is more eloquent and easy, especially for the case of very long spin-lattice relaxation time. The tunneling spectrum, $\omega_t^{SS'}$, of the methyl groups are obtained through the so-called "tunneling assisted maximum" of the spin-lattice relaxation rate, T_1^{-1}. Therefore, the examination was performed with respect to the problem that the behavior of the spin relaxation can be understood in the framework of the novel theory of symmetry restricted spin diffusion model (S.R.S.D.) or not, before the tunneling energy scheme of the methyl groups were discussed. The non-exponential recovery of the spin magnetization of the materials cited in this thesis and its dependence on the pulse sequence employed can be understood within the framework of S.R.S.D. theory (Subsection VI.1). The tunneling assisted minimum only appeared in the fast-relaxing component (T_{1f}) of the spin-lattice relaxation time, which is in consistent with the prediction by S.R.S.D. model. The tunneling assisted minima in the T_{1f} curve vs. temperature were clearly demonstrated in the β and γ phases of tetramethylsilane (Subsection VI.4).

The tunneling splittings of the torsional ground state of the methyl groups of trichloromethylsilane (CH_3SiCl_3) are 34.6 ± 0.5 MHz and 40.4 ± 0.5 MHz. The two kinds of splittings are attributed to the different methyl groups which are hindered by slightly different potential barriers due to different surroundings in the crystal. The strength of repulsive interaction between the methyl groups was estimated to be smaller than that of durene, tetramethylpyrazine, tetramethylsilane and hexamethylbenzene by the factor more than 10 (Subsection VI.2).

The tunneling splittings of durene and tetramethylpyrazine are three kinds in their torsional ground states. For durene, 29.3 ± 0.7 MHz, 25.3 ± 0.6 MHz, and 17.8 ± 0.5 MHz were observed and for tetramethylpyrazine 26.8 ± 0.8 MHz, 20.2 ± 0.8 MHz, and 14.3 ± 0.6 MHz (or 6.4 ± 0.7 MHz) were identified. The crystalographically inequivalent methyl groups are two kinds in both crystals of durene and tetramethylpyrazine. The three kinds of tunneling splittings are not deduced from the simple superposition of the energy schemes of a single methyl group . These experimental results are comprehended when we consider the mechanical coupling between the two methyl groups (Subsection VI.3).

The tunneling frequencies of the methyl groups of tetramethylsilane ($Si(CH_3)_4$) in its γ phase are 15.8 ± 0.9 MHz and 24.0 ± 1.4 MHz. The β phase showed more complicated tunneling spectra which distribute from about 2 MHz to about 70 MHz.

Hexamethylbenzene showed two tunneling splittings in it phase III. These are 9.6 ± 0.4 MHz (A) and 7.9 ± 0.4 MHz (B) at low temperature limit. The frequency B decreases into zero below 30.9 K whereas the frequency A was almost independent of the temperature up to 30.9 K.

These results of tetramethylsilane and hexamethylbenzene are not understood when we consider a single methyl group. They also indicate that the mechanical coupling between the adjacent methyl groups plays an important role in the rotational tunneling state of these methyl groups. The "coupled rotational tunnel state" in solids was demonstrated in this thesis in the first time. The magnitude of the coupling between the methyl groups in hexamethylbenzene molecule is strongest when we consider the distance between the adjacent methyl groups (Subsection VI.6).

For the complete explanation of the observed tunneling spectra of the methyl groups, we need the detailed tunneling energy scheme of the coupled methyl groups (rotor level scheme) and furthermore need the coupling of the nuclear spin states to the rotor states, because what we observe is the effect of tunneling splittings on the "spin-lattice relaxation" of the protons of methyl groups. The problem for a single methyl group has been investigated as shown in Section II. But for the coupled methyl groups the problem has not been solved until now and it is the problem to be solved in the next step of the study. A consideration was proposed in this thesis (Subsection VI.3).

The spin state is probably described by the simple superposition of the 3/2 spin-systems even in the case of mechanically coupled methyl groups, because the rigidity of the nuclear spins hold only in each methyl group in the case of rapidly rotating methyl groups, i.e. internuclear distances between the different methyl groups fluctuate due to relative rotation of the methyl groups in many case.

The decreases of the observable tunneling frequencies of tetramethylsilane and of hexamethylbenzene (peak B) with increasing temperature were directly observed. For trichloromethylsilane, durene and tetramethylpyrazine, the indirect evidences of decreases of tunneling frequencies were obtained (Subsections VI.2 and VI.3). These behaviors are considered to be the result of thermal averaging of the rotational states due to non-magnetic transitions induced by rotation-phonon interaction (H_{RP}).

The tunneling assisted rotation is important in the low temperature region for all materials studied in this thesis. The tunneling frequencies of the methyl groups are the same order as the Larmor frequency ($10^0 \sim 10^2$ MHz). The effects of tunneling rotational modes on the spin-lattice relaxation time of the protons of methyl groups were clearly observed. As the temperature rised, observable (effective) tunneling frequencies decreased and became zero below the T_1 minimum temperature of each material. This T_1 minimum is due to the rotation of the methyl groups about their symmetry axes. Near and above that temperature the jumping rotation over the top of the barrier is principal mechanism of the rotation of methyl groups. This change of the principal mechanism of the rotation of methyl groups was observed as the change of the behavior of the spin-lattice relaxation in the materials studied in this thesis. The average transition rate ω_3, with which the methyl group jumps (over the top of the barrier) from one well to the another well of the potential barrier was obtained for trichloromethylsilane and tetramethylpyrazine from the observed T_1 curve vs. temperature. It is

$$\omega_3 = 3.62 \times 10^{11} \exp(- 5.8 \text{ kJ mol}^{-1}/RT)$$

for trichloromethylsilane and it is

$$\omega_3 = 1.51 \times 10^{12} \exp(- 6.3 \text{ kJ mol}^{-1}/RT)$$

for tetramethylpyrazine.

The small reduction of the maximum slope width and second moment of N.M.R. absorption line of the tunneling methyl groups at low temperature ($10 \sim 50$ K) was assigned to that of intermethyl dipole broadning. The mechanism of this reduction is probabry due to the increase of the rate of non-magnetic transitions among the torsional states due to rotation-phonon interaction (H_{RP}) or due to the increase of the population in the higher torsional levels as temperature increases (Subsection VI. 7).